HAL
open science

Development of New Late-Stage Labeling Methods with Labeled Carbon and Fluorine-18

Malvika Sardana

To cite this version:

Malvika Sardana. Development of New Late-Stage Labeling Methods with Labeled Carbon and Fluorine-18. Radiochemistry. Université Paris-Saclay, 2020. English. NNT : 2020UPASF001 . tel-02954095

HAL Id: tel-02954095

https://theses.hal.science/tel-02954095

Submitted on 30 Sep 2020

HAL is a multi-disciplinary open access archive for the deposit and dissemination of scientific research documents, whether they are published or not. The documents may come from teaching and research institutions in France or abroad, or from public or private research centers.

L'archive ouverte pluridisciplinaire **HAL**, est destinée au dépôt et à la diffusion de documents scientifiques de niveau recherche, publiés ou non, émanant des établissements d'enseignement et de recherche français ou étrangers, des laboratoires publics ou privés.

université PARIS-SACLAY

Development of New Late-Stage Labeling Methods with Labeled Carbon and Fluorine-18

Thèse de doctorat de l'université Paris-Saclay

École doctorale n°571, Sciences chimiques :
Molécules, Matériaux, Instrumentation et Biosystèmes (2MIB)
Spécialité de doctorat : Chimie
Unité de recherche : Université Paris-Saclay, CEA,
Service de Chimie Bio-organique et de Marquage, 91191, Gif-sur-Yvette, France.
Référent : Faculté des Sciences d'Orsay

Thèse présentée et soutenue à Orsay,
le 10 Septembre 2020, par

Malvika SARDANA

Composition du Jury

Cyrille KOUKLOVSKY Professeur, Université Paris-Saclay	Président
Chris WILLIS Professeur, University of Bristol	Rapporteur & Examinatrice
André LUXEN Professeur, Université Liège	Rapporteur & Examinateur
Magnus SCHOU Associate Director Bioscience, AstraZeneca R&D	Examinateur
Chad ELMORE Director Isotope Chemistry, AstraZeneca R&D	Encadrant & Examinateur
Christophe DUGAVE ISOTOPICS project coordinateur, CEA-Saclay	Directeur de thèse
Davide AUDISIO Head of Carbon-14 Labeling Group, CEA-Saclay	Co-Encadrant
Fabien CAILLE Service Hospitalier Frédéric Joliot, CEA-Saclay	Co-Encadrant

Thèse de doctorat

NNT : 2020UPASF001

Development of New Late-Stage Labeling Methods with Labeled Carbon and Fluorine-18

Malvika Sardana

The thesis was prepared in the Isotope Chemistry team at AstraZeneca in Gothenburg, Sweden from January 2017 – March 2020. The project was funded by European Union's Horizon 2020 research and innovation program under the Marie Skłodowska-Curie grant agreement no. 675071.

© Malvika Sardana, September 2020

To her, who could not be here today…

Acknowledgement

Horizon 2020 Research and Innovation Program of the European Union under Marie Sklodowska-Curie grant agreement No.675071 funded my PhD studies. These past three years have been very memorable, and I have a lot to be grateful for. I must thank Dr Chad Elmore for giving me the opportunity to perform this PhD under his supervision, you have been a true mentor. It has been a pleasure to work with you, and to always find your door open for any discussion, for both chemistry and non-chemistry related discussions. I have learned a lot and hope to learn more ☺.

I would also like to express my gratefulness towards Dr Magnus Schou, Dr Christophe Dugave, Dr Davide Audisio and Chad for giving me vital advice and guidance throughout the PhD. I would also like to thank Lee Kingston, Jonas Bergare and Dr Cecilia Ericsson for helping with the carbon-14 chemistry, helping me around the lab and the great *fikas*. Obviously, I cannot forget Dr Markus Artelsmair for being in the similar PhD-*boat* with me at AstraZeneca. And I must mention Joakim Bergman, for helping me with the visible-light chemistry, your help has been very much appreciated. I would like to thank all past and present colleagues for making it an enjoyable work place.

I would like to express my gratitude towards the management team of this project: Dr Karen Hinsinger, Dr Christophe Dugave and Dr Emilie Nehlig. It has been an amazing journey meeting all the ESRs and having these fruitful consortium meetings. Moreover, I would like to thank both Karen and Christophe for being my translator and helping me with the registration at the university. I would like to acknowledge Dr Bertrand Kuhnast for evaluating the progress and quality of my PhD.

I would like to express my gratitude to the jury members Prof Chris Willis, Prof André Luxen, Dr Magnus Schou and Prof Cyrille Kouklovsky for reading and evaluating my PhD thesis. I would like to thank Dr Christophe Dugave and Dr Chad Elmore for correcting my thesis prior to submitting this thesis to the jury.

The Horizon 2020 project enabled me to do a secondment at Bioorganic Chemistry and Molecular Labeling department (Service de Chimie Bioorganique et Marquage) at the CEA, Saclay, France and at CEA Service Hospital Frédéric Joliot in Orsay France. I am grateful to Dr Davide Audisio, Dr Fabien Caillé and Dr Bertrand Kuhnast for welcoming me in their teams. The financial support from the Horizon 2020 project allowed me to attend conferences in UK, Czechia, Austria, and China. It was a memorable experience presenting my work as a presentation and posters.

I would like to thank my MSc students, Sylvia Wenker and Samiksha Sardana, it was a pleasure work with you two.

I would like to thank my husband, Deepak, for having confidence and going through this journey with me. My parents, Rajesh and Sarita, and my siblings, Samiksha and Sambhav, for supporting me not only throughout this PhD, but my whole life and making me capable to be where I am. When I was offered this PhD position, I was employed at Mercachem and I have many people to thank for supporting my decision. I will always remember the great support that I received from my colleagues back then.

Definitions – Terminology used in Radiochemistry

- Becquerel (Bq) – a SI unit to measure radioactivity, which is 1 disintegration per second. The traditional unit for radioactivity is Curie (Ci, 1 Ci corresponds to 3.7 10^{10} Bq.), which corresponds to the amount of radioactivity entitled by 1 g of Radium-222 (2.022×10^2 disintegration per minute.

- Specific Activity (SA) – the amount of radioactivity per molecule expressed in TBq/mmol or TBq/mg. A preferred terminology for long-lived radionuclides.

- Molar Activity (MA) – the amount of radioactivity per molecule expressed in GBq/µmol. A preferred terminology for short-lived radionuclides (PET).

- Decay-corrected – yield corrected to the same time point (A_0), to correct for the radioactivity lost due to the half-life time (t½) of the radionuclide. Formula used $A_t = A_0 e^{-\lambda t}$, with $\lambda = \frac{\mathrm{Ln}2}{t½}$.

Abbreviation

[^{11}C]PIB: 2-(4-([*methyl*-[^{11}C]amino)phenyl)benzo[d]thiazol-6-ol, Pittsburgh com

[^{18}F]FDG: 2-deoxy-2-[^{18}F]fluoro-D-glucose

^{11}C]PMP: 1-[^{11}C]methylpiperidin-4-yl propionate

2-MeTHF: 2-Methyltetrahydrofuran

ABC: ATP-binding Cassette

Ac: Acetyl

ADME: Administration, Distribution, Metabolism and Excretion

AIBN: 2,2'-azobis(2-methylpropionitrile)

aq: aqueous

Ar-X: Aryl-Halide

ATP: adenosine triphosphate

AUC: Area Under the Curve

BBB: Blood-Brain Barrier

BCRP: Breast Cancer Resistance Protein

Boc: *tert*-butyloxycarbonyl

Bq: Becquerel

C-11/^{11}C: Carbon-11

C-13/^{13}C: Carbon-13

C-14/^{14}C: Carbon-14

CEA: Commissariat à l'énergie atomique et aux énergies alternatives

Ci: Curie

CN: Cyanide

CO: Carbon Monoxide

COD: Cyclooctadiene

COgen: 9-Methylfluorene-9-carbonyl chloride

CORM: Carbon Monoxide Releasing Molecules

COware: Carbon Monoxide glassware, two-chamber system connected with a glass bridge

CRO: Contract Research Organization

d.c.: Decay Corrected

DCM: Dichloromethane

DDQ: 2,3-Dichloro-5,6-dicyano-1,4-benzoquinone

DIEA: Di-isopropylethylamine

DMF: N,N-Dimethylformamide

DMSO: Dimethylsulfoxide

EI: Electron Ionization

EOB: End of Beam

Equiv: Equivalents

ESI: Electrospray Ionization

ESR: Early Stage Researcher

Et: Ethyl

EtOAc: Ethyl Acetate

EtOH: ethanol

eV: Electron Volt

F-18/^{18}F: Fluorine-18

FDA: Food and Drug Administration

FeTTP: Iron Porphyrin

GE: General Electric

h: hours

H-2/^{2}H: Hydrogen-2, also known as Deuterium (D)

$H_2N^{14}CN$ [^{14}C]Cyanamide

H_2O: Water

H_2SO_4: Sulfuric acid

H-3/^{3}H: Hydrogen-3, also known as Tritium (T)

HIE: Hydrogen Isotope Exchange

HMBC: Heteronuclear Multiple Bond Correlation

HPLC: High Performance Liquid Chromatography

HRMS: High Resolution Mass Spectrometry

I-125: Iodine-135

*i*Pr: isopropyl

J: coupling constant

KIE: Kinetic Isotope Effect

LED: Light-emitting diode

LSC

M: Metal

MA: Molar Activity in TBq/mol

Me: Methyl

MeCN: Acetonitrile

MeOH: Methanol

min: Minutes

Mrp1: Multidrug Resistance-associated Protein

MS: Mass Spectrometery

N-15: Nitrogen-15

NET: Norepinephrine Transporters

PET: Positron Emission Tomography

P-gp: P-glycoprotein, also known as ABCB1 or MDR1

Ph: Phenyl

PMB: *para*-Methoxybenzene

prep: Preparative

PTFE: Polytetrafluoroethylene

qNMR: quantitative Nuclear Magnetic Resonance

QWBA: Quantitative Whole Body Autoradiography

RCY: Radiochemical Yield

S-35: Sulphur-35

SA: Specific Activity

sat: saturated

SCBM: Le Service de Chimie Bioorganique et de Marquage

SFC: Supercritical Fluid Chromatography

SHFJ: Service Hospital Frédéric Joliot

SI: *Système International* d'unités (International System of units)

SIL: Stable Isotope Labeled

SilaCOgen: methyldiphenylsilanecarboxylic acid

S_NAr: Nucleophilic aromatic substitution

SPE: Solid Phase Extraction

SPECT: Single photon emission computed tomography

$TBABF_4$: Tetrabutylammonium tetrafluoroborate

TEABr: Tetraethylammonium bromide

$TEAHCO_3$: Tetraethylammonium Bicarbonate

TFA: Trifluoroacetic Acid

TLC: Thin Layer Chromatography

TMS: Trimethylsilyl

TOF: Time of Flight

UPLC: Ultra-Performance Liquid Chromatography

UV: Ultra Violet

β^+: positron

γ: gamma

δ: Chemical Shift on NMR

λ: Wavelength

Table of Contents

ACKNOWLEDGEMENT 5

DEFINITIONS – TERMINOLOGY USED IN RADIOCHEMISTRY 7

ABBREVIATION 8

1. INTRODUCTION 19

1.1. Isotopic Labeling in Drug Discovery 19
1.1.1. Drug Development 19
1.1.2. Need of Isotopic Labeling in Drug Development 20
1.1.3. Stable Isotopes in Drug Development 21
SIL Compounds as Clinical Agents 23
1.1.4. Radionuclides in Drug Development 25
Radioligands for Lead Discovery 27
Administration, Distribution, Metabolism and Excretion 28
Clinical Trials 30
Considerations in Radiochemistry 31

1.2. Carbon-14 33
1.2.1. C-14 Building Blocks 34
[^{14}C]Cyanide 35
[^{14}C]Acetylene 36
[^{14}C]Cyanamide 38
[^{14}C]Carbon Dioxide 38
Last-stage carboxylations developed within ISOTOPICS 41

1.3. Carbonylation in Carbon Isotope Chemistry 43
Palladium-Catalyzed Carbonylation – Catalytic Cycle 43
1.3.1. General methods for Carbonylation using [^{14}C]Carbon Monoxide 44
[^{14}C]Calcium Carbonate Pyrolysis 45
[^{14}C]Formate based [^{14}C]carbonylation chemistry 46
^{14}COgen 50

1.4. Objectives 53

2. METHOD DEVELOPMENT: VISIBLE-LIGHT ENABLED AMINOCARBONYLATION OF UNACTIVATED ALKYL IODIDES WITH STOICHIOMETRIC CARBON MONOXIDE FOR APPLICATION ON LATE-STAGE CARBON ISOTOPE LABELING 59

2.1. Synthetic approaches towards carbonylation of unactivated alkyls 59
Radical Carbonylation – Thermal Initiator 60
Nickel-Catalyzed Carbonylation 60
Visible-light enabled carbonylation 62

2.2. Aim **65**

2.3. Development of Visible-light Enabled Palladium Catalysis **66**
2.3.1. Optimization of the reaction 67
2.3.2. Investigation of the Reaction scope 71

2.4. Conclusion and future perspectives **76**

3. METHOD DEVELOPMENT: REDUCTION OF $^{14}CO_2$ TO ^{14}CO, COMPARISON OF TWO METHODS 79

3.1. Aim **80**

3.2. Preliminary Results **81**
3.2.1. Electroreduction of $^{13}CO_2$ 81
3.2.2. Reduction of $^{13}CO_2$ by disilanes catalyzed by F^- 82

3.3. Summary and Future Perspectives **84**

4. METHOD DEVELOPMENT: RADIOSYNTHESIS OF [^{18}F]CRIZOTINIB, A POTENTIAL RADIOTRACER FOR PET IMAGING OF THE P-GLYCOPROTEIN TRANSPORT FUNCTION AT THE BLOOD-BRAIN BARRIER 87

4.1. P-glycoprotein **87**

4.2. Positron Emission Tomography **88**
4.2.1. Labeling with short-lived radionuclides 89
4.2.2. PET tracers for P-gp 90

4.3. Aim **93**
4.3.1. Fluorine-18 94
4.3.2. Synthetic approaches 95

4.4. Synthesis of Precursors **96**
4.4.1. Hypervalent Iodine(III) precursor 38 96
4.4.2. Deoxyfluorination precursor 50 97

4.5. Radiofluorination **100**

4.6. Conclusion and Future Perspectives **104**

5. SUMMARY OF FINDINGS AND FUTURE PERSPECTIVES 107

6. RESUME DE LA THESE 110

7. EXPERIMENTAL: VISIBLE-LIGHT ENABLED AMINOCARBONYLATION OF UNACTIVATED ALKYL IODIDES WITH STOICHIOMETRIC CARBON MONOXIDE FOR APPLICATION ON LATE-STAGE CARBON ISOTOPE LABELING 117

7.1. General Information 117
General Reactions 117
Reaction Setup 117
Reaction mixture 118
Purification 118
Analysis 119
LED report of the blue LEDs 121

7.2. General Procedures 122
General Procedure for Chamber B, CO Producing Chamber 122
General Procedure for Aminocarbonylation Chamber A, CO Consuming Chamber 122
Characterization data 123

8. EXPERIMENTAL: REDUCTION OF $^{14}CO_2$ TO ^{14}CO, COMPARISON OF TWO METHODS 146

8.1. General Information 146

8.2. Procedures and characterization 148
Electrochemical reduction 148
Reduction of $^{13}CO_2$ by disilanes catalyzed by F^- 151

9. EXPERIMENTAL: RADIOSYNTHESIS OF ^{18}F-CRIZOTINIB, A POTENTIAL RADIOTRACER FOR PET IMAGING OF THE P-GLYCOPROTEIN TRANSPORT FUNCTION AT THE BLOOD-BRAIN BARRIER 153

9.1. General Information 153
General Reactions 153
Reaction Setup 153
Reaction mixture 153
Purification 154
Analysis 154
Radio synthesis 155
Quality control 156

9.2. Procedures and characterization data 157
*Precursor synthesis: hypervalent iodine(III) precursor **38** 157*
*Precursor synthesis: Deoxyfluorination precursor **50** 164*
Failed strategies for protection and deprotection 174

10. REFERENCES 181

Introduction

1. Introduction

1.1. Isotopic Labeling in Drug Discovery

1.1.1. Drug Development

The process of discovering and developing new medical treatments is long and complex process, estimated to take between 10 to 15 years to go from project initiation to launch a drug on the market with costs around €2 billion per new entity (Figure 1).[1] The drug development process can be divided into eight stages. 1) It starts with the identification of an unmet medical need and finding a key target. 2) Next the drug discovery part, during which a drug candidate is identified that interacts with the earlier identified biological target (disease marker) and lead compounds are assessed for their pharmacokinetics and (early) safety properties.[2] 3) The preclinical phase comprises of *in vitro* and *in vivo* studies for toxicology screening and early administration, distribution, metabolism and excretion (ADME) studies. 4) During phase I of the clinical trials, a study is performed with a small group of healthy volunteers designed to test the safety and identify potential side effects, understand tolerability of the compound while investigating the dose range of efficacious doses. 5) Phase II studies cover the human ADME, tolerability and optimal dose determination in a small to medium group of patients to determine pharmacodynamics properties of the drug candidate and to assess its efficacy. 6) Phase III trials profiles the overall benefits and risks with a large group of patients. 7) When successful, it is necessary to gain approval from dedicated authorities to launch the drug on the market. 8) After launch of the medicine, it is important to keep up to date with the fate of the medicine (post-marketing surveillance) and to highlight the real benefit of the drug over existing treatments.

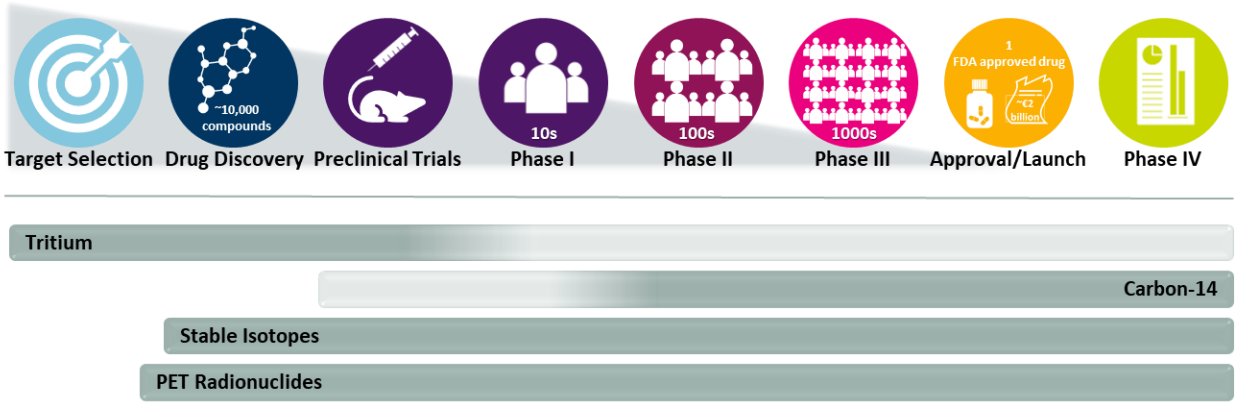

Figure 1 – Drug development process is depicted in eight stages here. The campaign starts with ~10.000 compounds and hopefully one of these reaches the market. The need of nuclides in different phases of the development can be seen in the bottom of the figure.

Multi-disciplinary teams work together over many years to develop new drugs to treat a particular disease.[2] Unfortunately, less than 10 percent of the potential drugs currently reach the market. These low success rates can primarily be ascribed to poor efficacy, poor understanding of the biology and rarely unexpected adverse effects, which are observed in Phase II clinical trials. Improved strategies are required to generate essential human pharmacokinetic and pharmacodynamic data in early drug discovery.

1.1.2. Need of Isotopic Labeling in Drug Development

During various stages of drug development, several *in vitro* and *in vivo* studies are performed to give a better understanding of the absorption, distribution, metabolism, and excretion of the drug candidate. The Food and Drug Administration (FDA)[3] recommends Phase 0 clinical trials to provide an alternative early drug development strategy by micro-dosing healthy volunteers with pharmaceuticals that are radiolabeled. To facilitate these studies drug candidates can be synthesized with stable nuclides (H-2, C-13 or N-15), long-lived radionuclides (H-3 or C-14) and/or short-lived radionuclides (C-11 or F-18). The synthesis of

radiolabeled compounds is generally a long and arduous process which requires the multistep synthesis of precursors for isotopic labeling. Moreover, the labeling position is an important aspect to be considered since the isotopic label must be chemically and biologically stable to enable the follow-up of *in vivo* fate of the drugs. Although, many drug metabolization pathways have been deciphered to date and help the medicinal chemist to recommend the labeling of chemical moieties reputed as biologically stable (to avoid loss of label), the (radiolabeling) of new drugs is often a complicated task. It may be necessary to synthesize several drug candidates with labels on various positions. Therefore, this is a complex process which mobilizes many radiochemists and is very time-consuming. In this respect, the late-stage or even last-stage incorporation of these (radio)nuclides is the ideal approach to streamline isotopic labeling of complex molecules. Unfortunately, there is a lack of such late-stage labeling methods in the toolbox of radiochemists. Therefore, the ISOTOPICS project[4] was initiated to train the next generation of isotope chemist, within academia and pharmaceutical companies. The project has 15 Early Stage Researchers (ESRs) who are trained to develop new late-stage methodologies to incorporate stable nuclides, long-lived radionuclides and/or short-lived radionuclides into drug molecules.[5–7]

1.1.3. Stable Isotopes in Drug Development

Natural carbon nuclides can be divided into the parent(most abundant), stable isotope, and radionuclide. Stable isotopes have the same number of protons but differ in the number of neutrons in the nucleus. A pivotal use of stable isotopes is in nuclear magnetic resonance (NMR), while protons are convenient to detect with ^{1}H NMR due to their spin ½; unfortunately, this does not hold true for C-12. To measure carbon atoms by NMR, we look

at C-13 as this too has a spin ½. Since the natural abundance of C-13 is only 1%, this explain the long measurements of a ^{13}C NMR. Stable isotope labeled (SIL) compounds are drug molecules in which at least one atom is substituted with a stable isotope. SIL compounds provide a key tool for the understanding of drug attributes: i.e. pharmacokinetics and pharmacodynamics, mechanism of toxicity and adverse effects; and bioavailability.[8] It can also be stored for a long time and can be handled without additional permissions, handling licenses or radiation safety measures.[9]

SIL compounds provide a MS signature that is a unique from the unlabeled compound, and can be useful for the absolute quantification of the parent compound and relative quantification of metabolites from biological samples (Figure 2).[10] To obtain a good resolution on MS, a mass increase of at least four is desired to avoid cross talk; this increase can be achieved by labeling with one or more stable nuclides or a mixture of different stable nuclides. If the compound contains a bromide or chloride atom, a higher mass increase may be necessary. For a proper quantification of the parent compound, it is key that the SIL contains very low to no unlabeled material.[11]

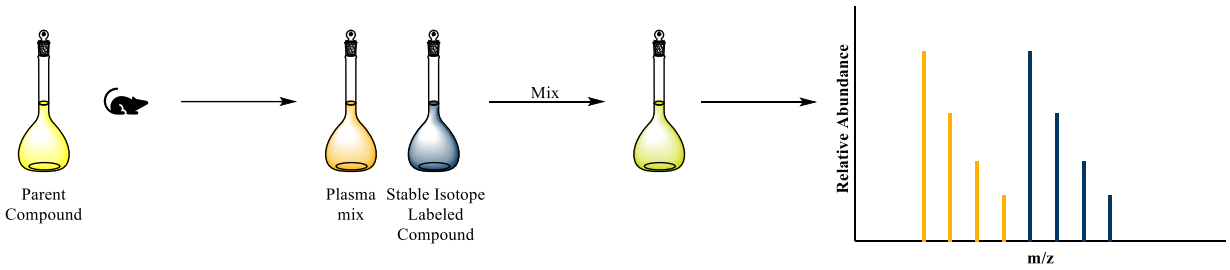

Figure 2 – Quantification of the parent compound with SIL compound. In this strategy the parent compound is processed in a biological matrix, mixed with the SIL compound, and analyzed on LC-MS. Adapted from Iglesias et al.[10]

The synthesis of SIL compounds often closely mirrors the synthesis of the parent compound, with some limitations related to the availability of the labeled starting material. SIL

compounds can also be used to optimize the synthesis and ensure reproducibility for radiosynthesis which will be discussed later.

The most commonly used stable isotopes are H-2, C-13 and N-15. The selection of which stable nuclides to use is often dependent on the commercial availability, costs, and synthetic route. While C-13 and N-15 do not significantly alter the drug molecule, deuterium can. The isotope effect is significant and can lead to chromatography issues, i.e. different retention time, depending on the location of the label. Moreover, it is important for the deuterium label not to be on an exchangeable position. Labeling with stable nuclides such as C-13 and/or N-15 is often used on a more metabolically stable position. Incorporation into these positions can be more time consuming and requires multiple steps. In contrast the incorporation of deuterium can be affected in a relatively fast and mild reaction with method such as Hydrogen-Deuterium (H-D) exchange allowing late-stage incorporation of the SIL.[9]

SIL Compounds as Clinical Agents

It is important to consider when substituting H for D, a large kinetic isotope effect (KIE) is observed, which can be explained by the large mass difference between these isotopes. The KIE can be used to improve the chemical stability, metabolic rate or residence time on the target of existing drugs.[12,13] Deutetrabenazine (Figure 3) is a drug approved for Huntington's disease. It is an improved treatment over tetrabenazine, as the hydrogens are replaced by deuterium atoms the drug has a better metabolic stability.

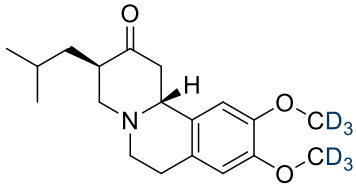

SD-809; Deutetrabenazine

Figure 3 – Deutetrabenazine, an approved treatment for Huntington's disease.

Thalidomide, a racemic drug (Figure 4), is an important and classic example of a marketed drug in 1950-60s with severe adverse effects, due to which the drug was withdrawn.[14] The side effects are caused by a single enantiomer, (*S*)-Thalidomide. However, the hydrogen atom in the chiral center is acidic, which epimerizes under physiological conditions. By replacing this hydrogen atom with a deuterium, the epimerization rate was reduced. The ability to stabilize a drug molecule with the isotope effect has an important added value in drug development.[15,16]

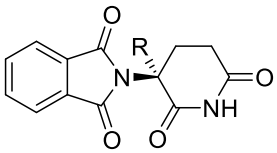

(S): R = H (*(S)*-Thalidomide)
R = D

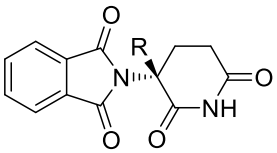

(R): R = H (*(R)*-Thalidomide)
R = D

Figure 4 – Two enantiomers of Thalidomide and of Deuterothalidomide.

Deuterated compounds have also found noteworthy application in positron emission tomography (PET) imaging tracers as well.[17] PET tracers (Figure 5) for mapping norepinephrine transporters (NET) and neurodegenerative diseases have shown an improved chemical stability due to the addition deuterium.[18–20]

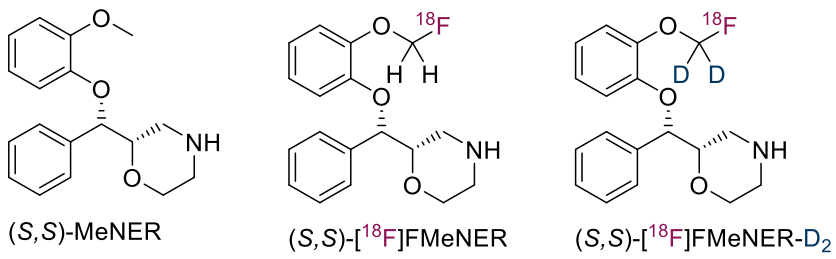

Figure 5 – Labeled analogues of (S,S)MeNER.

C-13 is also gaining interest as a clinical agent; [^{13}C]urea (Figure 6) is used in a breath test for *Helicobacter pylori* infection in the stomach.[8] While KIE can be observed for other nuclides such as B-11, C-13, N-15 and O-18, the effect is much smaller than H-2.[9]

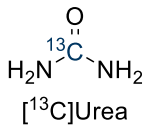

Figure 6 – Labeled urea used as a clinical agent.

1.1.4. Radionuclides in Drug Development

Radionuclides (Table 1) provide a sensitivity to molecules that allows an easier detection of these molecules in both *in vitro* and *in vivo* studies. Many compounds labeled with either long-lived radionuclides (i.e. H-3; C-14) or short-lived radionuclides (i.e. C-11; F-18) offer an array of advantages as they are easier to detect and trace, hence ease of visualization of organ and tissue distribution, and easy to quantify by scintillation counting or imaging methods. Basically, labeled molecules provide a practical way to both predict and later follow the fate of the drug candidate and the drug metabolites. Moreover, radiolabeling preserves the molecular structure, therefore introduces little if any change of chemical or biological property (depending on the radionuclide of choice).[21,22] Radionuclides offer an array of advantages that could contribute fruitfully to drug development program for use in preclinical, clinical and post-marketing studies.

Table 1 – Most commonly used radionuclides for clinical purposes, with their properties

Radionuclide	Decay product	Emission Type	Half-life time	Theoretical SA	Main Uses in Drug Discovery
Long-lived radionuclides					
Tritium	Helium-3	β-	12.43 years	1.07 TBq/mmol	Receptor binding, DMPK studies
Carbon-14	Nitrogen-14	β-	5730 years	2.30 TBq/mol	DMPK studies
Phosphorus-32	Sulfur-32	β-	14.3 days	338 TBq/mmol	Tumor detection, DMPK studies
Sulfur-35	Chloride-35	β-	87.4 days	55.4 TBq/mmol	Receptor binding
Iodine-125	Tellurium-125	EC	60 days	80.5 TBq/mmol	Receptor binding
Short-lived radionuclides					
Carbon-11	Boron-11	β+	20.8 min	341 TBq/µmol	PET radiotracer
Nitrogen-13	Carbon-13	β+	9.97 min	696 TBq/µmol	PET radiotracer
Oxygen-15	Nitrogen-15	β+	122.2 s	3426 TBq/µmol	PET radiotracer
Fluorine-18	Oxygen-18	β+	110 min	63 TBq/µmol	PET radiotracer
Galium-68	Zinc-68	β+/EC	67.7 min	101.8 TBq/µmol	PET radiotracer
Iodine-124	Tellurium-124	β+/EC	4.2 days	1.15 TBq/µmol	PET radiotracer

Data for PET radiotracers obtained from Weissleder et al.[23]

In the early drug discovery long-lived radiolabeled molecules are used in pharmacological studies (*in vitro* and *ex vivo*), such as binding site characterization and receptor binding/occupancy. In a more evolved phase of the drug discovery, the use of radiolabeled drug candidates is more focused on *in vitro* and *in vivo* preclinical to clinical ADME investigations. The distinctive feature of radionuclides is that the released radiation is independent of the structure, therefore an accurate quantification of the parent compound and metabolites can be achieved without an internal standard; however, it is important for the radionuclide to be in the metabolite.[11]

Radioligands for Lead Discovery

Radioligand binding assays have become an universal tool to characterize receptor, identify novel chemical structures that interact with the target receptor, and define ligand activity and selectivity in normal and diseased tissue.[9] Agonists or antagonist with a good affinity for the target receptor are labeled with radionuclides, often H-3, S-35 and I-125, which enables quantification of even very low concentration of target-radioligand complexes. Binding studies can be divided into three categories: kinetic, saturation studies and competitive binding experiments. Kinetic studies can provide valuable information about the time required to reach equilibrium between the unbound target and target-radioligand complex, this time data can be used for the saturation binding studies. Saturation binding studies determine the binding affinity of that ligand along with target concentration. This study is performed by increasing concentration of radioligand with a constant concentration of target at a specified time. Last but not the least are the competition experiments, this method is used to determine the affinity of new/unknown compounds. It is important to note that this is an indirect approach to determine the affinity of these new/unknown compounds, as we are looking into competition between the radioligand and the new/unknown compound. For this study it is a prerequisite to have the information from both the kinetic and saturation binding study for the radioligand.[24]

Photoaffinity labeling is a technique to study protein-ligand interactions and provides information about unknown molecular targets, off-target interactions, and structural elucidation of binding sites. Photoaffinity ligands used for these investigations usually have a ligand with an affinity for the target, a covalent binder upon light activation and a reporter tag for detection. This reporter tag can be a radiolabel (often H-3 and I-125), fluorescent dye

or partner for specific binding event (i.e. biotin). In contrast to the other reporter tags, radiolabeling with H-3 causes minimal change to the structure and still allows ease of detection with high sensitivity.[25]

Administration, Distribution, Metabolism and Excretion

ADME (and toxicology) studies start early in the drug discovery process. The pharmacokinetic studies (absorption, bioavailability, dose proportionality and kinetic parameters) are performed on rodents (mice, rats) and non-rodents (dogs or monkey), depending on the metabolic similarities between animal models and humans. While many drugs are ideally delivered orally, often intravenous studies are carried out to gain an understanding of the absolute bioavailability, clearance and volume of distribution of molecule to better understand the oral kinetics.[26]

Tissue distribution studies provide the valuable information about the distribution and pharmacokinetics of the parent drug and its metabolites in animal tissues and organs. These studies are performed using a radiotracer. The traditional method, tissue excision-Liquid Scintillation Counting (LSC), involves excision of the tissue followed by homogenization which provides whole organ concentrations; however, the results are dependent on the skills of the technician.[27] This traditional method has been replaced by quantitative whole-body autoradiography (QWBA), which is a well-known imaging method using a radiotracer to establish the whole-body tissue distribution of radioactivity. QWBA has numerous advantages as it provides a whole-body picture which can be easily visualized by radioactivity and provides clear picture of the distribution as well as the concentration of the radioactivity in major organs. QWBA also gives information about drug accumulation in potentially

toxicological or pharmacological sites of actions. These studies are typically performed on small rodents (< 5 kg) such as rats and mouse, but occasionally also on rabbits. Full distribution are primarily performed on male rodents; females and pregnant females are also used to compare any differences in radioactivity distribution (Figure 7).[22,26,28]

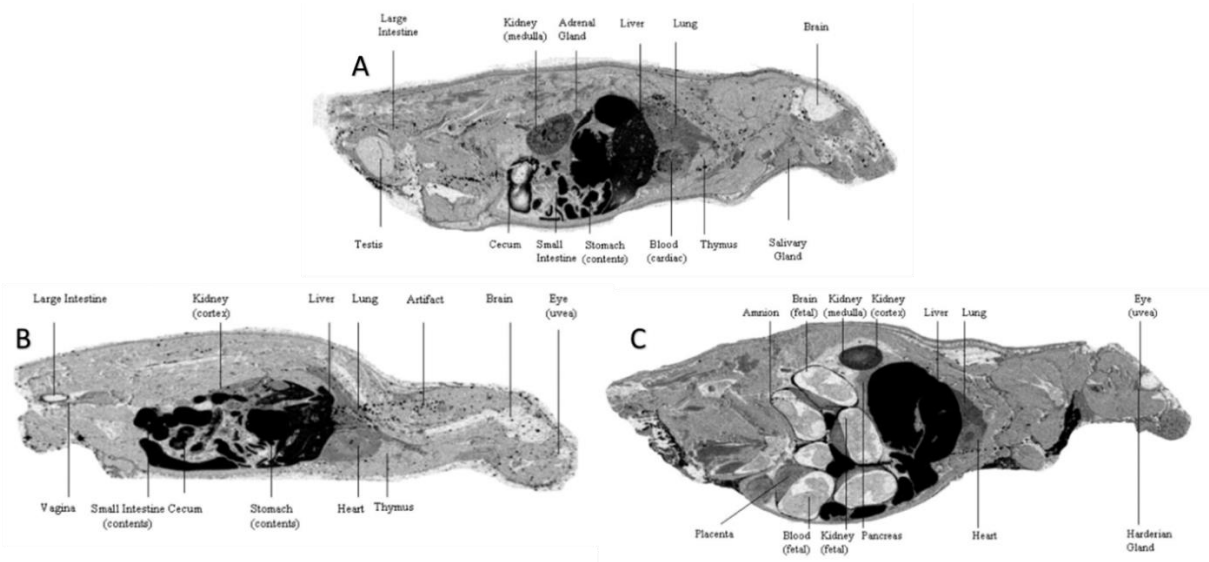

*Figure 7 – Examples of QWBA images with [^{14}C]Apixaban (5 mg/kg), radioactive distribution at 1 h after a single oral dose **A** male rat. **B** in female rat. **C** pregnant rat. Darker color shows higher concentration of the radioactive material. Image was reprinted from Wang et al.[29]*

The animal is then sliced into thin slices (40 µm) and exposed to photographic emulsions or phosphoimaging devices for localization and quantification of radiolabeled material in selected tissues. Long-lived radionuclides are the choice for the radiotracer as they provide good resolution. C-14 and H-3 have a long half-life time and are the most often used radionuclides for QWBA. C-14 labeled drugs are preferred over H-3 labelled drugs as less exposure time is needed for the final imaging and less β-emissions are absorbed by the tissues.[22,28] Direct imagers such as the Biospace Beta imager provides real-time imaging and higher resolution; however, this may still take overnight as only a few sections can be measured at a time.[30]

Typically, drugs undergo a biotransformation to metabolites in the body before they are excreted *via* the urine and feces. During the drug discovery campaign, the compounds are optimized for their metabolic properties with desired pharmacokinetic properties. It is important to determine the rates and routes of metabolism, to understand the effect of the metabolites on the body. Numerous *in vitro* and *in vivo* studies are performed and provide information about drug-drug interaction, the enzymes responsible for the metabolism, and potential effects of reactive metabolites are identified.[26]

Clinical Trials

Drug discovery is a costly and time-consuming process, with high failure rates late into the clinical trials. Therefore, new tools and strategies are continuously developed to improve the development new drugs. Phase 0 trial (Exploratory Investigational New Drug Studies) is a strategy to evaluate drugs by microdosing with radioligands at very low concentration in humans before going in the clinical trials. Critical human pharmacokinetic and pharmacodynamic data can be obtained from this trial. Based on the data obtained from Phase 0 combined with the preclinical data from the animals can aid in a better design and development of the subsequent trials. Results from Phase 0 can also highlight undesirable pharmacokinetic and pharmacodynamic properties before initiation of the more expensive clinical trials.[5,6,31]

However, till date Phase 0 is not a requirement; therefore, many drugs are often immediately submitted to Phase I clinical trials. Radiolabeled drugs are ubiquitous for human ADME studies during Phase I and Phase II trials and are often performed in a small group of healthy volunteers. Radiolabeled drug along with the parent compound are administered to the

establish the rates and routes of excretion of the parent compound and its metabolites. Although C-14 labeled drugs are more frequently used, because the label is incorporated in a more metabolically stable position; however, H-3 can be used as well.[22,32,33]

Considerations in Radiochemistry

The synthesis of compounds containing radionuclides can often be closely mirrored to non-radiolabeled synthesis. However, there are key considerations to be made for the incorporation of radionuclides and it might be necessary to alter the chemistry from the already developed routes.[11,32]

1. Purpose of the radioligand.

   The purpose of the radioligand in an assay will dictate which radionuclide, the specific activity and location of the radionuclide should be chosen.

2. Type of molecule to be labeled.

   Whether a small molecule is used or a biological, this may limit the choice of radionuclide as well as the chemistry that can be used for the labeling.

3. Choice of labeling position.

   The position of the nuclides can be of great importance depending on the study. It may be important to identify the metabolic position.

4. Existing strategies for labeling.

   Ideally the radionuclide is incorporated in a late stage, to reduce generation of expensive-to-dispose-of waste and less handling of radioactive material by the radiochemist. If the preparative method for labeling has not been well-

established, then it may be wise to develop the methodology on the non-radioactive nuclide.

Efforts have been made to develop fast and convenient late-stage methods that introduce the desired nuclide through an exchange method on the drug molecule. Hydrogen isotope exchange (HIE) has been extensively studied[9] and recently carbon isotope exchange is also gaining attention[34].

5. Available labeled starting material.

   Synthesis of a radioligand will heavily depend on the availability of suitable precursors.

6. Radiochemical purity requirements.

   The final purity requirement for radiolabeled compounds are generally higher due to the low detection limits of radioactivity.

1.2. Carbon-14

C-14 is a rare carbon radionuclide that occurs in 10^{-12} g per gram of carbon. Interestingly the occurrence of C-14 was unknown, until it was prepared in the laboratory by Samuel Ruben and Martin D. Kamen in 1940s.[35,36] Although the level of C-14 is almost negligible, yet it is enough to be a golden standard for determining the age of carbonaceous materials. C-14 is a β^--particle emitter with a half-life of 5730 years and decays into stable nitrogen.[36] The most common applications of C-14 labeled compounds in drug discovery are ADME studies, metabolic studies, QWBA, cross-species comparison and environmental fate studies.[22]

C-14 is produced on a commercial scale in a nuclear reactor by neutron bombardment of solid beryllium nitride, solid aluminum nitride, solid calcium nitrate or a saturated solution of ammonium nitrate, for a period of 1 to 3 years (Figure 8). C-14 is isolated by dissolving the target in H_2SO_4; the gasses that evolve from this process are hydrogen, [^{14}C]methane and $^{14}CO_2$. $^{14}CO_2$ is trapped in a $NaOH_{(aq)}$ scrubber. The remaining gasses are passed over a suitable oxidation catalyst to afford $^{14}CO_2$. This is absorbed by an aqueous solution of BaOH and is stored as $Ba^{14}CO_3$. $Ba^{14}CO_3$ is obtained with a C-14 content of 85-90%, equivalent to specific activity (SA) of 1.85-2.072 TBq/mol. $Ba^{14}CO_3$ with higher SA (up to 2.294 TBq/mol) can be obtained, but that is more expensive.

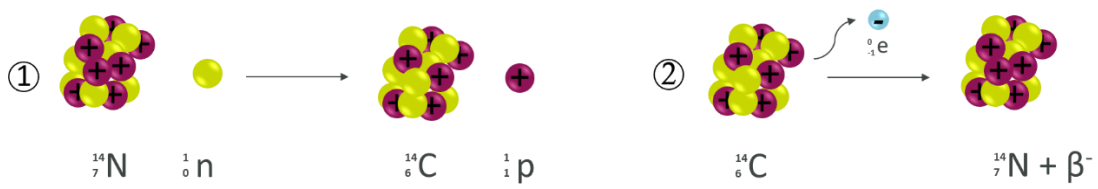

*Figure 8 – **1** Formation of carbon-14 and **2** decay of carbon-14. Plum: proton, Green: neutron, Blue: electron.*

Carbon-11 is another radionuclide of carbon that is frequently used for clinical purposes. This radionuclide can be obtained as $^{11}CO_2$ or $^{11}CH_4$ from the cyclotron; however, this radioisotope has a very short half-life (Table 1), due to which the starting material needs to be synthesized on demand and converted rapidly in the desired radioligand. Moreover, the amount of C-11 containing starting material obtained from the cyclotron is extremely limited, thus the other reagents used in the reaction are always used in a large excess.

1.2.1. C-14 Building Blocks

$Ba^{14}CO_3$ is a stable source of C-14 and serves as the precursor for four key building blocks metal [^{14}C]cyanide, [$^{14}C_2$]acetylene, [^{14}C]cyanamide and [^{14}C]carbon dioxide (Scheme 1).

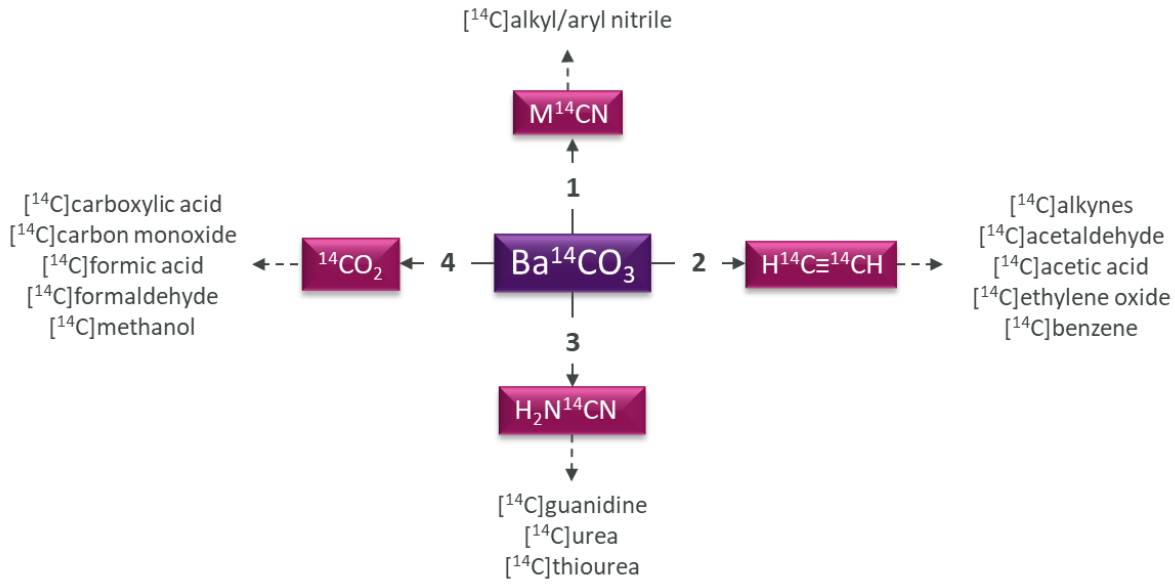

*Scheme 1 – **1** KN_3, sea sand, 350 – 700 °C or **a** H_2, Ni, 350 °C; **b** NH_3, Pt, 1150 °C; **c** aq. $KOH_{(aq)}$ or MeOH (~100 °C). **2a** Ba, heat to fuse; **b** H_2O. **3a** NH_3 (stream), 850 °C, **b** H_2SO_4. **4** H_2SO_4; r.t. or $PbCl_2$; heat. Adapted from Voges et al.*[37]

[^{14}C]Cyanide

A very versatile reagent in C-14 synthesis are metal [^{14}C]cyanides (M = Na, K, Zn, Cu) (Scheme 1, **1**). As M^{14}CN are salts (solids), they are easier to manipulate in comparison to other gaseous C-14 sources ($^{14}CO_2$ and ^{14}CO). While these solids are easier to handle, many M^{14}CN are hygroscopic and all are toxic; therefore, care must be taken when handling these. The reactivity of M^{14}CN can be tuned by changing the metal counterion, solvent, or tuning the leaving group it replaces. Finally, the obtained organic [^{14}C]nitrile can be subjected to an array of transformations to obtain a wide array of C-14 labeled compounds.[38,39]

M^{14}CN can be obtained in a convenient and safe method on a 1 to 10 mmol scale through a reduction of Ba$^{14}CO_3$ as summarized in Scheme 1. The most commonly used salt is K^{14}CN and can be prepared on a scale of 1 to 10 mmol by reducing Ba$^{14}CO_3$ with KN_3 at elevated temperature (450 to 700 °C). Na^{14}CN can be prepared in a comparable manner. Other commonly used M^{14}CN are Cu^{14}CN and Zn(^{14}CN)$_2$. Cu^{14}CN can be prepared by treatment of K^{14}CN with an excess of $CuSO_4 \cdot 5H_2O$ in presence of hydrogen sulfite at 20-60 °C. When K^{14}CN is treated with $ZnCl_2$, Zn(^{14}CN)$_2$ is isolated as a white solid.[38,39]

Matloubi *et al*[40] and Sunay *et al*[41] both published the synthesis of [^{14}C]clozapine using Cu^{14}CN (Scheme 2). The labeling reagent is then used in the synthesis of [^{14}C]2-amino-benzonitrile and in three additional steps [^{14}C]clozapine is synthesized with an overall radiochemical yield of 30%. Efforts have been made to improve upon the chemistry, in respect to late-stage introduction of the radioactive label, this will be discussed in a later in this thesis.

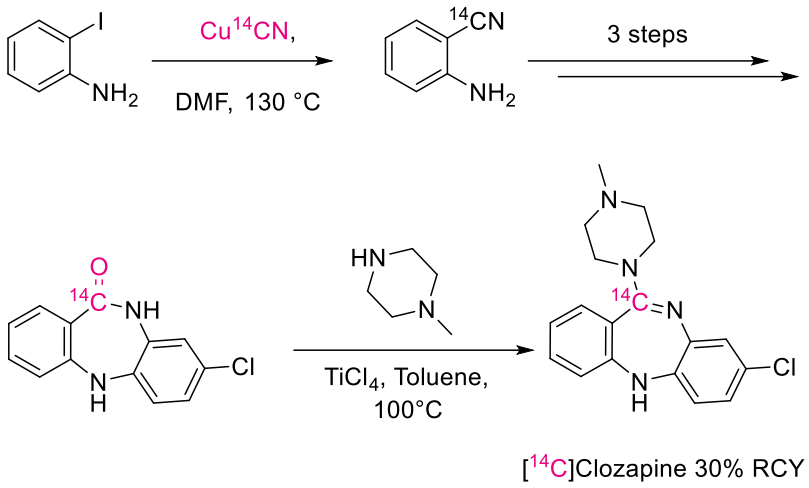

Scheme 2 – [^{14}C]Cyanation of Clozapine as presented by Sunay et al.[41]

New strategies have been developed to introduce the C-14 cyanation reagent in a later stage *via* a disconnection-reconnection approach. While HIE is a well-established field, carbon isotope change is challenging and is gaining more interest recently. Loreau *et al*[42] developed a palladium-catalyzed decarboxylative cyanation method using K^{14}CN as presented in Scheme 3. In two-steps C-14 labeled carboxylic acid is obtained with an overall yield of 54%.

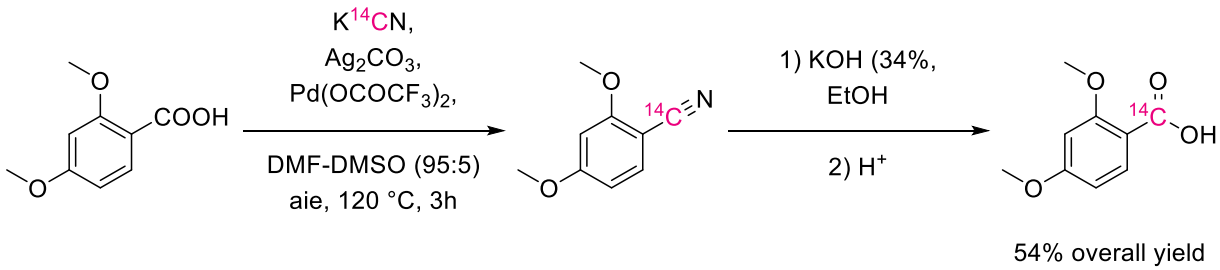

Scheme 3 – Carbon-isotope exchange [^{12}C]-[^{14}C] strategy in a two-step approach.

[^{14}C]Acetylene

[$^{14}C_2$]Acetylenes can be prepared in high yields from Ba$^{14}CO_3$. [$^{14}C_2$]Acetylene is a key reagent for the production [$^{14}C_6$]benzene and an array [$^{14}C_n$]aromatic derivatives (Scheme 1, **2**).

Heating a mixture of $Ba^{14}CO_3$ with Ba shavings under an atmosphere of He or H_2 produce exothermic formation of $Ba^{14}C_2$, and hydrolysis releases [$^{14}C_2$]acetylene. This method is useful on a scale of 1 to 20 mmol; however, on larger scale it is better to synthesize [$^{14}C_2$]acetylene *via* the reduction of $^{14}CO_2$ with molten lithium, followed by hydrolysis.[43]

Elmore *et al*[44] synthesized triphenylsilyl[$^{14}C_2$]acetylene for the use in Sonogashira reaction (Scheme 4). The synthesis was started with $Ca^{14}C_2$ was synthesized by passing [$^{14}C_2$]acetylene gas over a $CaCO_3$ column, followed by a K_2CO_3 column. To $Ca^{14}C_2$, a solution of ethyl magnesium bromide was added, followed by a solution of triphenylsilyl chloride, to give the triphenylsilyl[$^{14}C_2$]acetylene in 65% yield. While the yield was moderate, some difficulties were faced in the next step. The cumbersome purification made the Sonogashira reaction be more challenging. The issue was resolved by purifying triphenylsilyl[$^{14}C_2$]acetylene with prep-HPLC instead of silica purification. Moreover, homocoupling was also observed and by exchanging the atmosphere from argon to H_2, the yield was improved. Unfortunately, the yield of the reaction was still highly variable, from 15 to 75%; therefore, they chose to perform the Sonogashira reaction in smaller batches.

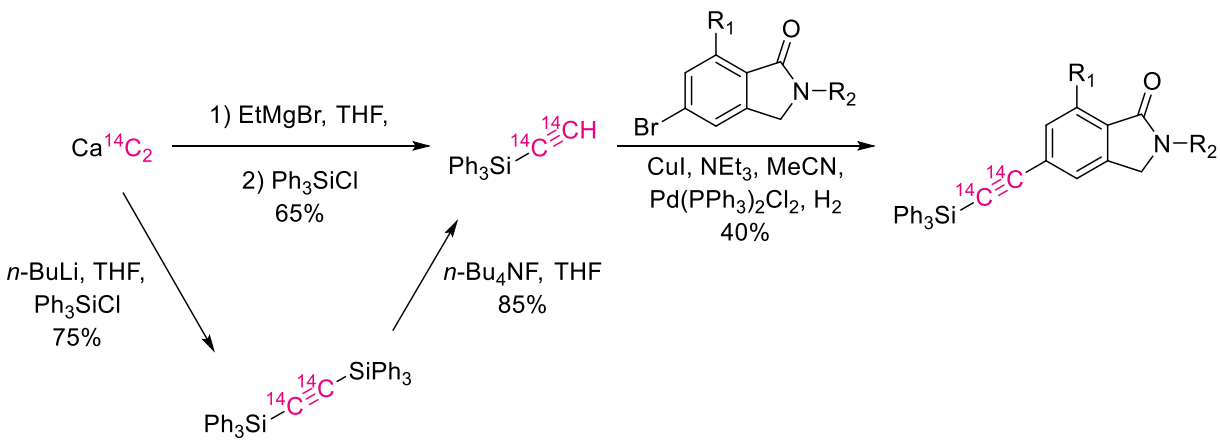

Scheme 4 – Use of [^{14}C]acetylene for Sonogashira coupling.

[^{14}C]Cyanamide

Reaction of $Ba^{14}CO_3$ with gaseous ammonia at 850 °C followed by hydrolysis results in [^{14}C]cyanamide (Scheme 1, **3**).[45] Its Ba-salt, $BaN^{14}CN$, canbe used to synthesize useful C-14 building blocks, [^{14}C]guanidine, [^{14}C]urea and [^{14}C]thiourea. [^{14}C]Cyanamide itself is a useful building block. Murthy *et al*[46] used $H_2N^{14}CN$ to successfully incorporate a C-14 label on position of a pyrimidine ring as shown in Scheme 5.

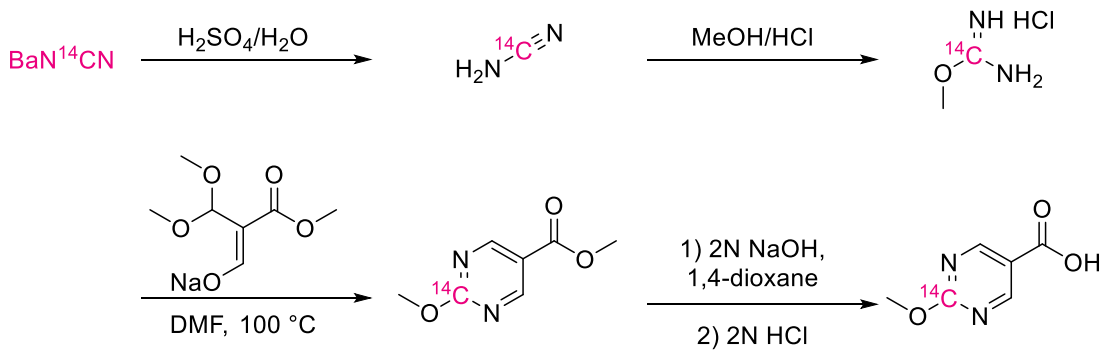

Scheme 5 – Synthesis of C-14 labeled pyrimidine using [^{14}C]cyanamide.

[^{14}C]Carbon Dioxide

$^{14}CO_2$ is a fundamental, one carbon synthon, which can be obtained from $Ba^{14}CO_3$ by reacting it with concentrated sulfuric acid[47] or $PbCl_2$[48] (Scheme 1, **4**). The later produces radioactive heavy metal waste; therefore, this method is usually avoided. Upon liberation of $^{14}CO_2$, it can be absorbed in a trap containing molecular sieves and stored at room temperature. Upon heating, $^{14}CO_2$ is released from the molecular sieves. The molecular sieve bed can be attached to a stainless-steel manifold (Figure 9) in order to facilitate the handling of $^{14}CO_2$.[49]

Figure 9 – Stainless steel manifold by RC Tritec, allowing safe working environment with radioactive gasses (and nonradioactive analogues of the gasses). Image reprinted with permission from www.rctritec.com

Carboxylation of $^{14}CO_2$ has long been known and is frequently used for incorporating C-14 into molecules. This is mainly due to the low cost of $^{14}CO_2$ in comparison to other C-14 labeled material. Coupling with organomagnesium or organolithium reagent is the traditional methods, but these methods require harsh conditions and have poor functional group tolerance; therefore, an early installation of C-14 is required as shown in Scheme 6. Hesk *et al*[50] recently published the synthesis of a potent and selective Adenosine A_{2a} antagonist. Furan-2-yllithium was carboxylated with $^{14}CO_2$. The resulting acid was converted in to the desired compound in 2 additional steps with 22% overall yield from $Ba^{14}CO_3$.

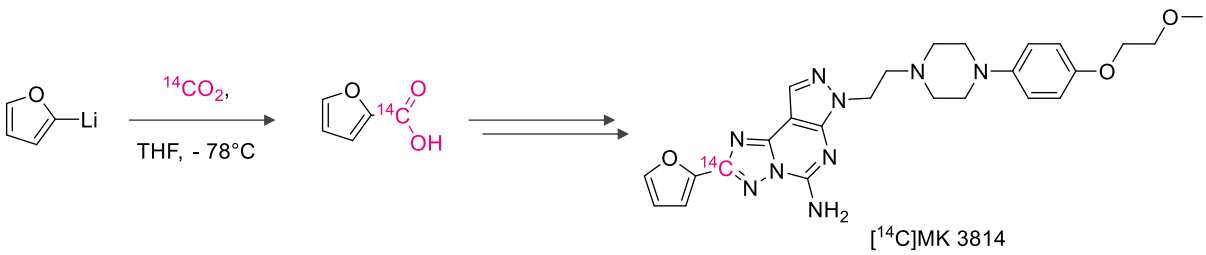

Scheme 6 – Carboxylation of furan-2-yllithium en route to [^{14}C]MK 3814.

When poor functional group tolerance prevents the use of Grignard or lithium reagents; cyanodehalogenation with $M^{14}CN$ is usually the preferred choice as presented by Latli *et al*[51] for the synthesis of C-C chemokine receptor 1 antagonists in Scheme 7. The arylbromide was subjected to the cyanation reaction using [^{14}C]zinc cyanide, followed by a hydrolysis with 87% overall yield. While the carboxylation with the turbo-Grignard conditions (*i*PrMgCl and LiCl) provided a poor yield in comparison. The [^{14}C]carboxylic acid was used in an amide coupling to provide the target compounds.

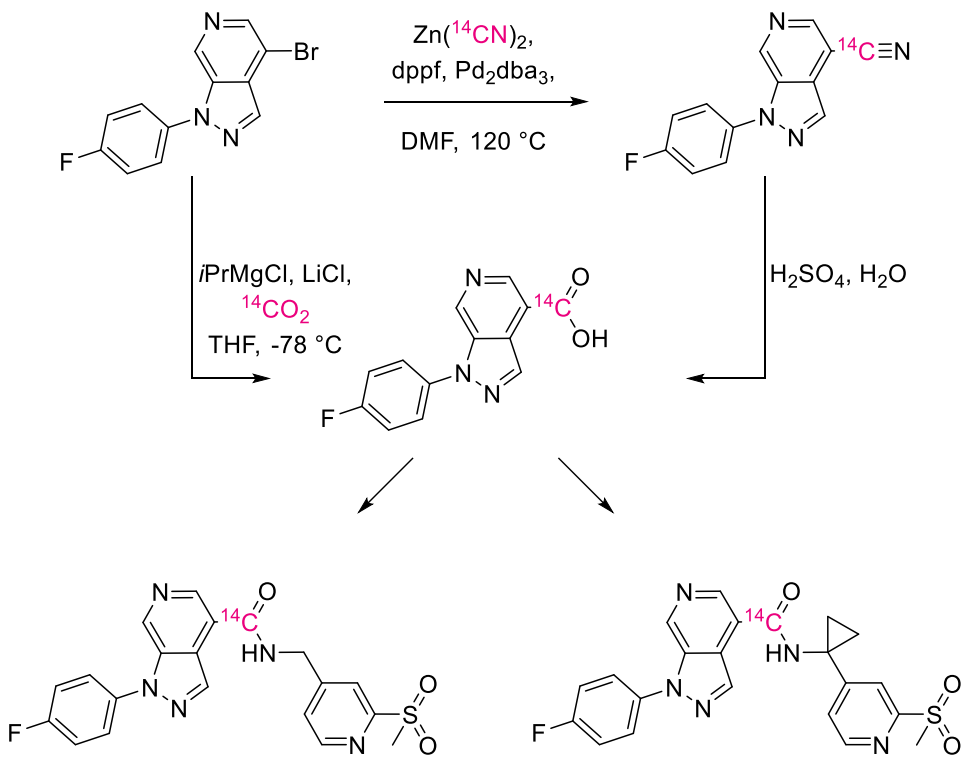

Scheme 7 – A comparison of [^{14}C]cyanation and [^{14}C]carboxylation to achieve C-14 labeled amide in CCR1 antagonists.

McGhee *et al*[52] sought to replace the use of phosgene with CO_2, which would eliminate the issues when using phosgene, such as high commercial price, inconvenient preparation and limited radiochemical stability. Dean *et al*[53] effectively applied this for the synthesis of m-tolyl

[^{14}C]isocyanate with 80% yield, which is a key intermediate for the synthesis of CCK_B antagonist, L-740,093 (Scheme 8).

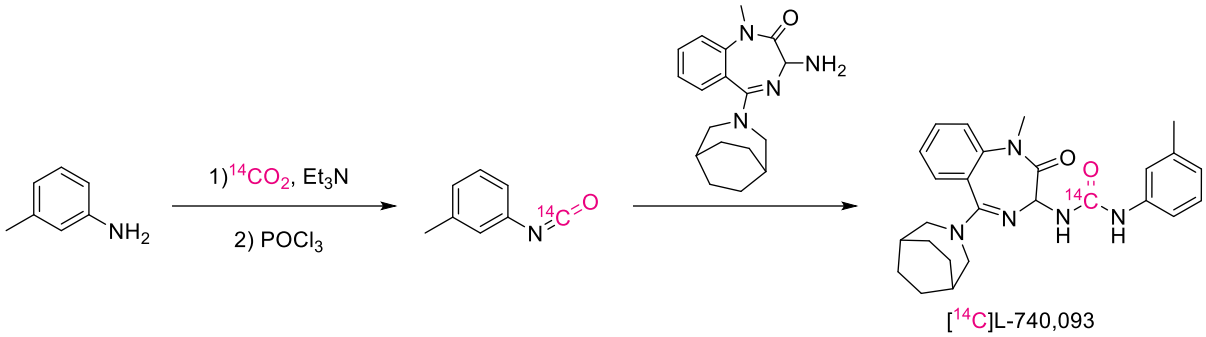

Scheme 8 – Using $^{14}CO_2$ as an alternative for [^{14}C]phosgene.

Last-stage carboxylations developed within ISOTOPICS

Del Vecchio *et al*[54] also pursued the replacement of [^{14}C]phosgene (and/or [^{14}C]urea) to label cyclic ureas. They established a click-chemistry-like protocol to incorporate $^{14}CO_2$ in cyclic ureas as shown in Scheme 9. Herein they reported using $^{14}CO_2$ directly in a sequential Staudinger/aza-Witting reaction with a high functional group tolerance. Ureas are a commonly used functional group found in various pharmaceutical compounds. The short reaction time of only 5 minutes allowed this method to be implemented with $^{11}CO_2$.

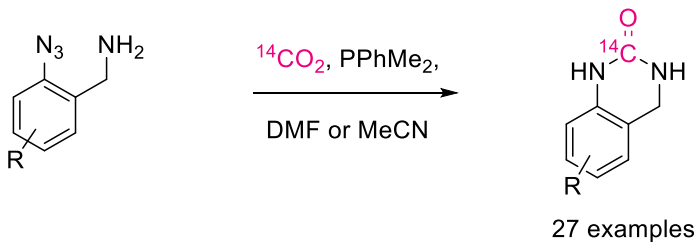

Scheme 9 – Late-stage labeling for the synthesis of [^{14}C]cyclic ureas.

Destro *et al*[55] were inspired by the HIE methods which allows a radionuclide to be introduced on previously synthesized drug in a single step (Scheme 10). This methodology was developed

to allow dynamic carbon isotope exchange, using the same principle; utilizing the desired drug molecule as the starting material without the need of any structural modification. Herein, carboxylate cesium salts were used for this exchange, using cheap copper catalyst in the presence of 3 equiv $^{14}CO_2$. The reaction is currently limited to aromatic substrates; moreover, it suffers from isotopic dilution. A major byproduct formed in the reaction is unlabeled CO_2, which can react like $^{14}CO_2$, providing a maximum of 75% isotopic enrichment.

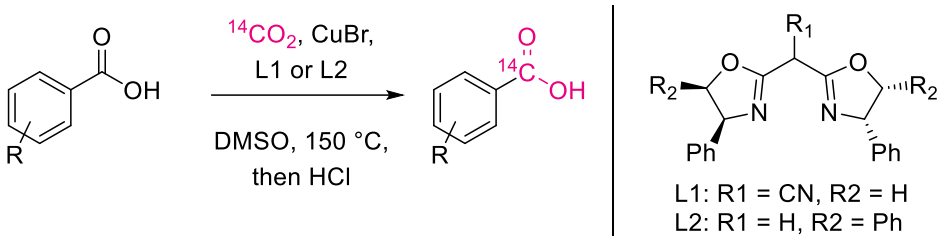

Scheme 10 – Carbon isotope exchange.

1.3. Carbonylation in Carbon Isotope Chemistry

Carbonylation reactions with carbon monoxide (CO) were first identified in 19th century.[56] Since the first reports of palladium catalyzed carbonylation, the substrate scope has expanded considerably.[57] CO can be introduced into complex molecules by adding a single carbon unit as a carbonyl group, which is prevalent in many bioactive compounds. The initial Heck carbonylation disclosed a three-component reaction, involving an electrophile, nucleophile and carbon monoxide, and was catalyzed by palladium.[58–61] Aryl, alkenyl and benzyl halides have been well documented as the electrophile constituent. In contrast, alkyl halides often encounter difficulties, due to slow oxidative addition step of the metal center. β-Hydride elimination can be an important step in many transition-metal catalyzed reaction, but it can be a major side reaction too, which is encountered when alkyl halides[62,63] are used as the coupling partner, this is depicted in Scheme 11.[64] The nucleophilic component of the carbonylation reaction can be an amine, alcohol, thiol or phosphine.[65]

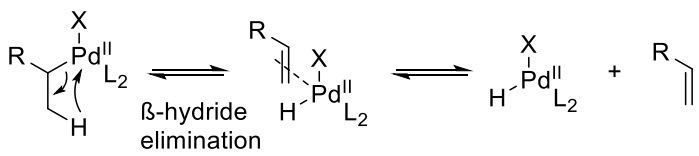

Scheme 11 – β-hydride elimination that leads to the formation of alkenes.

Palladium-Catalyzed Carbonylation – Catalytic Cycle

The general palladium catalyzed carbonylation for aryl halide can be depicted in a catalytic cycle as shown in (Scheme 12). The catalytic cycle is initiated with the oxidative addition of a 14-electron Pd(0) species across to an aryl-halide (Ar-X) bond. CO coordinates to the Pd(II) complex, followed by a 1,1-insertion of CO onto the Ar-Pd(II) bond, to give an acyl-Pd(II)

complex. The nucleophile attacks this acyl-Pd(II) complex; is immediately followed by a reductive elimination to give the carbonylated product. The base in the reaction scavenged the protons produced in the reaction which leads to the regeneration of the Pd(0) complex. If an organo-metallic reagent is used, a transmetalation occurs after the CO insertion, and the catalytic cycle is closed with a reductive elimination that gives the carbonylated product along with regeneration of the Pd(0) catalyst.[64]

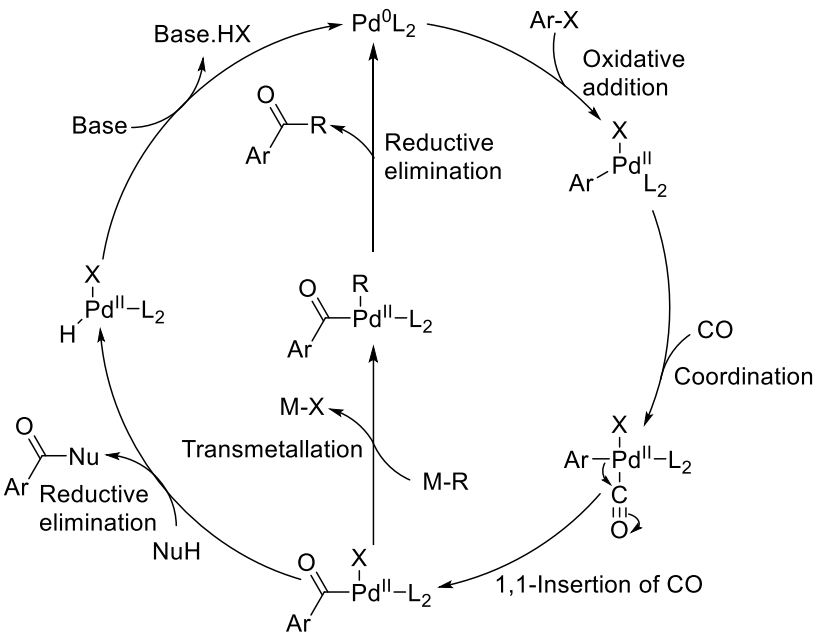

Scheme 12 – A catalytic cycle of palladium(0)-catalyzed carbonylation with either heteroatom (NuH) or an organometallic reagent (M-R).

1.3.1. General methods for Carbonylation using [^{14}C]Carbon Monoxide

Transition metal-catalyzed carbonylation reactions are already a powerful tool for incorporating labeled CO into advanced molecules, due to the high functional group tolerance of the method. However, the method is mostly limited to aryl, vinyl and benzyl (pseudo)-halides for late-stage labeling; there are a few examples of the carbonylation of alkyl halides

with unlabeled CO or ^{11}CO.[65] Carbonylation reactions are of particular interest due to the availability of isotopically modified carbon monoxide (^{11}CO, ^{13}CO and ^{14}CO).[65]

CO is inexpensive and readily available; on the contrary, ^{14}CO is very expensive and has a short shelf life, due to radiolytic decomposition[66]. Therefore, most procedures rely on *in situ* or *ex situ* generation of the labeled gas. In the late 1940s, three routes for the preparation of ^{14}CO were described (Scheme 13). Method **A** required heating of $Ca^{14}CO_3$ with zinc dust at 700 °C to give quantitative conversion to ^{14}CO.[67] A related method **B** $^{14}CO_2$ reduced over a zinc dust at 400 °C.[68] Both methods required very high temperature for reduction and specialized apparatus. While the zinc dust method is a frequently used method for producing ^{14}CO, the method is of great value for reduction of $^{11}CO_2$ to ^{11}CO.[69] The third method **C** is more laboratory-friendly as it involves dehydration of [^{14}C]formic acid prepared *in situ* from $^{14}CO_2$.[70]

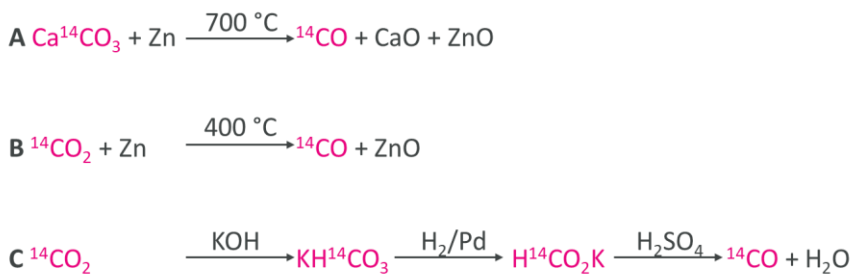

Scheme 13 – Classical methods to synthesize ^{14}CO on demand.

[^{14}C]Calcium Carbonate Pyrolysis

Jagadish and co-workers[71] applied the pyrolysis technique of $Ca^{14}CO_3$ on the synthesis of [^{14}C]imexon (Scheme 14). $Ca^{14}CO_3$ was prepared by absorption of $^{14}CO_2$ into $CaCl_{2(aq)}$. ^{14}CO was liberated by the pyrolysis of a mixture of $Ca^{14}CO_3$ and zinc powder in a ratio of 1:2 at 700 °C for 30 min to give ^{14}CO. A photolysis of ^{14}CO with slight excess of chlorine gas over 8h gives [^{14}C]phosgene with an overall yield of 85% over two-steps. While [^{14}C]phosgene can be

obtained with good yields; unfortunately, high heat and specialized equipment are a necessity for this method.

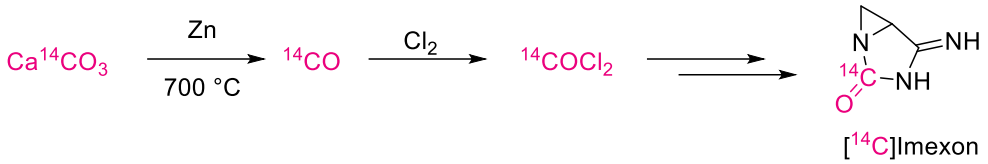

Scheme 14 – Pyrolysis of $Ca^{14}CO_3$ to synthesize [^{14}C]phosgene via ^{14}CO, for the synthesis of [^{14}C]imexon.

[^{14}C]Formate based [^{14}C]carbonylation chemistry

Elmore and co-workers[72] simplified the formic acid method by using a three-necked round bottom flask connected to the vacuum manifold, a septum with a needle and a round bottom flask with a 90° bent adapter. *Ex situ* generation of ^{14}CO was realized by heating [^{14}C]lithium formate with sulfuric acid. The formed ^{14}CO is then allowed to pass passively to the connected round bottom flask to undergo a palladium-catalyzed carbonylation. This procedure was applied on the synthesis of non-peptidyl GnRH receptor antagonists. The [^{14}C]carboxylic acid intermediate was isolated and subjected to an amide coupling (Scheme 15).[73]

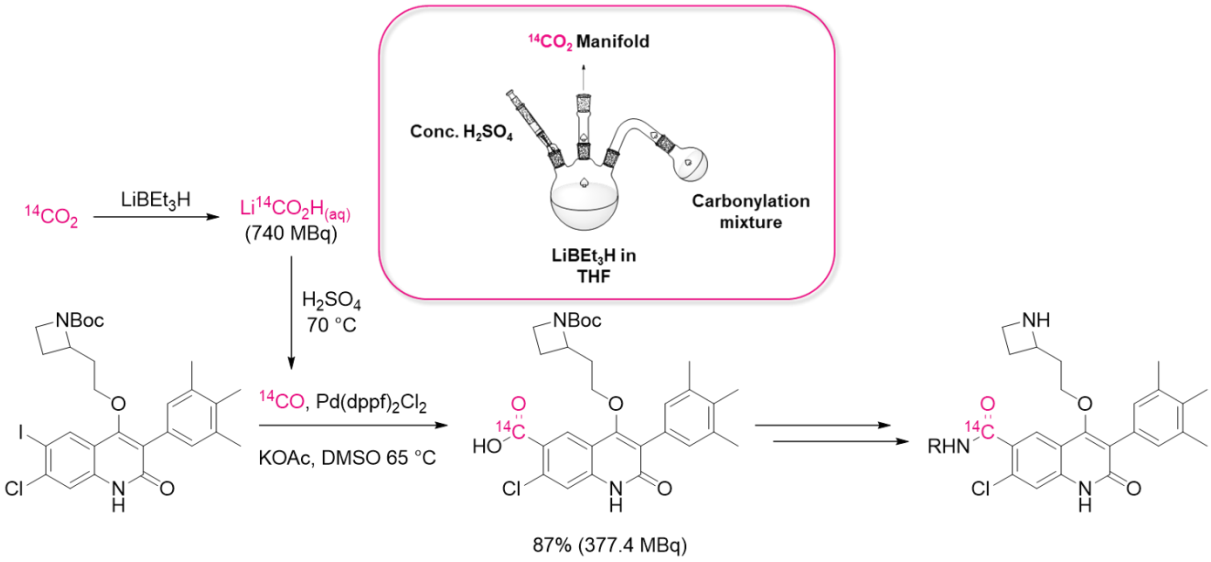

Scheme 15 – Carbonylation via dehydration of $^{14}CO_2H$ by sulfuric acid for synthesis of GnRH receptor antagonists.

An *in situ* [^{14}C]hydroxycarbonylation method was developed by Simeone *et al*[74] for a [^{14}C]-labeled Maxi-K channel blocker (Scheme 16). It is common to use a two-flask system, to liberate the ^{14}CO into a separate flask from the [^{14}C]carbonylation reaction. Simeone *et al* sought to use an operationally simpler setup to prepare [^{14}C]aryl carboxylic acids. For their procedure they liberated ^{14}CO by dehydrating [^{14}C]sodium formate with acetic anhydride,[75] this method provided the radiolabeled intermediate with 32% radiochemical yield. In three additional steps the final product was obtained.

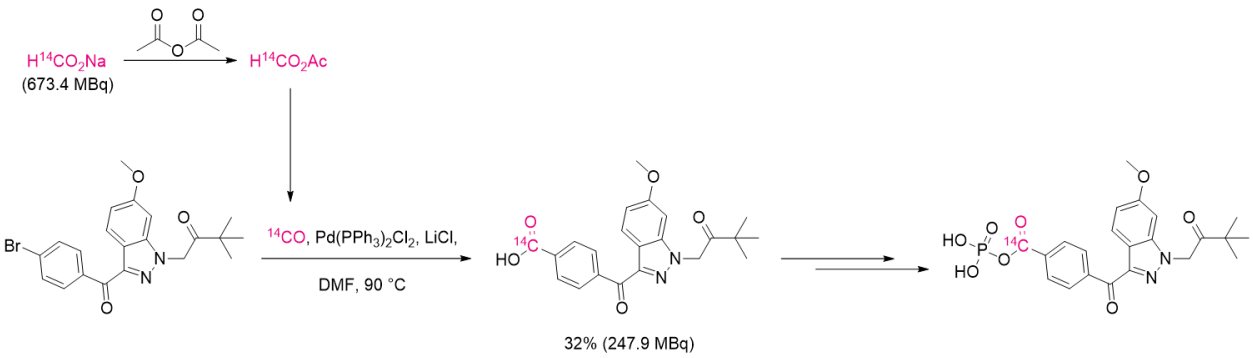

Scheme 16 – Hydroxycarbonylation via in situ ^{14}CO liberation as key step for synthesis of [^{14}C]-labeled Maxi-K channel blocker.

This one-pot approach was also being investigated by Latli *et al*[76] for a synthesis of a lymphocyte function-associated antigen-1 (Scheme 17), with potential treatment of inflammatory diseases. This method of introducing a C-14 label with this palladium-catalyzed [^{14}C]hydroxycarbonylation on the aryl amide position was quite suitable for the substrate as it contains two chlorine atoms and a nitrile. The [^{14}C]carboxylic acid was obtained in 35% radiochemical yield and of an amide bond formation completed the synthesis.

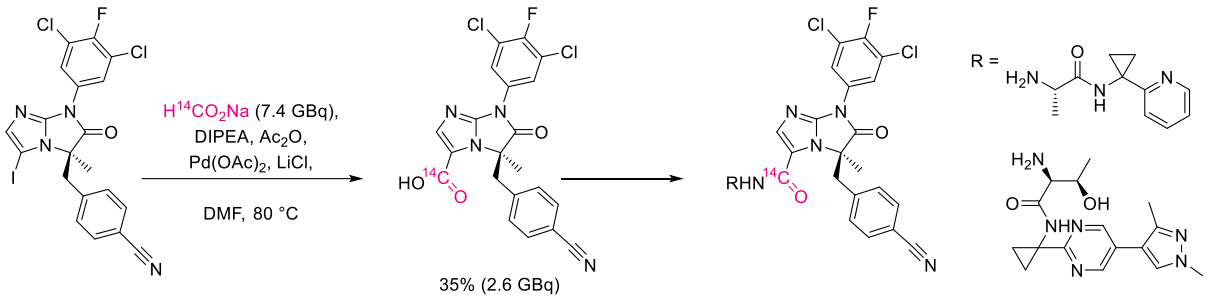

Scheme 17 – Hydroxycarbonylation using in situ generation of ^{14}CO for the synthesis of lymphocyte function-associated antigen-1 antagonists.

Elmore *et al*[77,78] used the previously discussed method for generation of ^{14}CO dehydration of $^{14}CO_2H$ by sulfuric acid. They chose to approach the labeling of C-14 labeled delta opioid antagonist *via* a carbonylative method, as this would allow the label to be incorporated in the last stage; moreover, the final labeled carbonyl group is also the obvious choice due to its metabolic stability. The same apparatus was used with the three necked flask connected to another round bottom flaks with an adaptor; however, *ex situ* generation of ^{14}CO was realized by heating [^{14}C]sodium formate with sulfuric acid (Scheme 18). The final product was obtained with 55.5 MBq (18% yield) of the desired delta opioid antagonist after preparative HPLC purification. While this may seem like a low yield, it is important to consider that the radionuclide was incorporated in the last step with ^{14}CO as the limiting reagent.

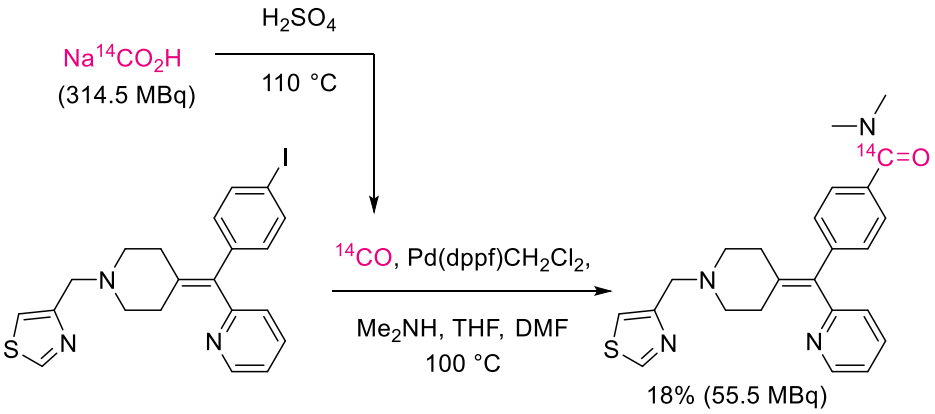

Scheme 18 – Carbonylation via dehydration of $^{14}CO_2H$ by sulfuric acid for synthesis of delta opioid antagonists.

Whitehead *et al*[79] reported a synthesis of [^{14}C]celivarone from ^{14}CO. Though, this method was not their first option; they only turned to ^{14}CO after failing to prepare the compound with routes using $^{14}CO_2$ and ^{14}CN, which gave poor yields or failed completely. To produce the ^{14}CO they drew inspiration from method reported by Villeneuve *et al*[80] and Roeda *et al*[81] for ^{14}CO, in which chlorophosphonium salt was used to convert [^{14}C]lithium formate to [^{14}C]formyl chloride, which is unstable at temperatures above -60 °C and liberates ^{14}CO. This approach was applied on the synthesis of the [^{14}C]celivarone with 53% yield with a single step of radiochemical handling (Scheme 19).

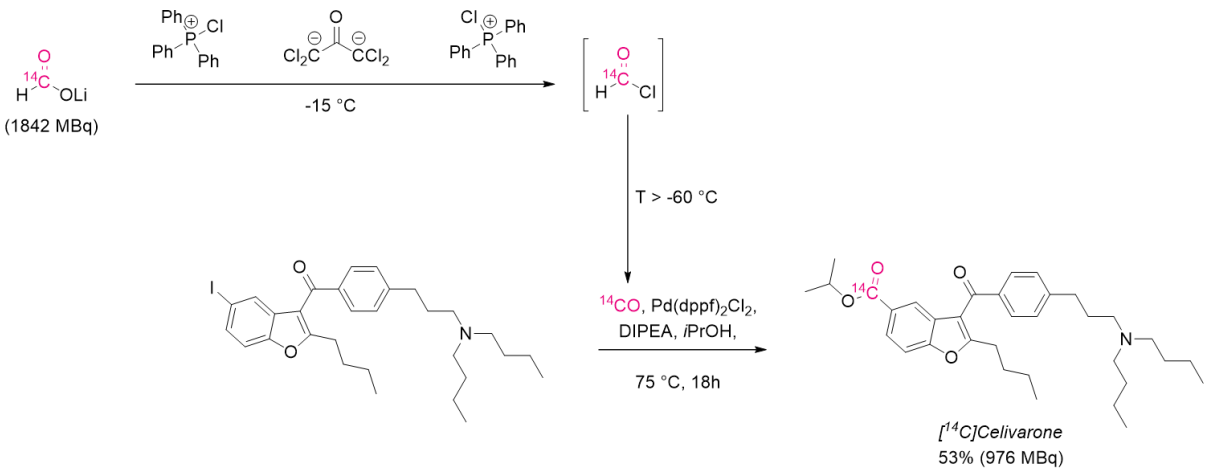

Scheme 19 – Carbonylation of [^{14}C]Celivarone via [^{14}C]Formyl Chloride.

Elmore *et al*[82] prepared a tricyclic ring systems containing C-14 in a late-stage fashion using ^{14}CO (Scheme 20). [^{14}C]Benzodiazepine, a precursor of [^{14}C]clozapine has previously been labeled *via* a [^{14}C]cyanation with 46% radiochemical yield (RCY) over 4 steps (Scheme 20).[40,41] While [^{14}C]cyanation reaction are mild, these cannot be achieve in the last step of a linear synthesis. This is due to the harsh conditions required to hydrolyze the [^{14}C]cyanide *via* hydrolyzation, reduction or other transformations, makes the overall procedure intolerant towards other functional groups. Therefore, efforts were made perform the last stage labeling

with ^{14}CO, although the [^{14}C]carbonylation method allowed late-stage labeling of [^{14}C]benzodiazepine, the method did not improve the overall yield, which is partly due to the cumbersome purification. On the other hand, the [^{14}C]carbonylation route provided access to C-14 labeled [^{14}C]benzodiazepine, [^{14}C]benzothiazepine, [^{14}C]benzoxazepine in a single step along with a reduction of radiochemical waste.

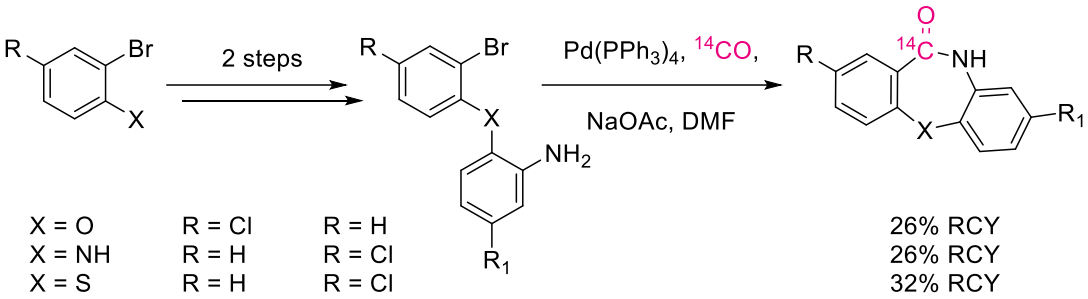

Scheme 20 – Carbonylation of [^{14}C]benzodiazepine, [^{14}C]benzothiazepine and [^{14}C]benzoxazepine.

^{14}COgen

While the [^{14}C]formate based methods are effective at preparing ^{14}CO, the method does have drawbacks. Furthermore, volatile gases remained on completion of the reaction. Typically, a large excess of sulfuric acid is used for the transformation, upon completion of the reaction contaminated concentrated sulfuric acid is left, which can be difficult and costly to dispose of. Lindhardt *et al*[83] sought to simplify the reaction method and to reduce the radioactive waste produced with the former method.

The group targeted the development of a carbon monoxide releasing molecule (CORM) (Scheme 21). In a preliminary study, pivaloyl chloride was investigated as a CORM, as it was commercially available, low cost, and has good atom economy. However, the low boiling point (105 °C) and liberation of isobutene gas leading to higher internal pressure caused

problems. Therefore, a bulkier acid chloride, 9-Methylfluorene-9-carbonyl chloride (COgen), was developed, which would produce a non-volatile byproduct, and allows incorporation of C-13 and C-14. The synthesis of COgen starts with the lithiation of 9-methyl-9*H*-fluorene, followed by a capture with CO_2 to produce the carboxylic acid. Oxalyl chloride and catalytic amount of DMF produce the imidoyl chloride which chlorinates the carboxylic acid intermediate to give COgen. The synthesis of unlabeled COgen is done with an excess of CO_2, high yield can be achieved with stoichiometric amounts of CO_2 and allows the use of C-13 and C-14 labeled CO_2.[84] Moreover, to allow safe and efficient handling of the generated CO, a new two-chamber glassware (COware) was produced.

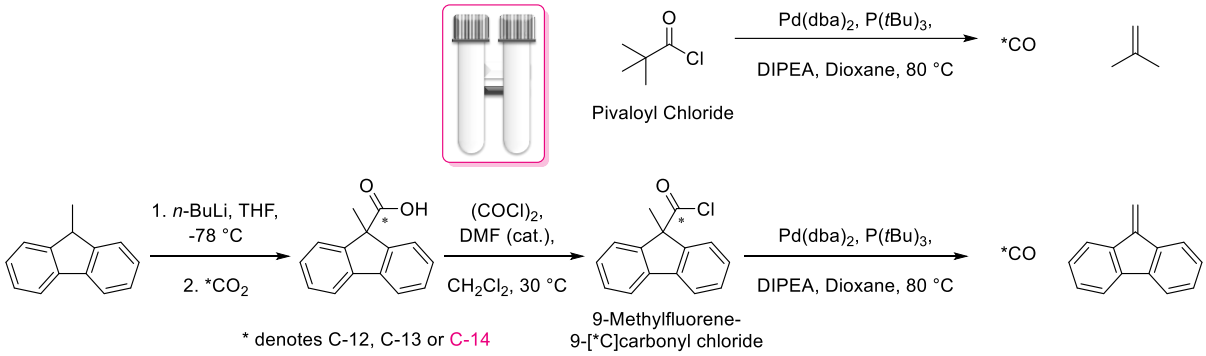

*Scheme 21 – Preparation of *COgen and liberation of *CO through a Palladium-catalyzed reaction.*

^{14}COgen has been used as the limiting reagent for aminocarbonylation, amidocarbonylation and carbonylative Suzuki-Miyaura couplings, to synthesize [^{14}C]thalidomide and [^{14}C]fenofibrate in good yields (Figure 10). As labeled COgen can be used for the generation of ^{12}CO, ^{13}CO and ^{14}CO, this reagent allows easy of translation of C-12/C-13 chemistry to radiochemistry with C-14.[83]

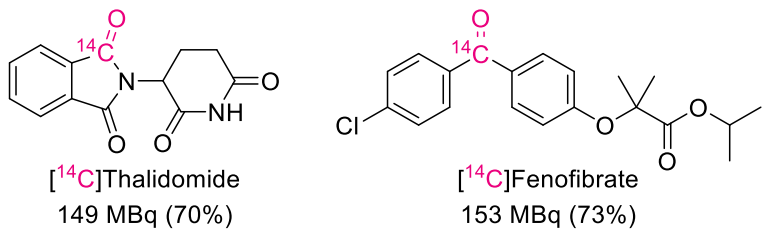

Figure 10 – C-14 labeled compounds using ^{14}COgen.

When working with ^{14}CO it may be important to consider the rules and regulations around venting radioactive gasses. It may be necessary to ensure full consumption of the radioactive gas; however, without the ability to test the progress of the reaction with analytical methods, this may not be an easy task. To address this issue, Lindhardt *et al*[83] developed a scrubber with *n*-BuLi, which enabled trapping of any surplus ^{14}CO. With this tool in hand, ^{14}CO can be used in a safe and simple manner, and in accordance with the regulations.

1.4. Objectives

As presented in the introduction, isotopic labeling is of immense value in drug discovery; however, the methods to achieve late-stage of the synthesis are limited. Carbonylation reactions are mild and allow the incorporation of a single synthon of carbon elegantly in growing molecules. Most methods are *only* suitable for carbonylation of aryl, alkenyl and benzyl substrates. Alkyl amides are prevalent in many drugs (Figure 11). Therefore, it is imperative to expand this methodology towards alkyl substrates.

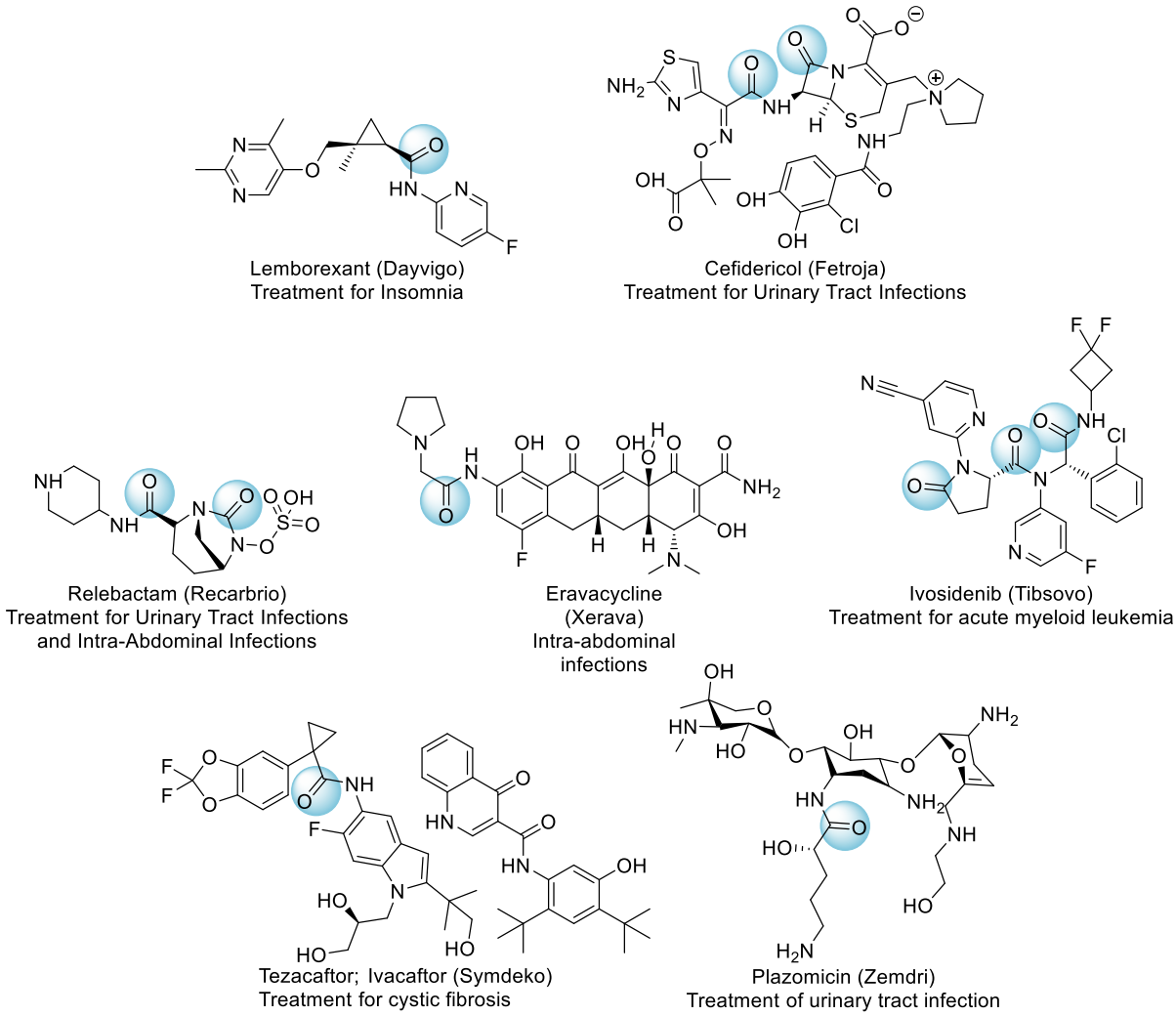

Figure 11 – FDA approved drugs with an alkyl amide moiety.

The objective of this PhD was to develop a new methodology that bridges the gap. Current methodologies rely on time-consuming multi-step synthesis that produces expensive-to-dispose of waste.

We desire to approach the alkyl amides *via* a three-component reaction (Figure 12), using alkyl halides (R-X), labeled CO (from labeled COgen) and amines as the nucleophile. Recent progress in the field of carbonylation enabled by visible light have shown elegant procedures to enable dehalogenation of alkyl halides that contain beta-hydrogens. While these methods still utilize multi equivalents of CO, it would be interesting to develop this towards isotopic labeling.

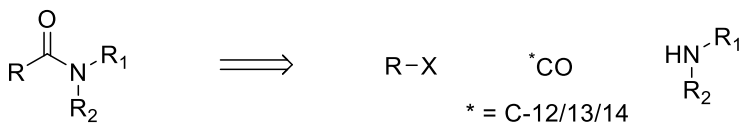

*Figure 12 – Retrosynthesis for labeling [*C-carbonyl]alkyl amides.*

Moreover, we propose late-stage labeling with CO, but it was important to consider that labeled COgen is synthesized in two steps. Therefore, we aim to evaluate methods that enable direct reduction of $^{14}CO_2$ to ^{14}CO.

Lastly, this PhD allowed a secondment in PET chemistry. Herein we will address the radiofluorination of crizotinib (Figure 13). Crizotinib contains a fluorine atom; therefore, PET labeling with F-18 will not modify the chemical structure, and the drug properties will be retained. The objective is to find a suitable radiolabeling precursor.

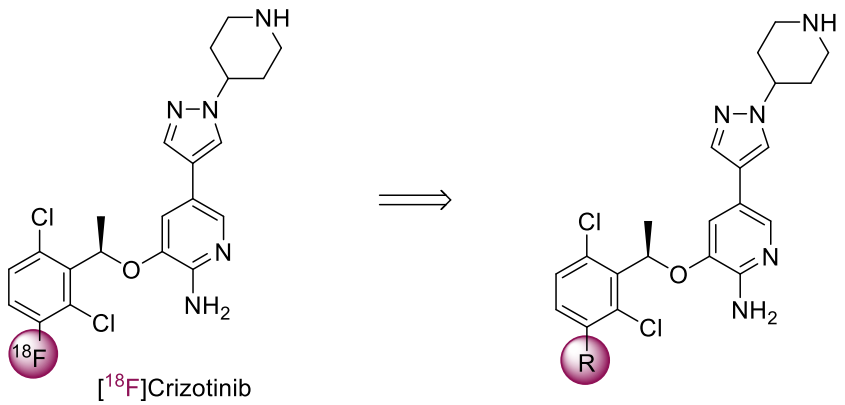

Figure 13 – Retrosynthesis of [^{18}F]Crizotinib

In summary, the aims of this thesis are:

1. To develop a convenient method for labeling alkyl substrates with labeled carbon monoxide. (Chapter 2).
2. To evaluate methods for reduction of $^{14}CO_2$ to ^{14}CO, without additional steps. (Chapter 3).
3. To develop a convenient route for radiofluorination of crizotinib. (Chapter 4)

Chapter 2:

Visible-Light Enabled Aminocarbonylation of Unactivated Alkyl Iodides with Stoichiometric Carbon Monoxide for Application on Late-Stage Carbon Isotope Labeling

2. Method Development: Visible-Light Enabled Aminocarbonylation of Unactivated Alkyl Iodides with Stoichiometric Carbon Monoxide for Application on Late-Stage Carbon Isotope Labeling

This work was published in The Journal of Organic Chemistry: Visible-Light-Enabled Aminocarbonylation of Unactivated Alkyl Iodides with Stoichiometric Carbon Monoxide for Application on Late-Stage Carbon Isotope Labeling.[85]

2.1. Synthetic approaches towards carbonylation of unactivated alkyls

Palladium catalyzed carbonylation reactions have found many applications in isotope chemistry. However, as discussed before, the method is mostly restricted to substrates such as aryl, vinyl, and benzyl (pseudo)-halides. Alkyl halides are mainly restricted by the competing β-hydride elimination of the metal-alkyl species formed by the oxidative additions. In the 1980s it was discovered that transition metal catalysis, combined with photoirradiation can improve carbonylation of alkyl iodides.[86,87] Since then, notable progress has been made in the functionalization of unactivated C(sp_3)-substrates with unlabeled carbon monoxide.[88]

C(sp_3)-halide substrates in combination photoirradiation promotes the generation of alkyl-metal species *via* a radical mechanism; this species undergoes CO insertion to form an acyl-metal species. Despite the compatibility of this radical dehalogenation with a range of alkyl halides, the carbonylation step often requires elevated CO pressures and highly specialized equipment.[88]

Radical Carbonylation – Thermal Initiator

Chow *et al*[89] developed a metal free aminocarbonylation using 2,2′-azobis(2-methylpropionitrile) (AIBN) as the radical initiator to generate isotopically labeled alkyl amides (Scheme 22). The radical is induced by AIBN and propagated by $(TMS)_3SiH$ to form alkyl radicals. The alkyl radicals react with ^{11}CO with a subsequent nucleophilic attack by an amine to produce C-11 labeled alkyl amides. Due to the toxic and explosive nature of AIBN the use of this method is limited, despite its success with carbonylation with sub-stoichiometric amount of labeled CO.

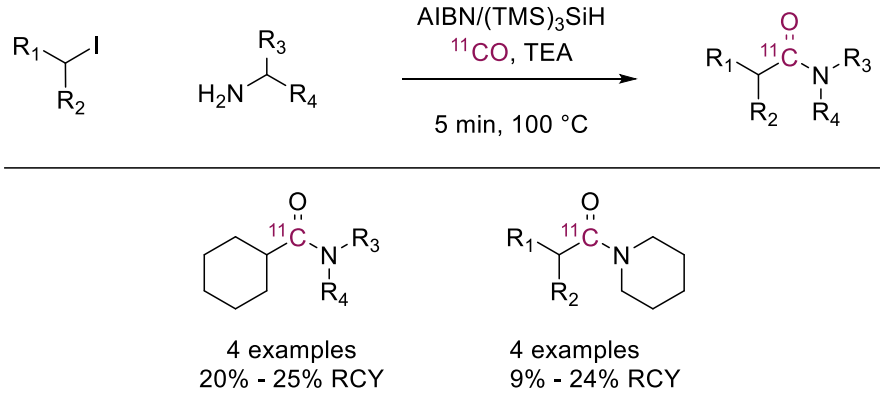

Scheme 22 – Aminocarbonylation with ^{11}CO, mediated by AIBN.

Nickel-Catalyzed Carbonylation

Pd-catalyzed chemistry is described to be limited in the choice of substrates ((hetero)aryl, alkenyl, benzyl halides), because alkyl halide substrates are prone to undergo β-hydride elimination. Obaidur *et al*[90] explored a Ni-catalyzed [^{11}C]carbonylation. While β-hydride elimination is possible with alkyl-nickel complexes, the energy barrier to rotate a Ni-C bond is significantly higher for nickel than palladium species; thus, this elimination is slower for alkyl-nickel complexes.[65,91] They demonstrated that $Ni(COD)_2$ with bathophenanthroline as a ligand

allowed the incorporation of ^{11}CO in *only* 5 minutes to produce the corresponding [^{11}C]alkyl amides (6 examples, Scheme 23). While this method provided the products with good RCY, its application on drug molecules is yet to be explored.

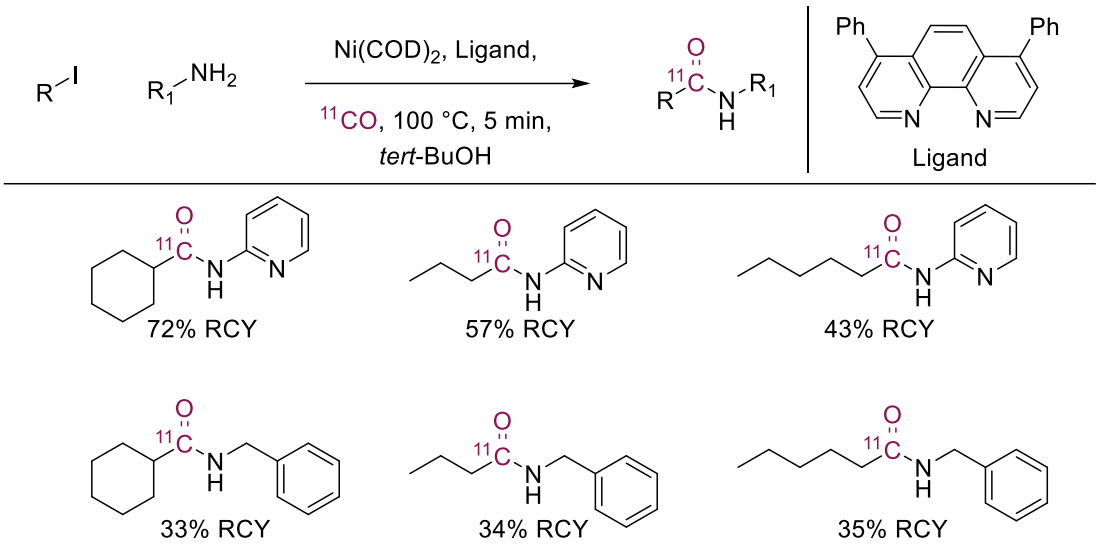

Scheme 23 – Ni-mediated [^{11}C]carbonylation of alkyl halides.

Neumann *et al*[92] further explored the synthesis of alkyl amides mediated by Ni-catalysis with a system that utilized Ni(II) complexes to avoid the generation of multi-carbonyl metal species, along with a transmetalation with a suitable alkylzinc reagent (Scheme 24). The transformation was achieved with 1.5 equiv of an *ex situ* CO-source, methyldiphenylsilanecarboxylic acid (SilaCOgen). SilaCOgen rapidly liberates CO at temperatures below 40 °C. This method was successfully applied to primary and secondary alkyl halides with primary, secondary, benzylic amines, and anilines.

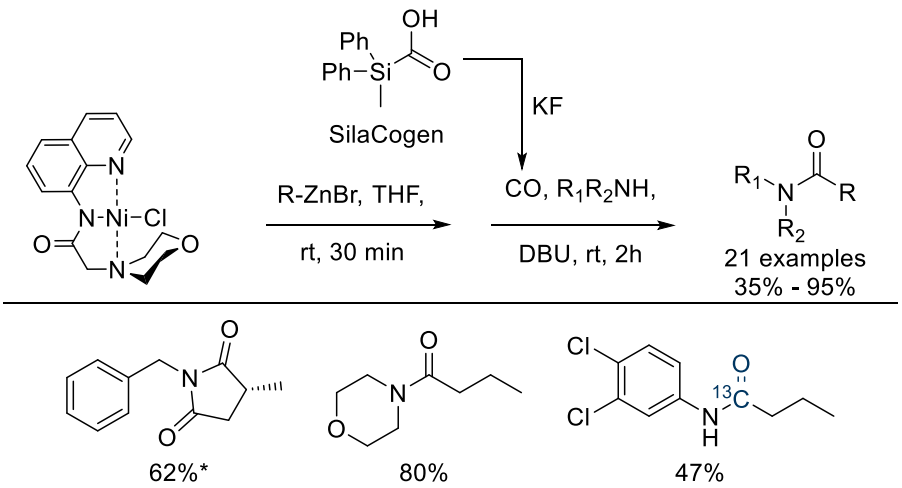

*Scheme 24 – Nickel-pincer catalyzed carbonylation to synthesize aliphatic carboxamides. *Note: The starting material is (S)-3-methoxy-2-methyl-3-oxopropylzinc bromide and benzylamine.*

Visible-light enabled carbonylation

Visible-light chemistry is a mild and facile method to produce radicals from alkyl, alkenyl and aryl iodides.[93] Chow and co-workers[94] were inspired by the recent developments in visible-light enabled chemistry and investigated the possibility to extend this methodology towards the aminocarbonylation of alkyl halides. This method requires inexpensive equipment (blue and white visible light) and generates the radicals under mild conditions. Moreover, the reaction does not require a high pressure of CO, which is an attractive attribute for translating the chemistry towards radiochemistry. Their method relied on the use of an iridium(III) photocatalyst, *fac*-Ir(ppy)$_3$, and Hantzsch ester in MeCN at room temperature, employing six equiv of CO (Scheme 25). The method was successfully applied on secondary and tertiary alkyl iodides. Unfortunately, primary alkyl iodides did not always perform well with this reaction, due to the competing S_N2 reaction.

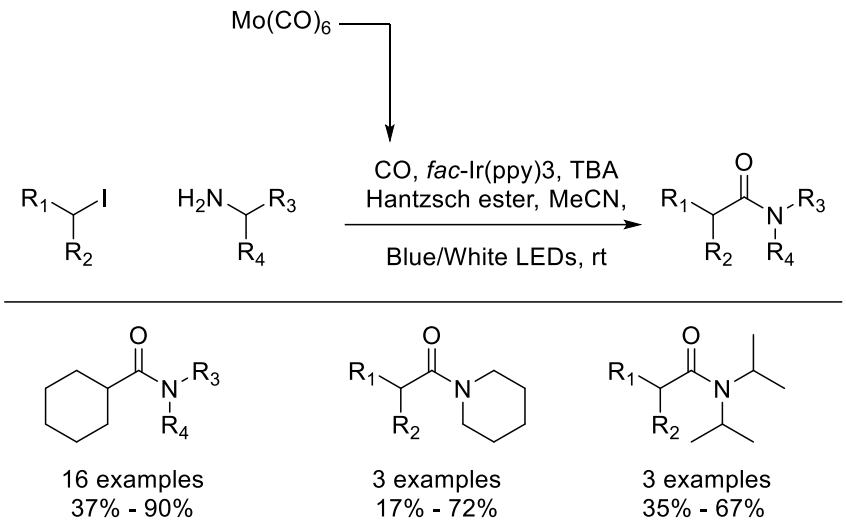

Scheme 25 – Visible-light mediated Ir(III)-catalyzed aminocarbonylation of alkyl halides.

Roslin *et al*[95] made efforts to apply this visible-light mediated Ir(III)-catalyzed chemistry to the synthesis of unsymmetrical ketones from alkyl halides and aryl boronic acid (Scheme 26). While their investigation began with a dual Ir/Pd catalytic system; to their surprise, a control experiment with *only* Pd-catalyst showed an increase in the yield, eliminating the need of the Ir-photocatalyst and improving the overall atom economy by removing the Hantzsch ester. In contrast to the Ir-catalyzed method described above, this method did not suffer from direct alkylation with primary iodides. Moreover, alkyl bromide could be used as well, but gave slightly lower yields.

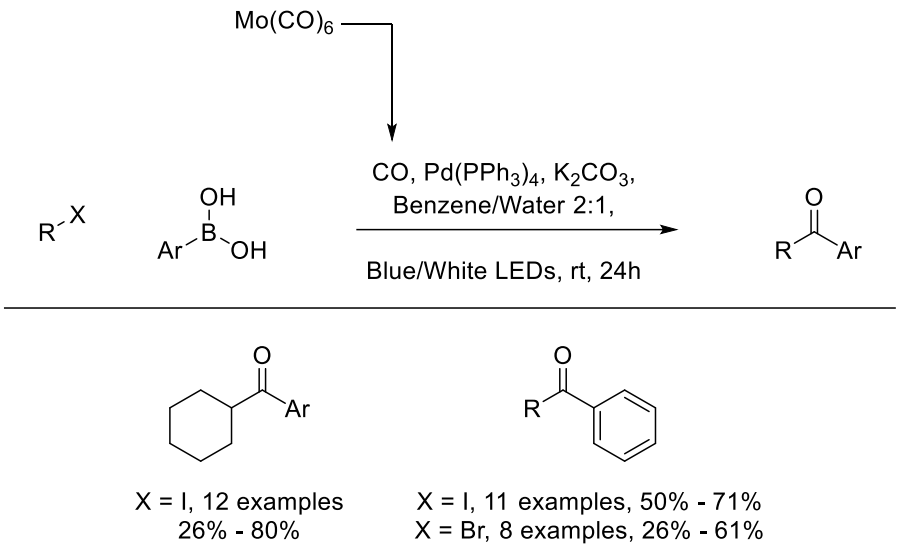

Scheme 26 - Visible-light mediated Pd-catalyzed carbonylation of alkyl halides.

2.2. Aim

Carbonylation with CO is a valuable technique for late-stage incorporation of carbon isotopes as it typically displays excellent functional group tolerance and can be applied to join two advanced intermediates.[72,83] Classical carbonylation methods utilize transition metal catalysis (i.e. Pd) to incorporate CO into complex drug-like molecules to afford ketones, carboxylic acids, esters, and amides.[65] However, most methods are only applicable with aryl or vinyl halides and triflate substrates.[96,97] Most procedures describing the use of alkyl halides typically use an excess of CO.[88] While unlabeled CO is a cheap gas, ^{14}CO is expensive and thus preferably used as a limiting reagent. Sub-stoichiometric ^{11}CO (short lived nuclide of carbon) carbonylation was achieved by Chow *et al*[89] using catalytic amounts of thermal radical initiator AIBN. Despite the applicability of the AIBN-mediated method on a wide range of functional groups, and compatibility with ^{11}CO, AIBN presents major drawbacks due to its safety profile and toxic nature. A milder approach using photochemistry with visible-light and 2-3 atm CO has been reported for the functionalization of unactivated alkyl halides using aminocarbonylation[94] and Pd-mediated cross-coupling with boronic acids[95]. Despite the synthetic utility of these methods and the advances that have been made in employing only moderate pressures of CO, in the context of isotope labeling further lowering the amount CO would be highly desirable. Inspired by the photochemistry works of Chow[94] and Roslin[95], we aimed to explore the synthesis of amides *via* carbonylation of alkyl iodides with amines using *only* stoichiometric amounts of CO.

2.3. Development of Visible-light Enabled Palladium Catalysis

After the evaluation the utility of several other carbonylation methods towards labeling, we aimed to evaluate visible-light conditions with Pd-catalysis.[94,95] Unlabeled CO was used as the limiting reagent with cyclohexyl iodide **1** and morpholine **2** as the model substrates. The CO was generated from COgen, which provides a readily transferable, solid form of CO and has been used with labeled CO ($^{13/14}CO$).[83] In order to limit costs and generation of waste, the optimization of the procedure and part of the scope were performed using unlabeled COgen. We paid particular attention to the set-up of the reaction in order to ensure direct implementation of the protocol onto C-14 radiolabeling. The dual chamber system (COware, (Figure 14**A**)) was used as previously described.[96] As COgen is moisture sensitive and undergoes hydrolysis, fresh batches of COgen were made before each experiment.[98]

To facilitate the visible-light chemistry in a parallel fashion, a photoreactor was constructed (Figure 14**B-C**). Blue LEDs surround a central compartment, which contains a heating block to enable the liberation of CO from COgen at 70 °C. The carbonylation chamber was kept at room temperature; a fan was used to circulate the air in the reactor to regulate the heat emitted from the LEDs. The setup could facilitate six parallel reactions; however, this setup could potentially be used for larger libraries, too.

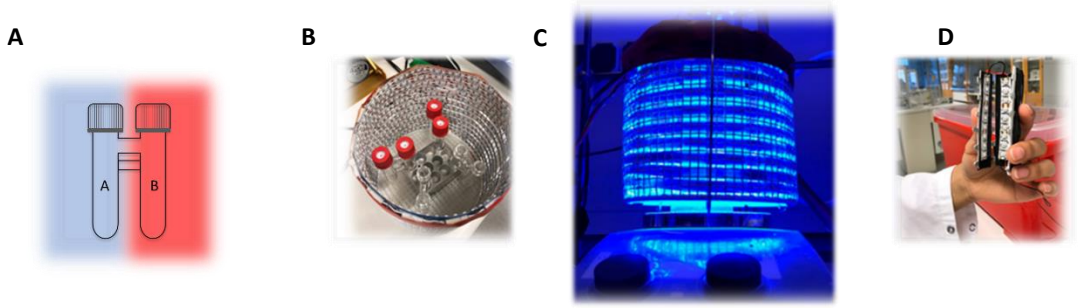

Figure 14 – A Schematic view of the COware, red represents the heating of the chamber and blue represents the blue visible-light irradiation. B top view of the elevated photoreactor. C Elevated photoreactor, enabling 6 reactions in parallel, with heating block in the middle to allow heating of Chamber B while Chamber A is kept at room temperature. D Single chamber photoreactor system.

2.3.1. Optimization of the reaction

The initial conditions used were from Roslin *et al*[95]. The COware was loaded with 0.30 mmol cyclohexyl iodide **1**, 1.5 equiv of morpholine **2**, 0.05 equiv $Pd(PPh_3)_4$, 1 equiv K_2CO_3, benzene:water (2:1, 3 mL) in the CO consuming chamber (chamber A), and the CO releasing chamber was loaded with 1 equiv COgen and the requisite reagents to release the CO (chamber B). Chamber B was heated to 70 °C for 24 h while chamber A was kept at room temperature and illuminated by blue LEDs, to give a conversion of 44% to cyclohexyl(morpholino)methanone (**3**) (Table 2, entry 1). The yield of the carbonylated product were monitored by addition of 1 equiv of anisole after the work up, which serves as an internal standard. Increasing the equivalents of morpholine to 3 equiv gave a yield of 64% (Table 2, entry 2). However, increasing morpholine beyond 3 equiv gave no further improvement (Table 2, entry 3).

Table 2 – Investigation of the Reaction Concentration

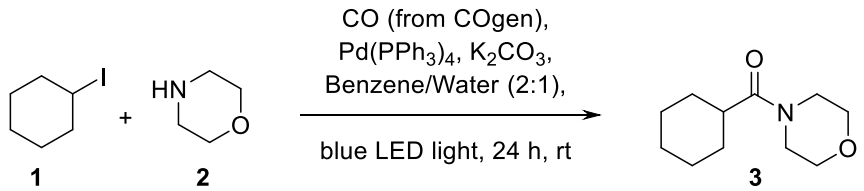

Entry	Amine 2 (equiv)	Solvent volume (mL)	Concentration 1 (M)	Yield of 3 (%)
1.	1.5	3	0.10	44
2.	3	3	0.10	64
3.	6	5	0.12	56
4.	3	5	0.12	70 [55]
5.	3	5	0.12	93[a]
6.	3	5	0.24	[38]
7.	3	5	0.24	[36][b]

Reaction condition: $Pd(PPh_3)_4$ 5%, K_2CO_3 (0.6 mmol), 5 mL Benzene/water 2:1, 1 equiv CO. [a] 2 equiv of CO is used. [b] ^{13}CO is used. Yields mentioned within the square brackets represent isolated yield.

Motivated by this initial success, we optimized the reaction with respect to solvent, catalyst, and base. The systematic variation of reaction conditions enabled a better understanding of the factors governing the carbonylation process. To improve the poor solubility of CO in most organic solvents[99] the reaction volume was maximized and the concentration of all reagents was increased. This led to a decrease in headspace, thus increasing the CO partitioning into the solvent to give a yield of 70% of **3** (Table 2, entry 4). When the reaction was done with 2 equiv of CO an increase to 93% was observed (Table 2, entry 5). While the goal remained to adapt the chemistry towards late-stage labeling, an increase in equiv of CO corresponds to an increase of the internal pressure that improved the yield. A drop to 38% in (isolated) yield was observed when the reaction was performed on the 1.2 mmol scale to give cyclohexyl(morpholino)methanone **3** (Table 2, entry 6), which may be related to a scalability issue when using the same size glassware. A similar result was observed by Roslin et al.[95] When the transformation was performed with ^{13}COgen on the same scale, no differences in isolated yield was observed (36%, Table 2, entry 7).

Due to the carcinogenic nature of benzene, finding an alternate solvent was imperative. A plethora of solvents were tried as shown in Graph 1. Replacing benzene in the solvent system with toluene lowered the yield. Solvents with a higher density than water were the most detrimental for the reaction efficiency. Greener alternatives such as 2-MeTHF and CPME, showed comparable yield to benzene. 2-MeTHF showed good conversion with (81%) and without water (54%).

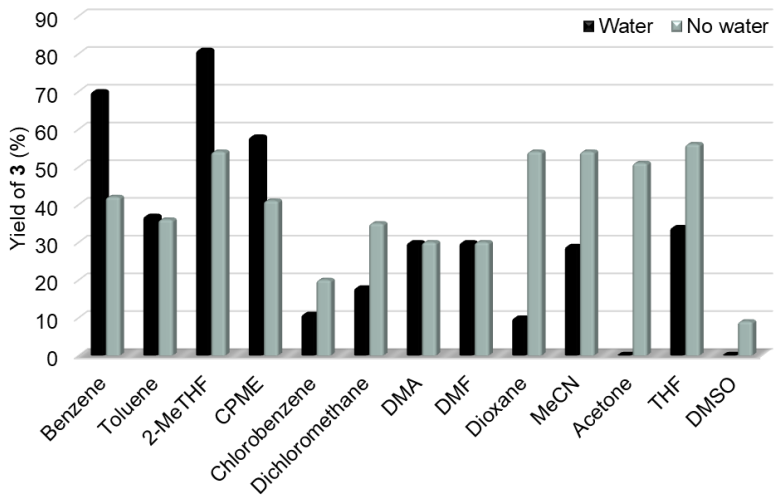

Graph 1 - Investigation of various solvents, with and without water
*Reaction conditions: iodocyclohexane **1** (0.6 mmol), morpholine **2** (1.8 mmol), $Pd(PPh_3)_4$ 5%, K_2CO_3 (0.6 mmol), solvent total volume (5 mL), CO (0.6 mmol).*

The reaction demonstrated no product formation in the absence of either visible-light or transition metal catalyst (Table 3, entry 1 and 2). As the presence of a transition metal catalyst is fundamental for the transformation to take place, in the next step we first investigated the role of the ligand on the catalyst as shown in Table 3. A control experiment was performed with $PdCl_2$ (Table 3, entry 3), and no product formation was observed. When ligands such as Xantphos or PPh_3 were used on the Pd catalyst (Table 3, entry 4 and 5), moderate yields of the product were seen. Other Pd(0) catalysts were also screened but furnished no product (Table 3, entry 7 and 8).

Ir(III) catalyst is well-known as a photocatalyst and has been used for aminocarbonylation mediated by visible light.[94] In our hands with 1 equiv of CO the yield of the reaction was higher when using $Pd(PPh_3)_4$ (Sigma Aldrich, € 51/g), than using an expensive photocatalyst such as the Ir(III) catalyst (Sigma Aldrich, € 612/250mg). Subsequently, the influence of loading of $Pd(PPh_3)_4$ was explored. As with any catalytic reaction, a low catalytic loading results in a lower yield, whereas a high catalytic loading disrupts the penetration of photons, which results in a lower yield. In this case, a loading of 5% was the most efficient.

Table 3 – Investigation of the catalyst and loading

Entry	Catalyst (%)	Yield of 3 (%)
1. [a]	$Pd(PPh_3)_4$ (5)	-
2. [b]	-	-
3. [b]	$PdCl_2$ (5)	-
4. [b]	$PdCl_2(PPh_3)_2$ (5)	56
5.	$PdCl_2$ Xantphos (5)	44
6. [b]	PPh_3 (5)	-
7. [b]	$Pd(dba)_2$ (5)	-
8. [b]	$Pd(dba)_2$, $P(t\text{-}Bu)_3$ (5)	-
9.	$Ir(ppy)_3$ (1)	58
10.	$Pd(PPh_3)_4$, $Ir(ppy)_3$ (5, 1)	57
11.	$Pd(PPh_3)_4$ (1)	10
12.	$Pd(PPh_3)_4$ (2)	37
13.	$Pd(PPh_3)_4$ (5)	70 [55]
14.	$Pd(PPh_3)_4$ (10)	54
15.	$Pd(PPh_3)_4$ (20)	48

*Reaction conditions: iodocyclohexane **1** (0.6 mmol), morpholine **2** (1.8 mmol), K_2CO_3 (0.6 mmol), 2-MeTHF/Water 2:1 (5 mL), CO (0.6 mmol). [a] no visible-light is used. [b] Benzene/water 2:1 (5 mL). Yields mentioned within the square brackets represent isolated yield.*

A variety of bases were screened as shown in Table 4, both organic and inorganic bases were shown to be effective. Surprisingly, when KOH was employed as a base, the yield dropped significantly. As most of the optimization was performed with K_2CO_3, and no significant improvement was observed when using other bases, K_2CO_3 remained as the base of choice.

Table 4 – Investigations of organic and inorganic bases

Entry	Base	Yield of 3 (%)
1.	K_2CO_3	81 [61]
2.	TEA	59
3.	Pyridine	51
4.	KOH	27
5.	K_3PO_4	52
6.	Cs_2CO_3	55

*Reaction conditions: iodocyclohexane **1** (0.6 mmol), morpholine **2** (1.8 mmol), $Pd(PPh_3)_4$ 5%, Base (0.6 mmol), 2-MeTHF/Water 2:1 (5 mL), CO (0.6 mmol). Yields mentioned within the square brackets represent isolated yield.*

Photochemistry can be a slow process when performed in batch synthesis.[93] Therefore, the time of the reaction was monitored. Seven reactions were set up in parallel and stopped at different time points to determine the yield. The maximum yield of the reaction was observed after 18 h (Graph 2).

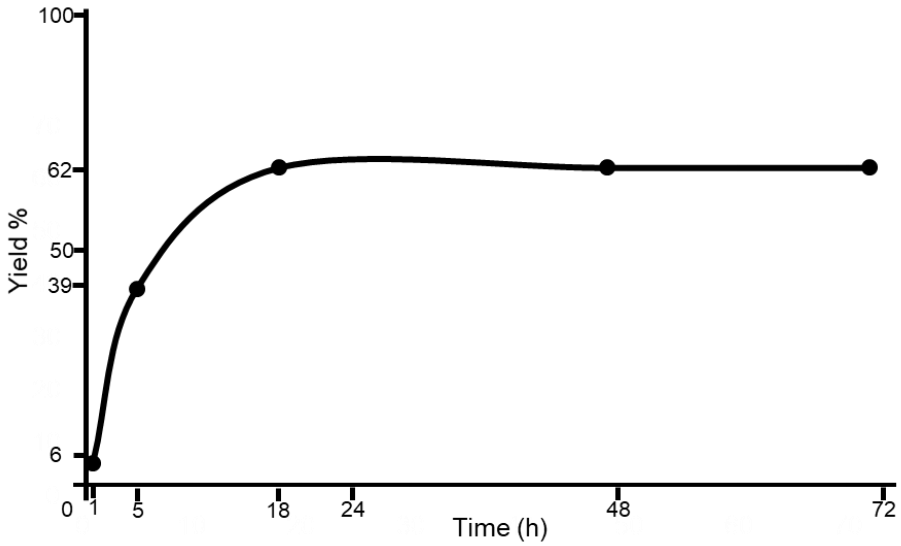

*Graph 2 - Investigations of time in hours. Reaction conditions: iodocyclohexane **1** (0.6 mmol), morpholine **2** (1.8 mmol), $Pd(PPh_3)_4$ 5%, K_2CO_3 (0.6 mmol), 2-MeTHF/Water 2:1 (5 mL), CO (0.6 mmol).*

2.3.2. Investigation of the Reaction scope

With the optimized conditions in hand, the scope of the amine coupling partner was investigated including primary, secondary, and aryl amines, to establish the versatility of this protocol and probe the limitations. The results are summarized in Scheme 27. Good yields were obtained for primary and cyclic secondary amines providing the amide products **3-6** in 37 to 61% yield. Yields of substituted piperazine (**4-5**) were lower than those obtained with the model substrate morpholine **2**. Surprisingly, cyclohexylamine did not show any product formation with 2-MeTHF/water solvent system, which may have been due to its partitioning into the water layer. When employing anhydrous conditions, product **6** was obtained in 57%

isolated yield. 2-Aminopyridine afforded 18% yield for product **7**. Whereas aniline only showed a trace of product **9** as monitored by GC-MS. 2-Aminopyridine is more basic than aniline and therefore likely demonstrates the lower limit of nucleophilicity the reaction will tolerate. Substituted benzyl amine performed well as a substrate giving moderate yield of the desired product **8**.

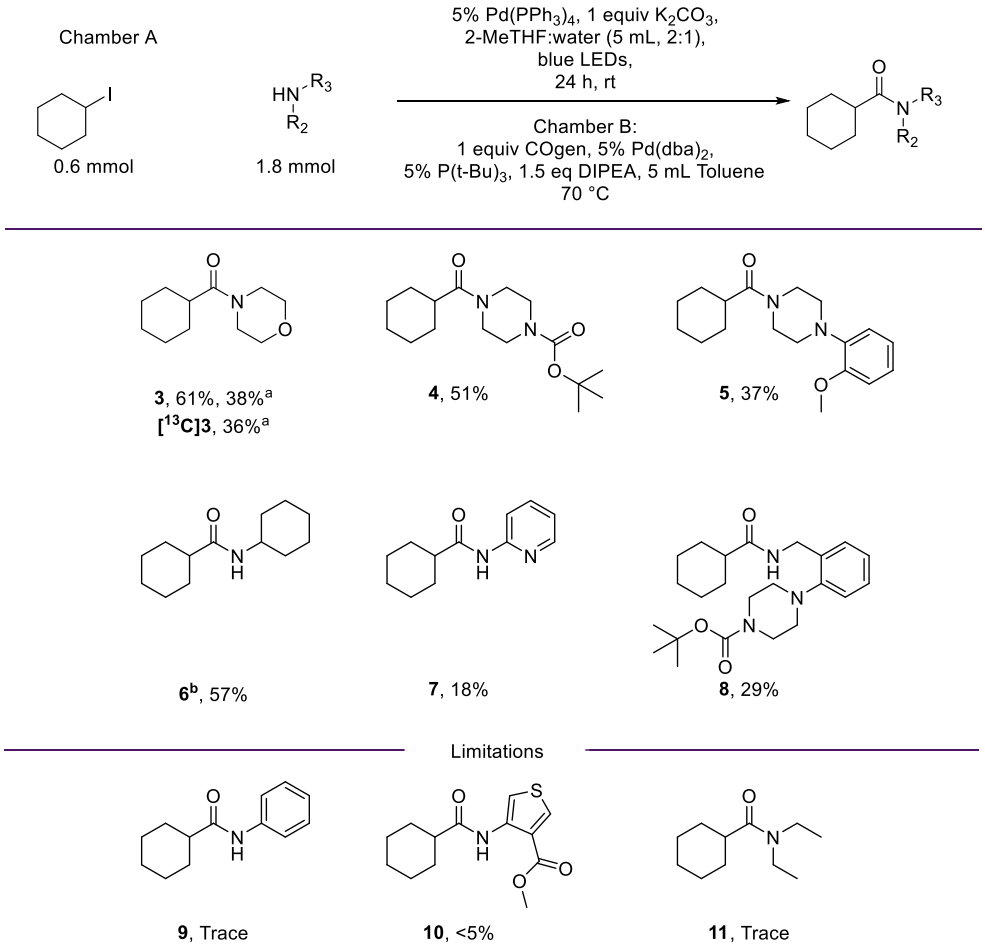

Scheme 27 - Synthesis of alkyl amides by carbonylative coupling of cyclohexyl iodide and amines. [a] 1.2 mmol scale. [b] Anhydrous conditions, 5 mL of 2-MeTHF was used in Chamber A.

Cyclohexyl iodide performed well with a range of amines. Therefore, the substrate scope was extended to a range of primary and tertiary iodides (Scheme 28). Under the optimized conditions, a series of iodides were reacted with morpholine as the nucleophile. Tertiary

iodides reacted satisfactorily to afford the amide products (**12-13**) in moderate yield, whereas 1-iodoadamantane returned the desired product **12** in higher yield compared to *tert*-butyl iodide. The less reactive 1-bromoadamantane afforded the expected product **12** in a 13% yield. Primary alkyl iodide, iodomethylcyclopentane, gave the product (**14**) with a yield of 41%. However, the lack of or low product (**15** and Scheme 29: **23**) formation for (2-iodoethyl)benzene and iodopropane is indicative of the competing direct alkylation reaction, which is favored over the pathway towards carbonylation.

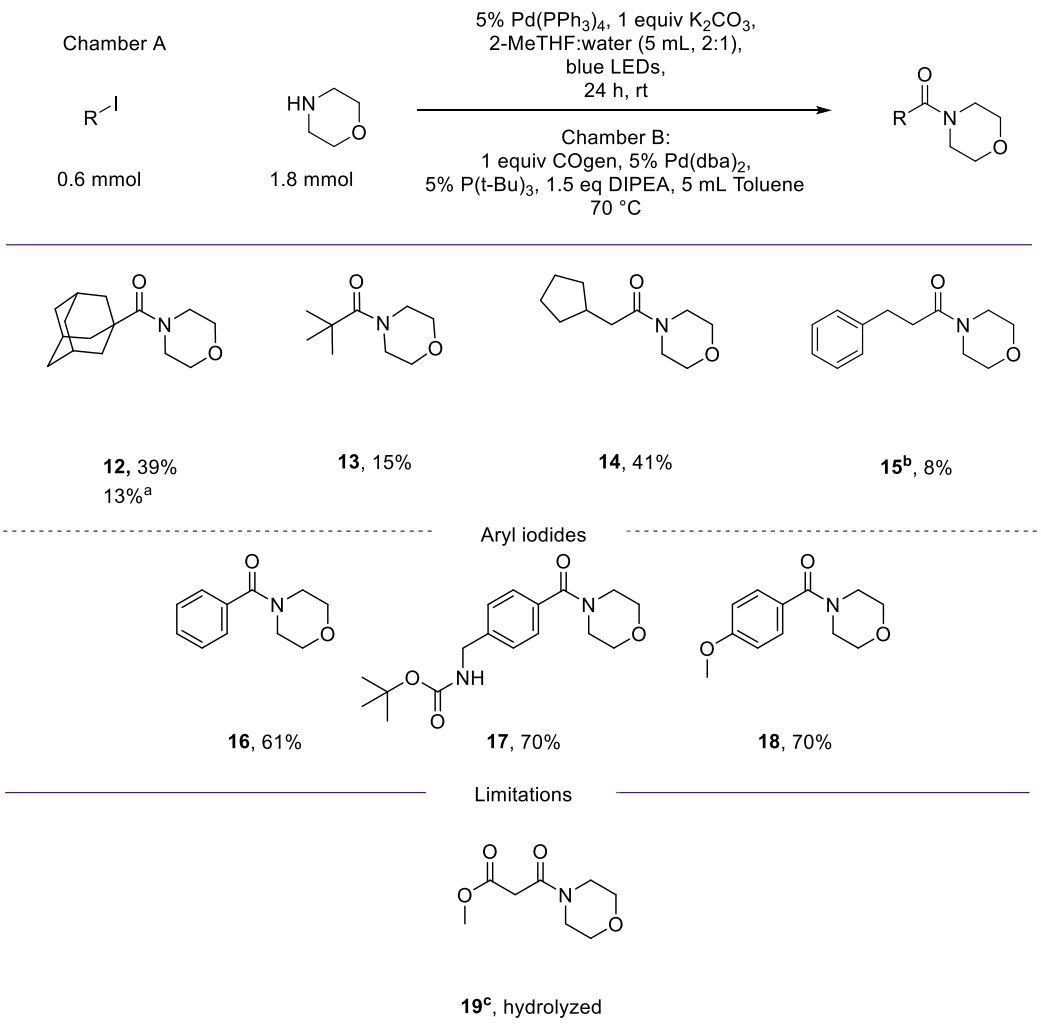

Scheme 28 - Synthesis of alkyl amides by carbonylative coupling of alkyl iodides and morpholine. [a] 1-Bromoadamantane was used. [b] S_N2 product was observed. [c] Product was hydrolyzed.

The generality of this method was further evaluated by performing the aminocarbonylation method with iodobenzene and, to our delight, morpholino(phenyl)methanone **16** was isolated with good yields. *Para* substituted aryl iodides, *tert*-butyl (4-iodobenzyl)carbamate, and 1-iodo-4-methoxybenzene were used to give good yields, 70% (**17**) and 69% (**18**), respectively.

Lastly, pharmaceutically relevant compounds were carbonylated with the optimized conditions (Scheme 29). Bucinnazine analogue **20** and Praziquantel **22** gave a yield of respectively 19% and 13%. However, attempting synthesis of Bucinnazine **23** by carbonylation of isopropyl iodide and the corresponding piperazine gave predominantly the propylated piperazine. Adamantyl amide **21** was isolated with moderate yield; surprisingly, with aqueous conditions no product formation was observed.

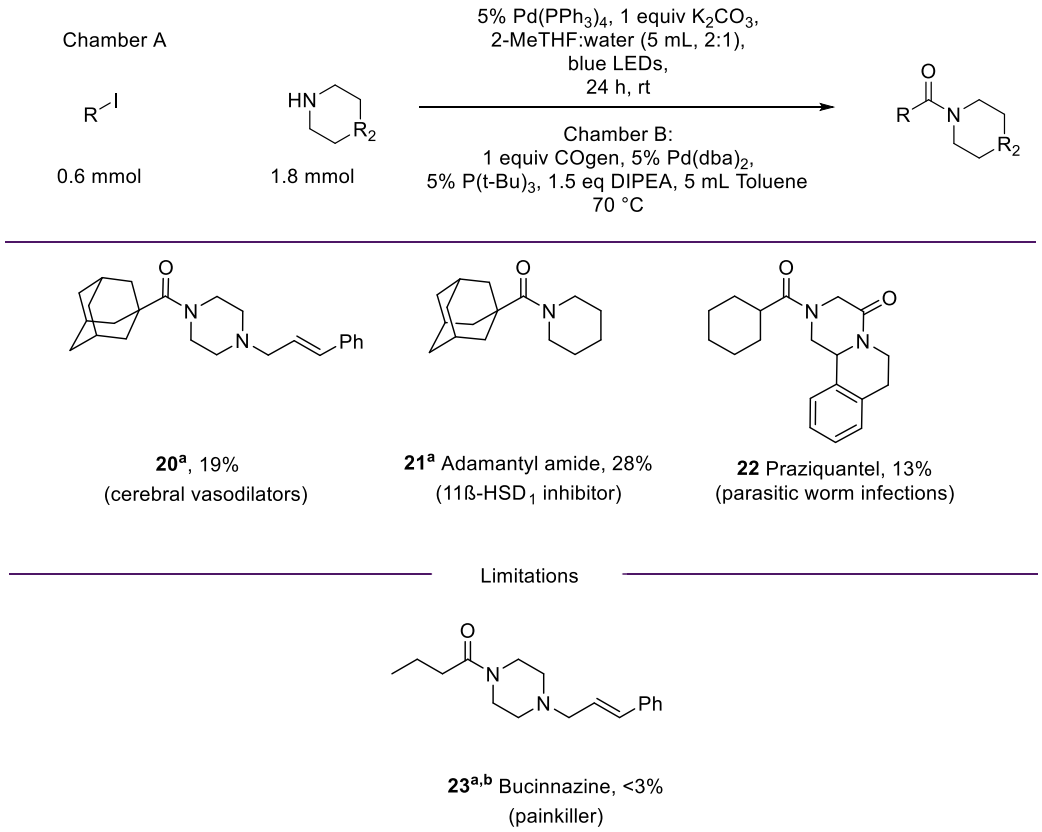

Scheme 29 - Synthesis of pharmaceutically relevant alkyl amides by carbonylative coupling of alkyl iodides and amines. [a] Anhydrous conditions, 5 mL of 2-MeTHF was used in Chamber A. [b] S_N2 product was observed.

The utility of this method towards C-14 labeling was demonstrated first using the model reaction with cyclohexyl iodide **1** and morpholine **2**. To reduce the radioactive waste, ^{14}COgen was diluted with unlabeled material, thus 5% ^{14}COgen was used with a specific activity of 0.110 TBq/mol. The result was in good agreement with the unlabeled carbonylation of cyclohexyl(morpholino)methanone **3** (Scheme 30) and the protocol was easily translated to a single photoreactor system (Figure 14**D**). [^{14}C]Cyclohexyl(morpholino)methanone **[^{14}C-*carbonyl*]3** was isolated with 50% yield with the expected specific activity within the error margin (Scheme 30).[100] Bucinnazine analogue **[^{14}C-*carbonyl*]20** was labeled to give 23% yield with the expected specific activity. To the best of our knowledge, no C-14 labeling procedures have been reported for either compounds.

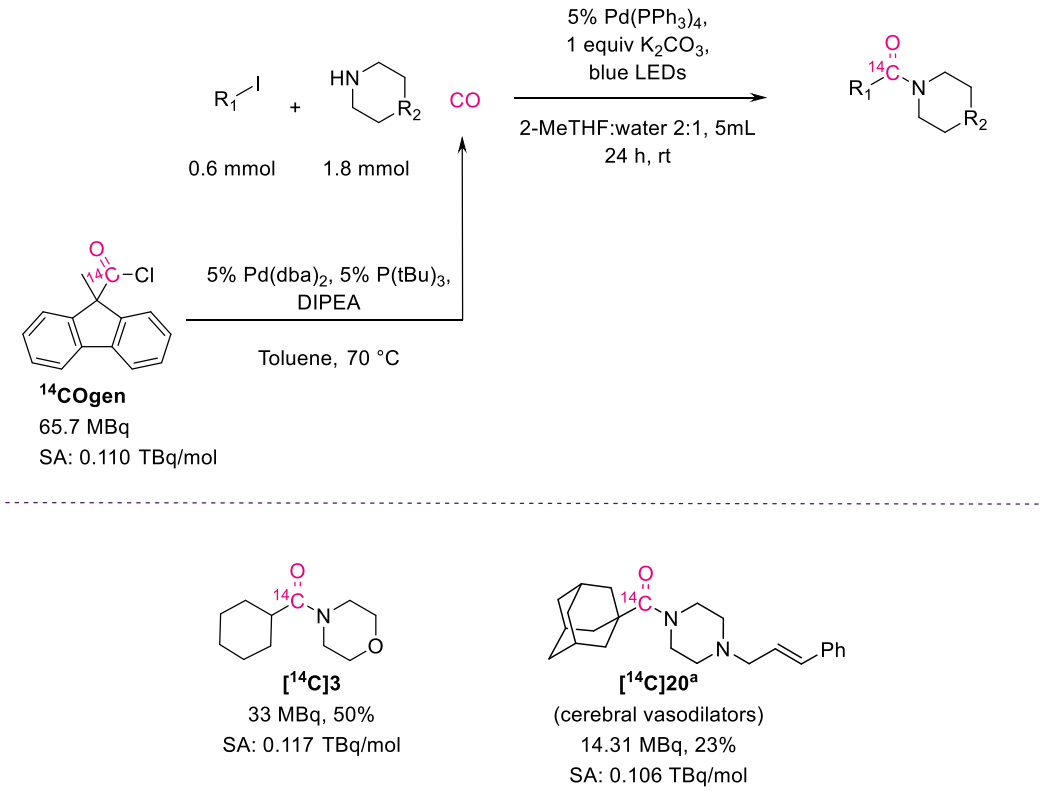

Scheme 30 - ^{14}CO reaction with model substrates, and drug-like compound. [a] Anhydrous conditions were used (5 mL of 2-MeTHF).

2.4. Conclusion and future perspectives

In summary, a mild and versatile radical aminocarbonylation protocol was developed for the late-stage isotopic labeling by carbonylation with good substrate compatibility. By using visible-light irradiation and palladium catalysis, alkyl halides were coupled with amines at ambient temperature with stoichiometric amounts of CO. Moderate to low yields were obtained for late-stage labeling with labeled CO. It is noteworthy that the reaction was enabled by $Pd(PPh_3)_4$, which is cheap and readily available. Additionally, the use of COgen allowed easy translation between unlabeled reaction and labeled reaction. As for the substrate scope, a wide range of alkyl substrates can be carbonylated, such as the unactivated secondary and tertiary iodides. On the contrary, primary iodides are difficult to achieve due to the competition with direct alkylation. To generalize the method, aryl iodides also reacted smoothly and were isolated with good yields; however, more investigations should be done to understand the mechanism and scope of this reaction. Overall, promising results have been achieved. These advances provide a powerful and broadly accessible tool for the labeling of functionalized alkyl amides.

Chapter 3:

Reduction of $^{14}CO_2$ to ^{14}CO, comparison of two methods

3. Method Development: Reduction of $^{14}CO_2$ to ^{14}CO, comparison of two methods

The previous chapter covered the development of a late-stage carbonylation methods. We used COgen as the CO source to allow easy handling of the toxic gas and the ease of incorporating unlabeled CO, ^{13}CO and ^{14}CO. However, the synthesis of $^{14}COgen$ requires two steps of radioactive handling, which is a drawback.

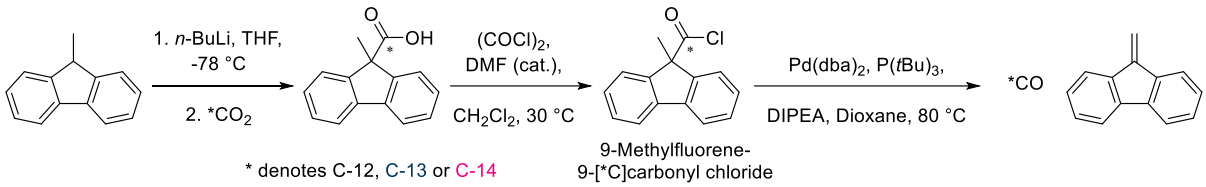

Scheme 31 – Synthesis of COgen in two steps, and 1 additional step for CO liberation.

There are two previously reported methods for reduction of $^{14}CO_2$ to ^{14}CO, unfortunately these methods come with several limitations. The earliest method for a single step reduction of $^{14}CO_2$ is the zinc-bed reduction. Apart from the specialized equipment and elevated temperature that are required for the transformation, the method is not very efficient and usually requires several passes of $^{14}CO_2$ to obtain full conversion to ^{14}CO. Moreover, the need of mercury-based Toepler vacuum pump, leaves the chemist with heavy metal waste that is contaminated with radioactivity, which can be costly to dispose of. Lastly, the apparatus is large and scaling down below 1 mmol of $^{14}CO_2$ (1.85 GBq) resulted in low yields.

Another method that does not require isolation of the any intermediate for the liberation of ^{14}CO involved the reduction of $^{14}CO_2$ using of the dehydrative nature of sulfuric acid. When concentrated sulfuric acid is heated with [^{14}C]formate for 2 h, ^{14}CO is liberated. However, at

the end of the synthesis the chemist is left with a large amount of concentrated sulfuric acid which is contaminated with radioactivity and can be difficult and costly to dispose of.

3.1. Aim

For the development of a new $^{14}CO_2$ reduction method, two methods were considered. The first method that caught our attention for the transformation was the electroreduction of CO_2 reported by Jensen *et al*[101]. The electrochemical conversion is performed in a CO_2 saturated solution of DMF using iron porphyrin (FeTTP) in the presence of trifluoroethanol (Scheme 32). A variety of palladium-catalyzed carbonylation reactions have been conducted successfully.

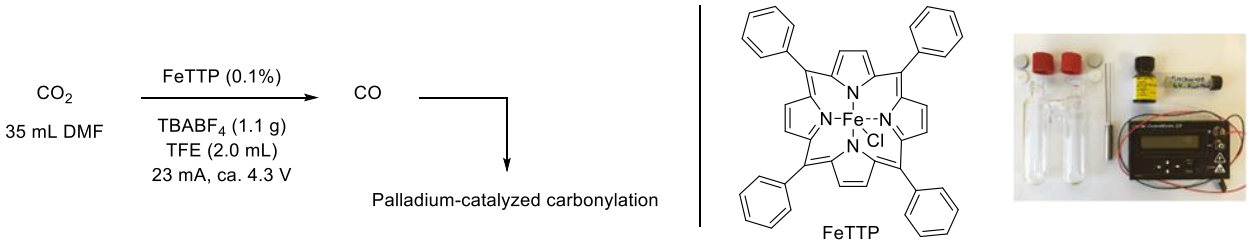

Scheme 32 - Electroreduction of CO_2. Image adapted from Jensen et al.[101]

The second method that has demonstrated it utility in PET chemistry for the conversion of $^{11}CO_2$[102] and unlabeled CO_2[103]. It involves a simple and mild protocol for the conversion of CO_2 to CO in the presence of a catalytic fluoride salt and disilane at room temperature (Scheme 33).

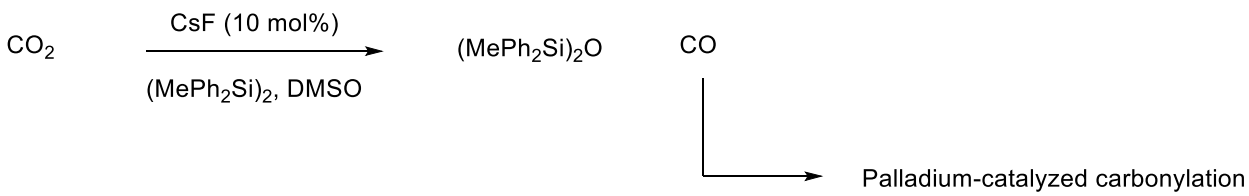

Scheme 33 – Disilane reduction of CO_2.

The main objective of this project was to expand the toolbox of radiochemist by demonstrating alternate route from $^{14}CO_2$ to ^{14}CO.

3.2. Preliminary Results

To attain new collaborations between industrial and academic partners within the Marie-Curie program (ISOTOPICS), ESRs employed at industrial partners performed two secondments at the site of the academic partners. My first secondment gave me the opportunity to spend three months at CEA-SCBM in Paris, France under the supervision of Dr Davide Audisio and Dr Antoine Sallustrau. The $^{14}CO_2$ reaction, in this chapter, was performed by Olivier Loreau.

3.2.1. Electroreduction of $^{13}CO_2$

As mentioned before, two methods were considered for $^{14}CO_2$ reduction to ^{14}CO. The two-chamber system, along with the electroreduction apparatus were provided by Professor Skrydstrup. The chambers were loaded according to the procedure described in Section Electrochemical reduction from page 148. To ease the quantification of the reduction, iodoanisole **24** and N-substituted morpholine **25** were chosen to measure the formation of CO-gas (Scheme 34). Given the literature report on electroreduction[101] of CO_2, a saturated solution of 35 mL DMF used for the transformation to give 48% of moclobemide **26**. When attempting the reaction with only 0.5 mmol of $^{13}CO_2$ in 12 mL DMF, no formation of product **26** was observed. Therefore, the method was abandoned.

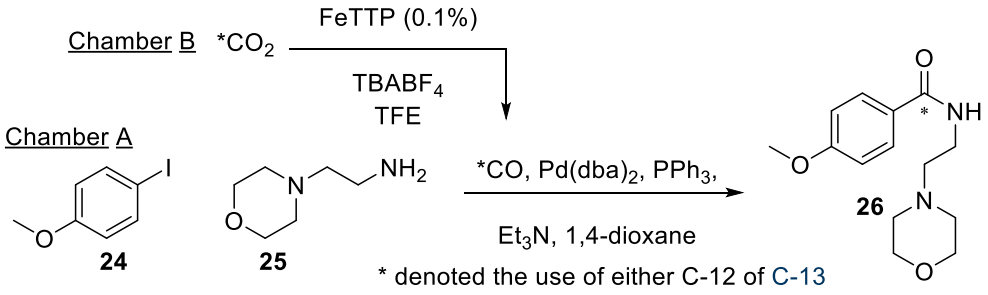

Scheme 34 – Model reaction for the quantification of CO.

3.2.2. Reduction of $^{13}CO_2$ by disilanes catalyzed by F^-

For the reduction of $^{13}CO_2$, the same glassware was used as described above and loaded as described in Table 5. When performing the reaction with 1.7 equiv of unlabeled CO_2, 68% of the desired product **[^{13}C]28** was isolated. The Tritec manifold was used to perform the reactions with $^{13}CO_2$, when the reaction was carried out with 1 equiv of $^{13}CO_2$, 62% of the desired product **[^{13}C]28** is isolated (Table 5, Entry 1). In attempts to improve the yield, different variables were investigated. The CO_2 reducing chamber was stirred at room temperature, when increasing the temperature and increasing the amount of KHF_2 to 1 equiv, a conversion of 1:1 4-iodoanisole **24**:product **[^{13}C]28** is seen. Taddei *et al*[104] showed that $(Me_2PhSi)_2$ in combination with TBAF was more efficient for the reduction of substoichiometric amounts of $^{11}CO_2$ to ^{11}CO; however, in our hands no product formation was observed (Table 5, Entry 3). As reasoned before, the solvent volumes were increased (Table 5, Entry 4-6) to force the CO to dissolve into the solvent.

Table 5 – Preliminary screening of disilane, fluoride source, solvent volumes.

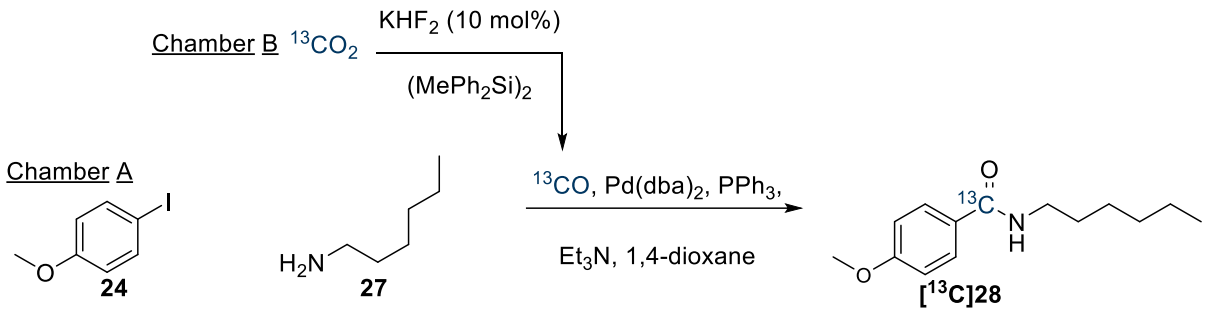

Entry	Changes from model reaction	Yield of [^{13}C]26 (%)
1.	N/A	62
2.	1 equiv KHF_2 and heating at 80 °C	- (not isolated)
3.	TBAF as F^--source and $(Me_2PhSi)_2$ as disilane in THF as solvent	-
4.	9 mL solvent in Chamber B	75
5.	12 mL solvent in Chamber B	54
6.	5 mL in Chamber A and 12 mL in Chamber B	70

*Reaction condition: Chamber A 4-iodoanisole **1** (0.5 mmol, 1 equiv), n-hexyl amine **27** (2 equiv), $Pd(dba)_2$ 5%, PPh_3 10%, Et_3N (2 equiv), 3 mL 1,4-dioxane, 80 °C, 18 h. Chamber B KHF_2 10%, $(MePh_2Si)_2$ (0.4 mmol), 3 mL DMSO, 1 equiv $^{13}CO_2$, rt, 18 h. Yield of **[^{13}C]28** are only isolated yields.*

While these results were preliminary, the method was tried using the conditions Table 5, Entry 5 with 4-iodoanisole **24** and 2-morpholinoethan-1-amine **25**. When the reaction was performed with 1 equiv of $^{13}CO_2$ an average (n = 2) yield of 25% was obtained. When *only* 0.2 equiv of $^{13}CO_2$ is employed 49% of the desired product is isolated. A test reaction with 1 equiv of $^{14}CO_2$ gave a yield of 44% of **[^{14}C-*carbonyl*]26**.

*Table 6 – Preliminary results with the synthesis of moclobemide **3**.*

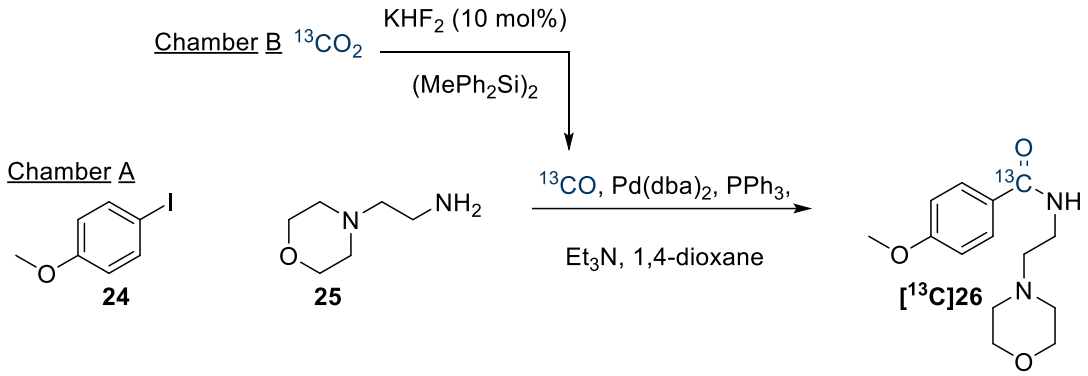

Entry	Changes from model reaction	Yield of [^{13}C]26 (%)
1.	N/A	25 (n = 2)
2.	0.2 equiv $^{13}CO_2$	49*
3.	1 equiv $^{14}CO_2$	44

*Reaction condition: Chamber A 4-iodoanisole **1** (0.5 mmol), 2-morpholinoethan-1-amine **25** (2 equiv), Pd(dba)$_2$ 5%, PPh$_3$ (5%), Et$_3$N (2 equiv), 3 mL 1,4-dioxane, 80 °C, 18 h. Chamber B KHF$_2$ 10%, (MePh$_2$Si)$_2$ (0.4 mmol), 12 mL DMSO, 1 equiv $^{13}CO_2$, rt, 18 h. Yield of **[^{13}C]26** are only isolated yields. * Yield based on $^{13}CO_2$.*

3.3. Summary and Future Perspectives

In summary, to expand the radiochemical toolbox for employing ^{14}CO in carbonylation reactions, we attempted to decrease the number of radiochemical steps to obtain this radioactive gas when using $^{14}COgen$.

New literature has emerged that enables one-pot reduction of CO_2 and carbonylation with CO. We compared two methods, while the electroreduction of CO_2 to CO works well with excess of unlabeled CO_2; unfortunately, it is not possible to limit the amount of CO_2 for labeling purposes.

On the other hand, the reduction of CO_2 with disilanes seems much more promising. The yields are preliminary; therefore, it is difficult to conclude with these results. First experience with C-14 has given a good yield.

The results are *only* preliminary and further optimization needs to be done. This method will be a useful addition to the radiochemical toolbox, when CO_2 in the atmosphere does not interfere with the carbonylation reaction.

Chapter 4:

Radiosynthesis of [^{18}F]Crizotinib, a potential radiotracer for PET imaging of the P-glycoprotein transport function at the blood-brain barrier

4. Method Development: Radiosynthesis of [^{18}F]Crizotinib, a potential radiotracer for PET imaging of the P-glycoprotein transport function at the blood-brain barrier

4.1. P-glycoprotein

The blood-brain barrier (BBB) is a firmly connected cell layer, which has the important function of protecting the brain from foreign substances. The movement of drug molecules can be either passive or active. Active transport of the drugs requires adenosine triphosphate (ATP). P-glycoprotein (P-gp, also called ABCB1 or MDR1) is a member of the ATP-binding cassette (ABC) efflux transporters family. P-gp is expressed can be observed in various tissues throughout the body. While the main function of P-gp at the BBB is to maintain the homeostasis of the brain, this transporter effectively transports several drugs out of the brain, including anticancer agents thus leading to lowered efficacy of the treatment in the brain in the central nervous system. Tumors can also express high levels of P-gp. Therefore P-gp is well-studied for its role in drug resistance.[105,106]

Studying the function of P-gp in human diseases is a challenging task. An important method to study this is using PET and Single photon emission computed tomography (SPECT). Several groups have been involved with the development of PET/SPECT radiotracer for P-gp, and this has been reviewed by Mairinger *et al*[107] and Syvänen *et al*[106].

4.2. Positron Emission Tomography

PET is a non-invasive imaging method and maps the location of positron-emitting radionuclides (short-lived radionuclides) that are injected into living subjects. This technique is used increasingly for studying biological processes *in vivo* and is mostly applied in the clinical research of cardiology, neurology, and oncology. It also allows studying *in vivo* pharmacological processes such as receptor occupancy, metabolism, and pharmacokinetic parameters, while its application is broad, it would be more extensively used if there would be more tracers available to assess target engagement as well as biologicals/disease process.[108]

Molecules labeled with radioactive radionuclides, release a positron upon decay from the nucleus.[109] The positron travels for a finite distance in the tissue, while losing the kinetic energy from the radioactive decay to the surrounding tissue. After losing most of its energy, the positron meets a random electron that results in an annihilation. The annihilation produces two photons (γ-rays), each with an energy of 511 keV, which are emitted in in opposite (180 °) directions. The rays are detected by a ring of crystals in the PET scanner (Figure 15).

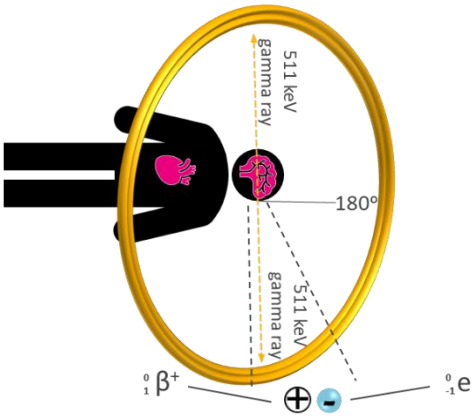

Figure 15 – A schematic overview of the PET imaging principle.

PET radiotracers can be either endogenous compounds ([^{15}O]H_2O), modified endogenous compounds (2-deoxy-2-[^{18}F]fluoro-D-glucose, [^{18}F]FDG) or novel radiotracers optimized specifically for the study, Pittsburg compound B ([^{11}C]PIB), [^{11}C]Nicotine and 1-[11C]methylpiperidin-4-yl propionate ([^{11}C]PMP) (Figure 16).[110] [^{18}F]FDG has become a standard radiotracer for PET neuroimaging and cancer mapping, as it allows visualization of glucose metabolism.[111]

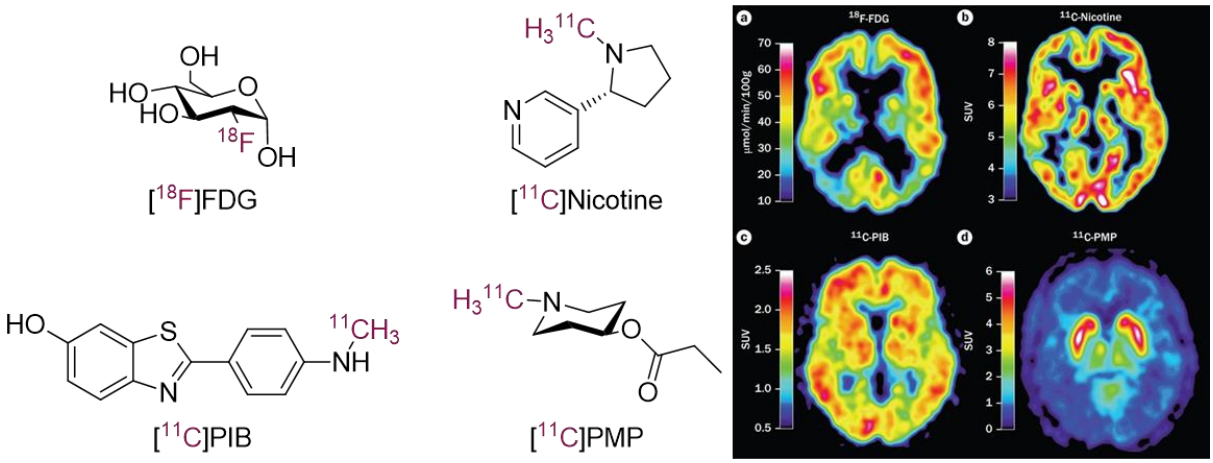

*Figure 16 – Structures of radiotracers and the corresponding PET image, herein a multitracer study on a patient with mild Alzheimer disease using **a** [^{18}F]FDG, **b** [^{11}C]Nicotine, **c** [^{11}C]PIB, **d** [^{11}C]PMP. Low uptake of [^{18}F]FDG implies a deficit in glucose metabolism. A deficit in cholinergic activity is seen by a low [^{11}C]Nicotine binding. [^{11}C]PIB retention is a measure of fibrillar amyloid load. The level of [^{11}C]PMP binding indicates the level of acetylcholinesterase activity. Right image reprinted from Nordberg et al.*[112]

4.2.1. Labeling with short-lived radionuclides

PET radionuclides are neutron deficient and decay mostly by positron (β^+) emission, where the proton is transformed into a neutron with simultaneous release of a positron. Typical radionuclides used for PET studies are C-11, F-18, N-13 and O-15 with half-life of about 20.8 min, 110 min, 9.96 min and 2.04 min, respectively. All these radionuclides are generated in a cyclotron *via* a nuclear reaction. Due to the short half-life of C-11, N-13 and O-15, for studies requiring this nuclide it is necessary for the cyclotron to be located at the site of the study.

On the other hand, F-18 labeled molecules can be transported to a remote imaging facility. Ideally, the synthesis is completed within two or three times the half-life of the radionuclide; therefore, ideally the radionuclide is incorporated in the last-stage. Reaction conditions, work up, purification, and formulation need to be optimized to fit in the time frame. The synthesis is performed on microscale; the non-radioactive reagents can be used in >1000-fold excess. Due to the scale of the reaction and the short half-life, powerful analytical methods such as NMR cannot be used. Typically, the labeled compounds are identified using pre-established HPLC methods. Due to the high radioactivity, the reactions are performed in lead-shielded hot cells, ideally using automated synthesis equipment.[113]

4.2.2. PET tracers for P-gp

The most widely used PET tracers for P-gp are *(R)*-[^{11}C]verapamil, *rac*-[^{11}C]verapamil, [^{11}C]Loperamide and [^{11}C]dLop (Figure 17). *rac*-Verpamil is a L-type calcium channel blocker, and the most extensively used P-gp PET radiotracer. While *rac*-[^{11}C]verapamil has a reasonable specificity towards P-gp, it also interactive with breast cancer resistance protein (BCRP). However, the main drawbacks the radiotracer is the formation of radiolabeled metabolites that contribute to the PET signal.[106,114] While (*R)*-[^{11}C]verapamil has a higher brain uptake than *rac*-[^{11}C]verapamil when P-gp is inhibited[115], (*R)*-[^{11}C]verapamil also suffers from the formation of radiolabeled metabolites.

Loperamide is an over the counter treatment for acute diarrhea. [^{11}C]Loperamide is also a well-known P-gp substrate and was investigated as a PET tracer for imaging the P-gp function. [^{11}C]Loperamide showed uptake in the brain in the absence or inhibition of P-gp. However, similar to [^{11}C]verapamil, metabolite of [^{11}C]loperamide contributed to the PET signals.

Therefore, the development of the PET tracer shifted towards its metabolite, N-desmethyl loperamide ([^{11}C]dLop). Studies have shown that [^{11}C]dLop does not interact with other ABC transporters (BCRP and multidrug resistance-associated protein, Mrp1). The main issue identified with this PET radiotracer is the very low baseline concentration which probably makes it unfeasible to detect an upregulation in P-gp function and makes it unsuitable for mapping the P-gp function.[106]

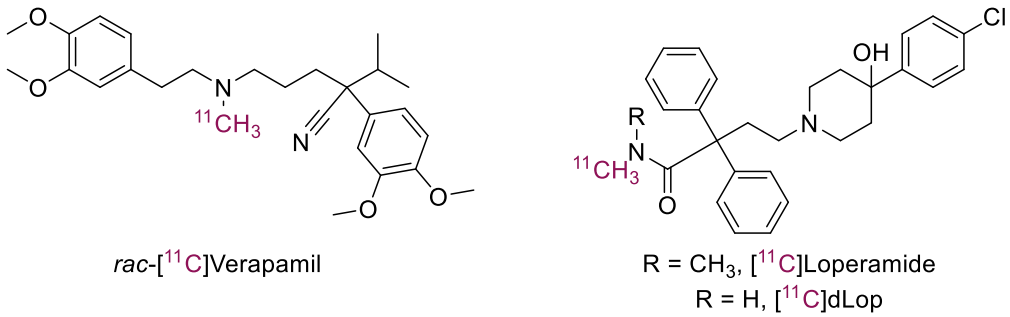

Figure 17 - Most widely used PET tracers for P-gp, [^{11}C]verapamil (depicted as racemate here), [^{11}C]Loperamide and [^{11}C]dLop.

Other radiotracers that have been investigated for P-gp imaging includes: [^{11}C]laniquidar, [^{11}C]tariquidar and [^{11}C]elacridar (Figure 15). These three compounds show P-gp inhibition at pharmacological doses, but at tracer doses, these drugs mostly behave like substrates for P-gp. [^{11}C]Laniquidar metabolizes extensively, and these labeled metabolites enter the brain and contribute to the PET signal, making it unsuitable for use in imaging of P-gp.

On the other hand, [^{11}C]tariquidar has a better metabolic stability, but it is not selective for only P-gp. It also inhibits BCRP, but with higher affinity for P-gp. [^{11}C]Elacridar has similar properties as [^{11}C]tariquidar, a better metabolic stability and a substrate for both P-gp and BCRP at tracer dose.[106]

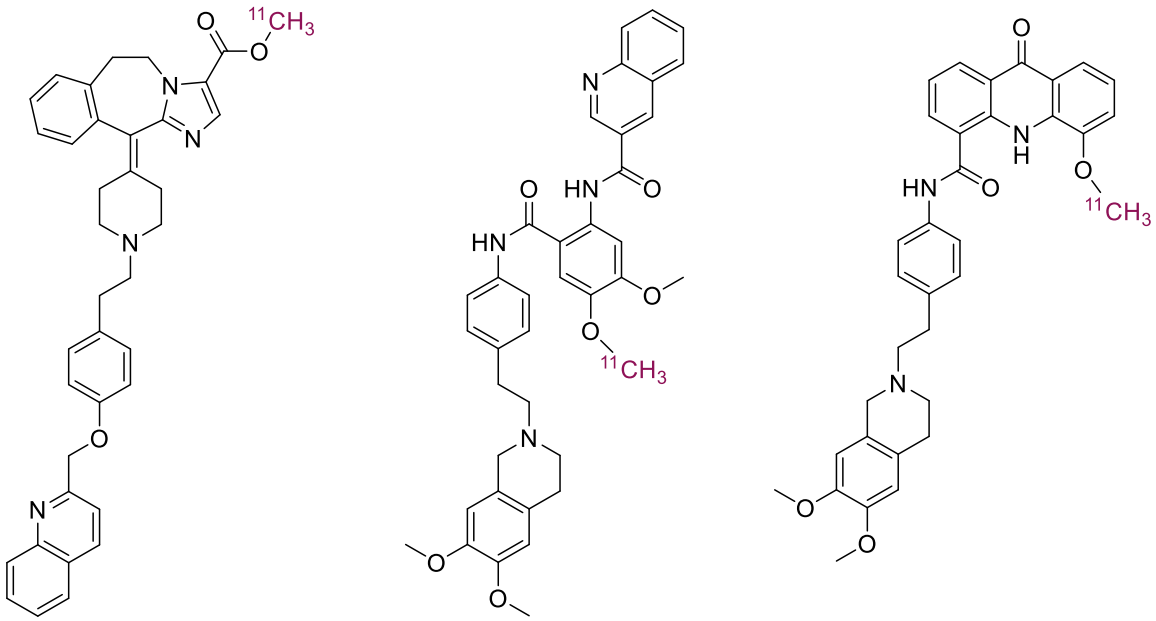

Figure 18 – P-gp inhibitors developed as PET radiotracers for P-gp , [^{11}C]laniquidar, [^{11}C]tariquidar and [^{11}C]elacridar

4.3. Aim

As mentioned before, active transporters in the brain such as P-gp effectively transport many xenobiotics out of the brain, including anticancer agents thus leading to lowered efficacy of the treatment in the central nervous system.[116–118] Crizotinib is an oral tyrosine kinase inhibitor and an approved treatment for non-small cell lung carcinoma (NSCLC), and its brain accumulation is mainly restricted by P-gp. It is not a substrate for the other ABC efflux transporters (MRP1 or BCRP), but *only* a P-gp substrate, this selectivity for P-gp makes it a promising radiotracer to image this transporter.

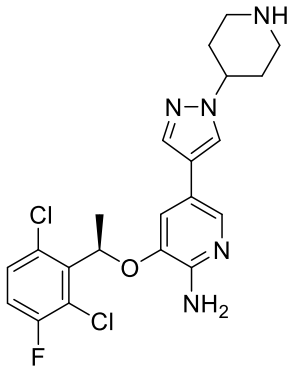

Crizotinib

Figure 19 – Crizotinib, approved treatment for NSCLC.

An additional aim is to investigate the use of labeled crizotinib to improve brain delivery of crizotinib. This is important because crizotinib is used to treat NSCLC. The patients are often diagnosed in advanced stages and have extremely poor prognosis (~8 months) and are likely to develop brain metastases.[116] For this reason, multiple groups have targeted the development of F18 labeled analogues of crizotinib,[119,120] as well as other inhibitors for the therapy of NSCLC.

4.3.1. Fluorine-18

During my PhD, there was an opportunity to do another secondment for three months at CEA-SHFJ in Orsay, France under the supervision of Dr Bertrand Kuhnast and Dr Fabien Caillé. Part of this time was spent on deprotection of PMB-protected phenol **47** and synthesis of the deoxyfluorination precursor **50**. The other half of the time was invested in the development of the radiolabeling protocol of crizotinib. This secondment provided a great opportunity to expand my skills with the field of radiochemistry and obtain an improved understanding of the challenging field of F-18 chemistry.

F-18 can be delivered as two reagents directly from the cyclotron: $[^{18}F]F_2$ or $^{18}F^-$. $[^{18}F]F_2$ is useful for electrophilic radiofluorination; however, due to technical reasons related to its high reactivity and a low molecular activity (MA), unlabeled F_2 gas is needed to release the radioactivity from the target. $^{18}F^-$ does not suffer from this issue is thereby used more frequently. $^{18}F^-$ is an effective reagent for nucleophilic aromatic substitutions (S_NAR) or nucleophilic substitutions (S_N2). As $^{18}F^-$ is produced from ^{18}O-enriched water, it is necessary to remove the water for the reaction. The removal of water is achieved by passing this over an ion exchange cartridge, which only traps the $^{18}F^-$ and eluted the water. $^{18}F^-$ is then removed by elution with aqueous acetonitrile and a counter ion such as $TEAHCO_3$. Subsequent evaporation steps allow removal of the remaining water. $^{18}F^-$ can then be used as a nucleophile in the desired reaction.[121,122]

4.3.2. Synthetic approaches

Crizotinib contains a fluorine atom and is a viable candidate for radiofluorination. Nucleophilic aromatic substitution (S_NAr) is a widely used reaction method to functionalize aromatic molecules. It is one of the most commonly used method to allow radiofluorination on arenes for use in PET imaging. Two routes were selected to achieve radiofluorination, a hypervalent iodine(III) complex[123,124] (Scheme 35) and a phenofluor activated phenol[125] (Scheme 36) were synthesized as precursors for radiosynthesis with $^{18}F^-$.

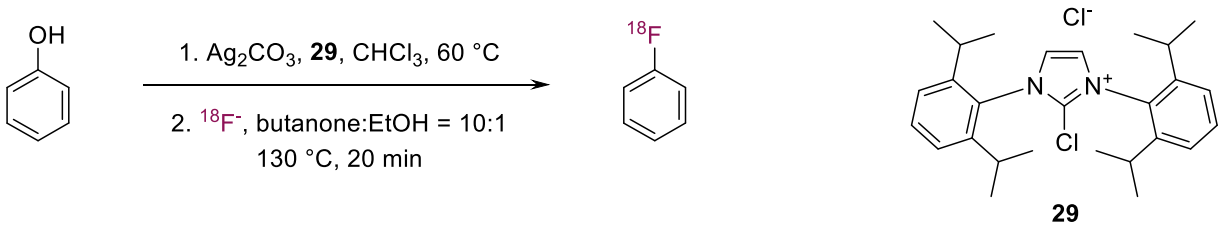

Scheme 35 – Deoxyfluorination to allow nucleophilic aromatic substitution.

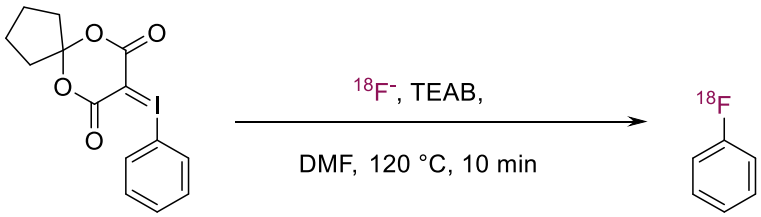

Scheme 36 – Nucleophilic aromatic substitution using spirocyclic hypervalent iodine(III) complex.

4.4. Synthesis of Precursors

4.4.1. Hypervalent Iodine(III) precursor 38

The synthetic route towards precursor **38** was developed by a contract research organization (CRO) prior to the start of this PhD project. Below is described the synthesis of this precursor done by this CRO.

The synthesis of hypervalent iodine(III) precursor **38** starts with the synthesis of mesylate **32** was synthesized in two steps (Scheme 37). The regioselective lithiation of 2,4-dichloro-1-iodobenzene **30** followed by nucleophilic addition to acetaldehyde gave rise to the corresponding alcohol **31** in 69% yield. This alcohol **31** was then mesylated to give compound **32** as an off-white solid in 67% yield. Compound **32** was used in a later step for a nucleophilic substitution reaction.

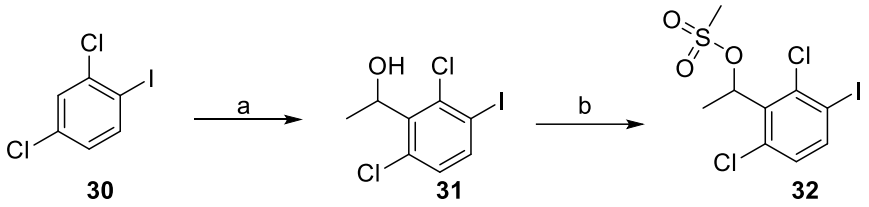

Scheme 37 - Reagents and conditions: a) n-BuLi, iPr_2NH, acetaldehyde, THF, -78 °C, 1 h, 69%, b) $NEtiPr_2$, MsCl, CH_2Cl_2, 0 °C, 1.5 h, 67%.

The synthesis of the hypervalent iodine(III) precursor **38** is shown in Scheme 38 and starts with a Suzuki coupling of boronic ester **33** and bromopyridine **34** to give **35** in 48% yield. Phenol **35** was reacted with mesylate **32** to give ether **36** in a 48% yield. Aminopyridine **36** was reacted with di-*tert*-butyl dicarbonate ($(Boc)_2O$) to give the *bis*-Boc protected aniline **37** as a white solid in 71% yield. The aryl iodide **37** was converted in to the hypervalent iodine(III) precursor **38** which was isolated as an off-white solid with 15% yield.

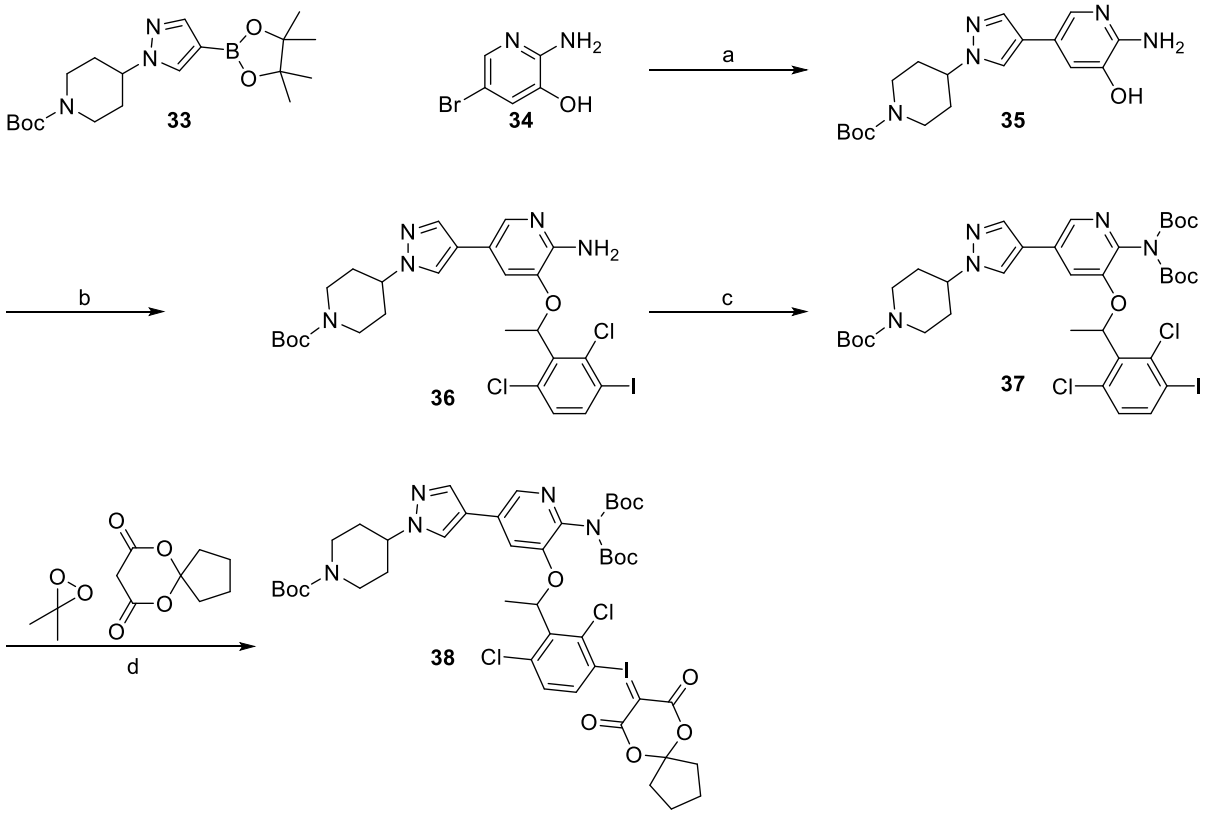

*Scheme 38 – Reagents and conditions: a) Pd(dppf)Cl_2, Na_2CO_3, H_2O, 1,4-dioxane, 100 °C, 16 h, 48%, b) Cs_2CO_3, **32**, MeCN, 60 °C, 4 h, 48%, c) $(Boc)_2O$, $NEtiPr_2$, DMAP, THF, 25 °C, 16 h, 71%, d) Na_2CO3 (10%), AcOH, EtOH, acetone, 25 °C, 2 h, 15%.*

4.4.2. Deoxyfluorination precursor 50

The deoxyfluorination reagent **29** can be prepared in a five-step sequence from cheap and commercially available precursors as shown in Scheme 39. Condensation of 2,6-diisopropylaniline **39** with glyoxal **40** gave diimine **41** as a yellow solid. Diimine **41** was treated with paraformaldehyde in the presence of chlorotrimethylsilane in hot ethyl acetate afforded imidazolium chloride **42**. Imidazolium chloride **42** was deprotonated by potassium *tert*-butoxide and the resulting carbene **43** was treated with hexachloroethane in tetrahydrofuran to afford chloroimidazolium salt **29** as an off-white solid in 72% yield over three steps. Finally, Ag_2CO_3 is mixed to give the precursor **44** which is used in the next step for produce the final radiofluorination precursor.

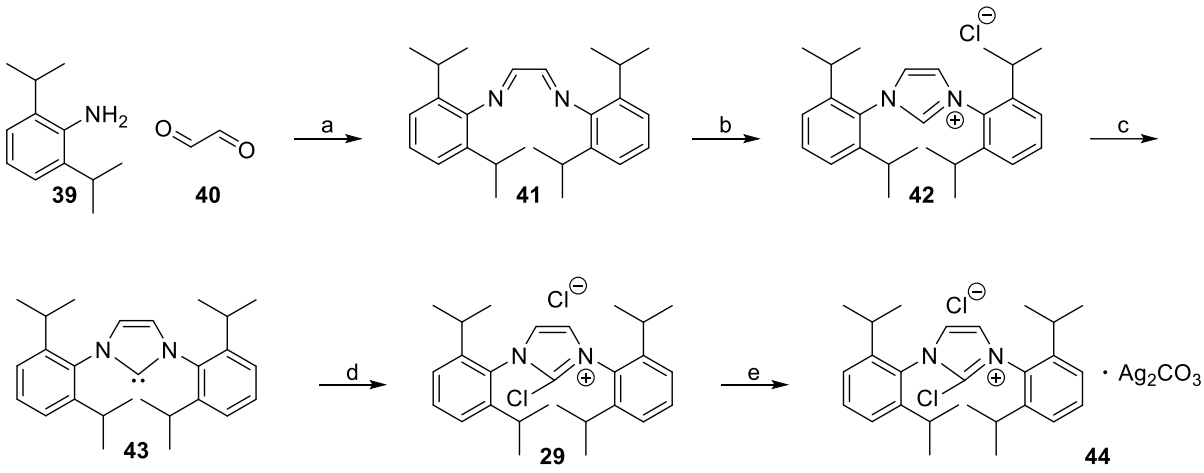

Scheme 39 – Reagents and conditions: a) AcOH, MeOH, overnight, 50 °C to rt, 75%, b) paraformaldehyde, chlorotrimethylsilane, EtOAc, 70 °C, 2.5 h, c) KOtBu, THF, rt, 3.5 h, d) hexachloroethane, THF, -78 °C to rt, 20 h, 72%, e) Ag_2CO_3.

To prepare the precursor **50** (Scheme 40), the synthesis originated from crizotinib, which was Boc-protected, followed by a nucleophilic aromatic substitution with alcohol **46**. Several attempts were made to deprotect the *para*-methoxybenzene (PMB) group in presence of the Boc-protected piperidine. However; little conversion was observed, and the purification was cumbersome. Therefore, an acidic deprotection of the PMB was done, which also led to deprotection of the piperidine. A re-protection of the piperidine and amide was attempted, and a product was isolated with addition of two Boc-groups. This product was reacted with imidazolium salt **44** to give uronium **50**; however, the subsequent synthesis of uronium **50** was not achieved. This may have been due to the a possible Boc-protection of the phenol. To avoid this, *only* the piperidine was protected by using *only* of 1 equiv of $(Boc)_2O$, and then converting the phenol **49** to the uronium **50**. Finally, uronium **50** was then prepared from chloroimidazolium **44** and phenol **49** and this can be directly used for the radiofluorination. The experimental on the alternative strategies attempted to achieve deprotection of the phenol and retain the protection on the free amines, can be seen in Section Failed strategies for protection and deprotection.

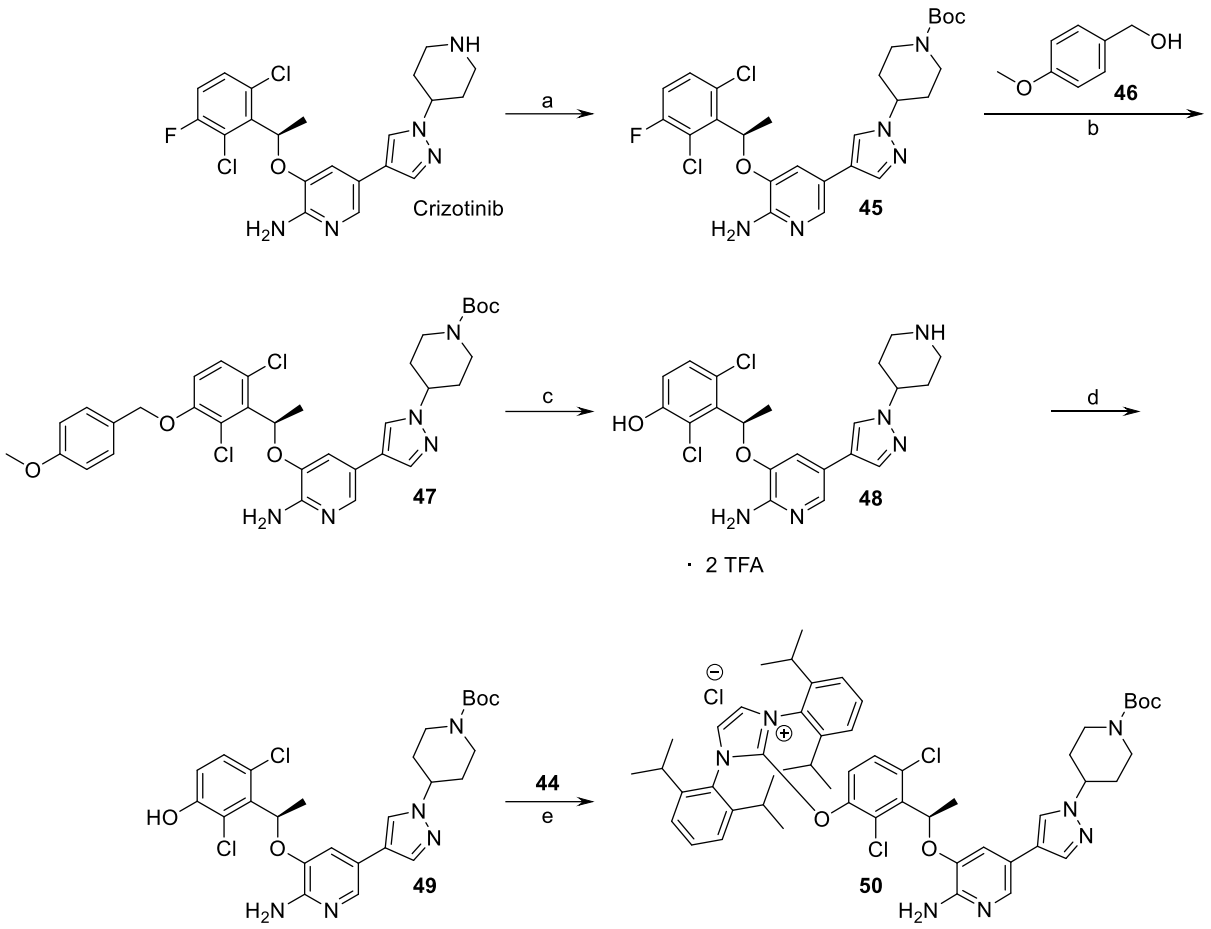

Scheme 40 - Reagents and conditions: a) $(Boc)_2O$, DMAP, THF, rt, 18 h, 91%, b) ***46****, NaH, DMF, µW, 120 °C, 30 min, 55%, c) TFA, CH_2Cl_2, rt, 1 h, quant, d) $(Boc)_2O$, $NaHCO_3$, 1,4-dioxane, rt, overnight, quant, e)* ***44****, $CHCl_3$, 60 °C, quant.*

4.5. Radiofluorination

Radiofluorination for both precursor **38** and **50** was attempted. For the radiofluorination we used the GE Tracerlab Fx_{FN} (Figure 20. This system allows semi-automation of the radiosynthesis, reducing unnecessary radiochemical handling and thus radiochemical exposure to the chemist. The radioactive material ($^{18}F^-$) comes from the cyclotron and is passed over the ion exchange cartridge (V10). $^{18}F^-$ is then eluted with the eluting solvent and counterion (V1). This is then sent to the reactor (V13) and the remaining water in the solution is dried azeotropically. After the drying, the precursor is loaded (V3). After the reaction is finished, the reaction mixture is sent to the prep HPLC (V14). After which, the purified product is collected.

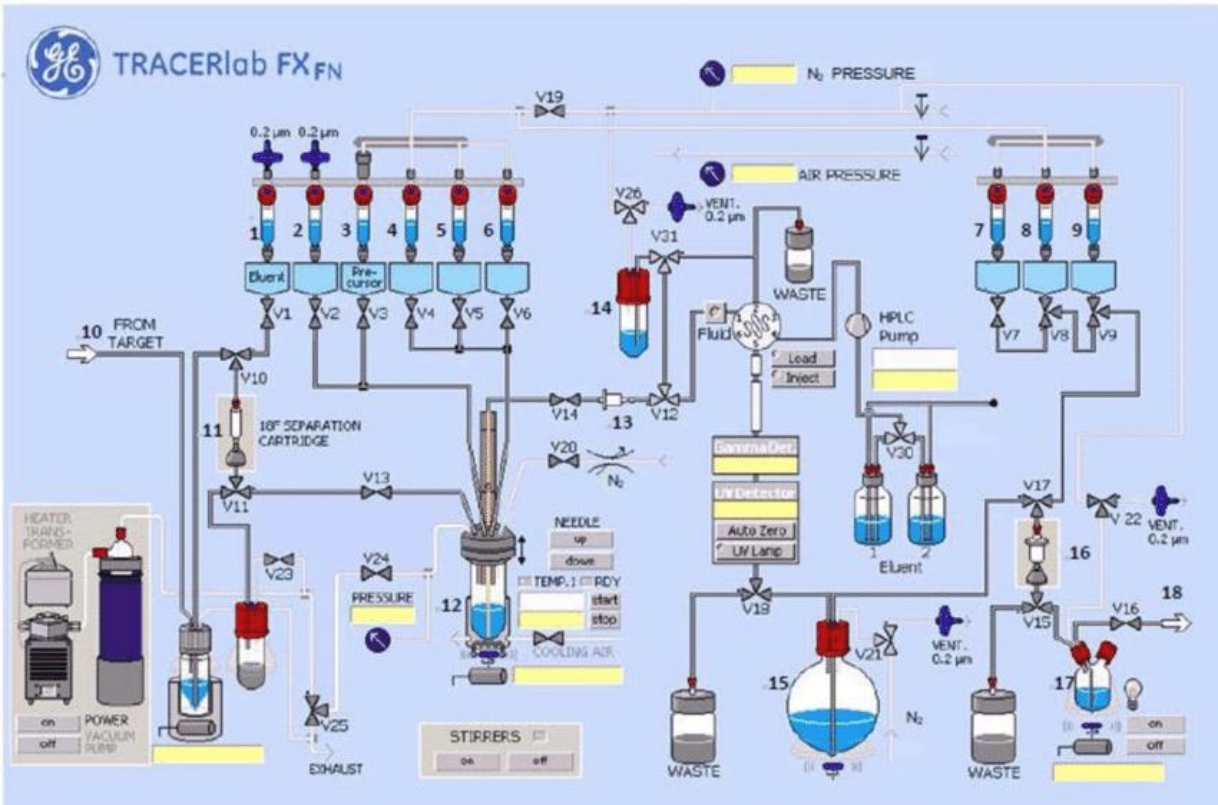

Figure 20 – User interface of GE Tracerlab FX_{FN}. Image was reprinted from Liang et al.[126]

When using this semi-automated system there is some flexibility; however, the flow of solvents is limited to one direction *only*. For radiofluorination using the deoxyfluorination reagent, Neumann *et al*[125] suggested elution of $^{18}F^-$ by using the precursor and thereby removing the azeotropic drying step. However, with our apparatus, this elution method could not be achieved easily. To maximize the elution efficiency, after trapping the $^{18}F^-$ on the cartridge, this cartridge needed to be inverted, followed by the elution with the precursor. But this semi-automated system *only* allowed the flow in one direction; therefore, the reaction had to be performed manually.

A first attempt was made with the precursor **50** and $KHCO_3$ as the additive, but only 15% of the $^{18}F^-$ was recovered from the ion exchange cartridge. After the radiofluorination a 60% conversion of the $^{18}F^-$ was observed; however, no product was observed after the HCl deprotection. In the second attempt 25% of the $^{18}F^-$ was recovered from the ion exchange cartridge; unfortunately, no product was seen after the first step of the reaction. A final attempt was made, but the radioactive material isolated from this reaction did not have the same retention time as unlabeled crizotinib and therefore this precursor and method were abandoned.

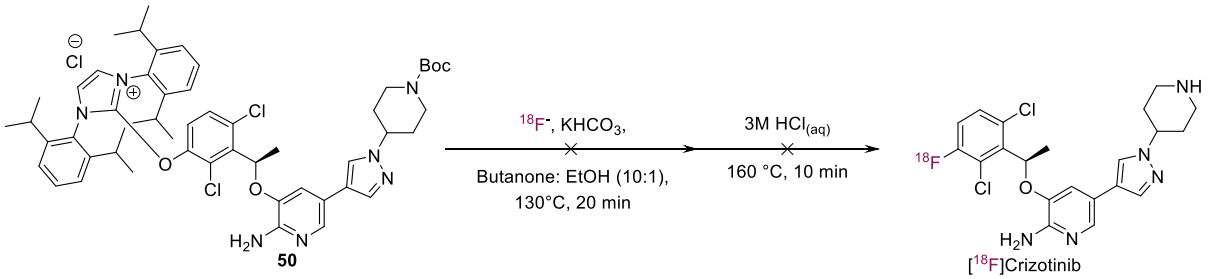

*Scheme 41 - Radiofluorination of activated phenol precursor **50**.*

Efforts were made to develop the F-18 labeled racemic crizotinib from hypervalent iodine(III) precursor **38**. In the first attempt, Et_3NBr was used to elute $^{18}F^-$ from the ion exchange cartridge; however, the recovery of $^{18}F^-$ was low. The reaction was attempted with the recovered $^{18}F^-$ at 120 °C for 10 min and gave 25% conversion. When the reaction was heated for an additional 10 min, a radiochemical conversion of 32% of the $^{18}F^-$ to *(R,S)*-[^{18}F]crizotinib was observed, along with 4% degradation (Table 7, Entry 1). Next step was to remove the Boc-protection of the amine and aniline. For this, the product was diluted with water, and trapped on C-18 cartridge, rinsed with water to remove all DMF and the F-18 labeled material was eluted with 1,4-dioxane. TFA/H_2O (2:1) was added and heated for 120 °C for 10 min. *(R,S)*-[^{18}F]Crizotinib, was observed on HPLC.

To avoid the solvent switch for the deprotection, 3M HCl was added to the reaction mixture and used for the deprotection of $(Boc)_2O$; however, only partial deprotection was observed (Table 7, Entry 2).

*Table 7 - Radiofluorination with hypervalent iodine(III) **38**.*

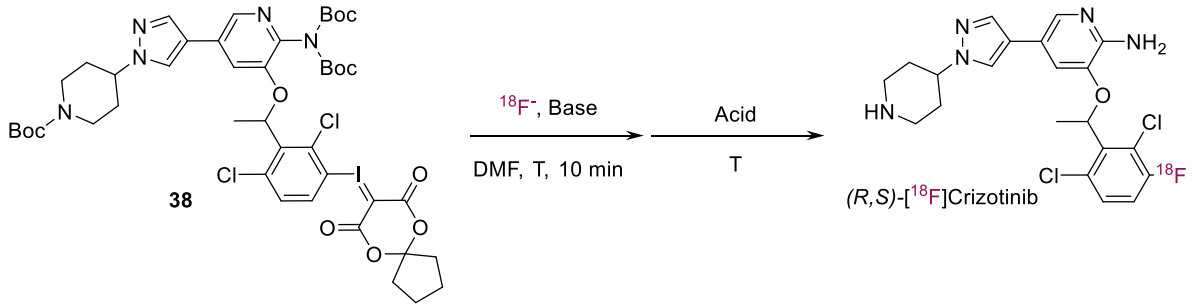

	Radiofluorination				Deprotection		
Entry	**Base**	**T_1 °C**	**t_1 (min)**	**RCC after radiofluorination**	**T_2 °C**	**t_2 (min)**	**Acid**
1.	Et_3NBr	120	10 (+10)	25% (32%)	120	10	TFA
2.	Et_3NBr	120	10	56%	120	10	3M HCl
3.	Et_3NHCO_3	140	10	15%			
4.	Et_3NHCO_3	160	10	52%	160	10	3M HCl

To achieve a better elution of $^{18}F^-$, the base was switched to Et_3NHCO_3. In addition, the reaction temperature was raised to 140 °C; then 160 °C, which gave a conversion of 52% after 10 min and deprotection with 3M HCl at the same temperature for 10 min gave full conversion to F-18 labeled crizotinib (Table 7, Entry 4).

With the optimized conditions in hand, the purification setup up was investigated by varying columns, eluents (MeOH, MeCN) and pH (3 and 10). The main issue that was observed was the poor solubility of crizotinib in classical prep-HPLC eluents, these eluents are usually MeOH or MeCN based. To improve the solubility of crizotinib for the purification, THF was added to the eluents. The final purification as performed with H_2O/MeOH/THF/TFA (70/20/10/0.1, v/v/v/v) using Symmetry® C18 column (300 x 7.8 mm, 7 µm). With these purification conditions, *(R,S)*-[^{18}F]crizotinib, was isolated by Dr Fabien Caillé with 15 ± 5% RCY d.c. and MA of 60 ± 10 GBq/µmol (n = 7). Synthesis of the *(R)*-[^{18}F]crizotinib is currently ongoing instead of racemate.

4.6. Conclusion and Future Perspectives

Two precursors were synthesized for the radiofluorination of crizotinib. [^{18}F]Crizotinib was prepared in a two-step one-pot protocol from the hypervalent iodine(III) precursor **38** using the GE Tracerlab FX_{FN}. *rac*-[^{18}F]Crizotinib was obtained with 15 ± 5% RCY and MA of 60 ± 10 GBq/µmol (n= 7).

Investigations to radiolabel *(R)*-[^{18}F]crizotinib and PET imaging of the P-gp function at the blood-brain barrier of rodents are ongoing.

Summary of Findings

5. Summary of Findings and Future Perspectives

Isotopically labeled drugs have found many applications in the drug discovery programs. However, incorporation of an isotope into drug molecules is not trivial. There is a limited availability of starting materials and it is important to consider the generation of radioactive waste when using radionuclides. The work presented in this thesis was focused on the development of a late-stage labeling method.

Amide groups are a very prevalent functional group in drugs and are often metabolically stable as well. While there are many robust methods for the labeling of amides with carbon labeling, they are often limited to aryl, alkenyl and benzyl substrates. The work presented in chapter 2 has explored visible-light mediated palladium catalysis to enable incorporation of labeled CO (Scheme 42). This method can easily be used with C-12, C-13 and C-14, when using *COgen as the labeled CO source. Moderate to low yields were obtained for this late-stage labeling for a wide range of alkyl substrates. In addition, aryl iodides could also be used as substrates for this reaction. It would be interesting to expand the substrates chemical diversity and gain more understanding of the mechanism.

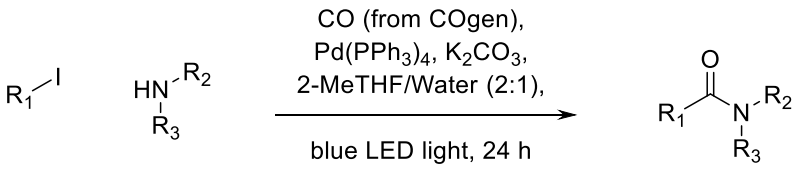

Scheme 42 – Late-stage labeling of alkyl amides with labeled carbon monoxide.

While the work above is focused towards labeling with labeled CO, the labeled CO releasing molecule which we used was synthesized in two-steps plus an additional step for the liberation of labeled CO. Therefore, efforts were made to adapt recent advances in direct

reduction of labeled CO_2 to labeled CO; thereby, eliminating the need of isolating and additional handling of radioactive material (Scheme 43). Preliminary results in chapter 3 have shown that reduction of labeled CO_2 with disilane is very promising. This methodology needs further development, and its applicability on a wide variety of pharmaceutically relevant compounds needs to be shown.

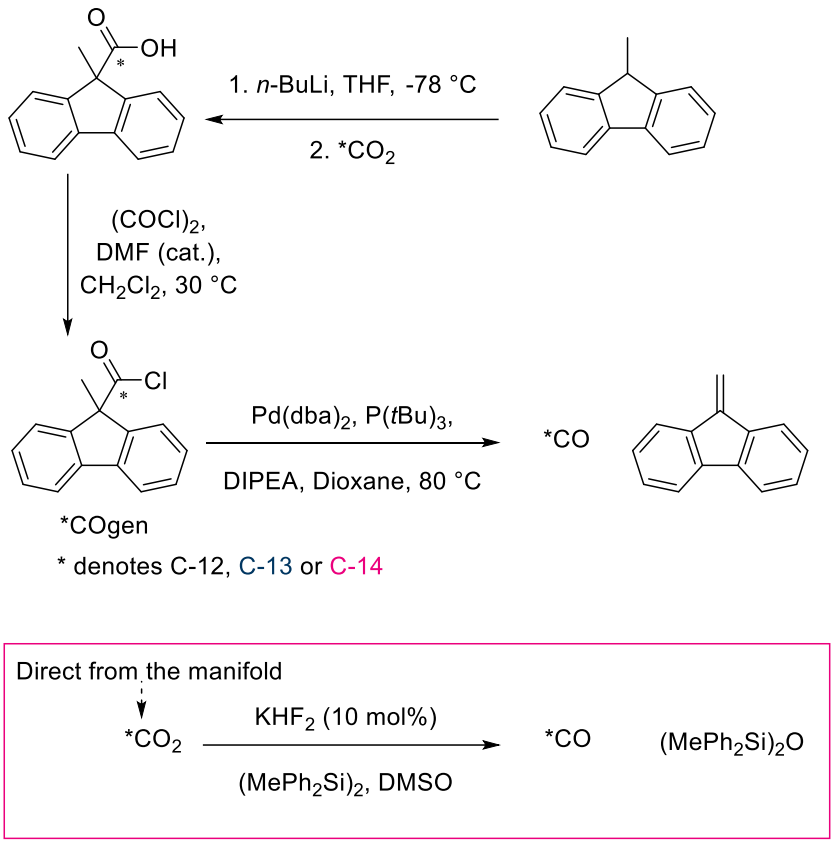

*Scheme 43 – Comparison of two-step synthesis of *COgen along with one-step for the liberation of *CO, versus a one-step reduction of *CO_2 to *CO.*

Lastly, within the ISOTOPICS consortium there was an opportunity to spend three months at a PET facility. For this PET project we aimed to develop crizotinib as a PET tracer for P-gp. Crizotinib is a tyrosine kinase inhibitor and a treatment for non-small cell lung carcinoma and its brain accumulation is restricted by P-gp and is unable to treat brain metastasis. For this purpose, we aimed to label crizotinib with F-18 as this would not alter the chemical structure

and the biological properties would be retained. Suitable conditions were identified for the synthesis of *(R,S)*-[^{18}F]crizotinib (Scheme 44). Currently, the investigations to radiolabel enantiomerically pure *(R)*-[^{18}F]crizotinib are on-going to perform rodents imaging studies.

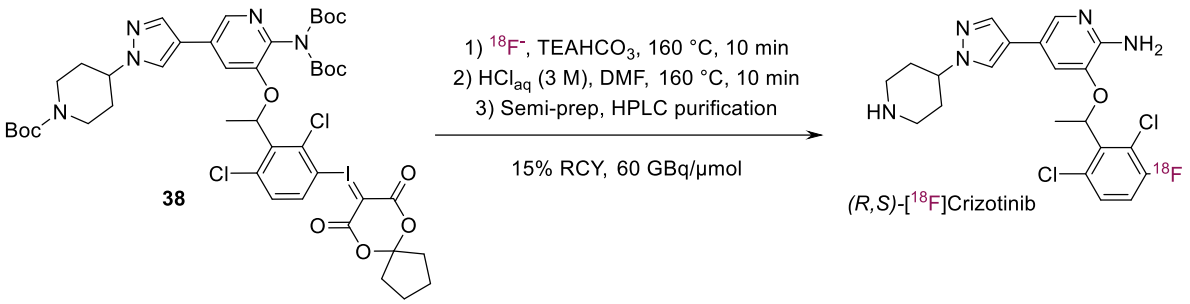

Scheme 44 – Radiofluorination of crizotinib for the imaging of P-gp at the blood-brain barrier.

6. Résumé de la thèse

La découverte et le développement de nouveaux médicaments et un processus complexe qui s'étend sur une quinzaine d'années avant qu'un nouveau traitement ne soit commercialisé (Figure 21).[1] Le coût de développement d'une nouvelle entité chimique thérapeutique est élevé (environ 2 milliards d'euros) avec un taux de réussite faible puisque moins de 10% des candidats médicaments entrant en essais cliniques sont finalement mis sur le marché. Ce fort taux d'attrition peut être attribué à une faible efficacité des molécules, une mauvaise compréhension du comportement des médicaments *in vivo* et une évaluation insuffisante des effets secondaires, notamment au cours des essais cliniques de phase II. De nombreuses études impliquant le marquage de candidats médicaments à l'aide de différents isotopes sont réalisées durant les différentes étapes de développement afin de mieux comprendre les divers aspects de l'absorption, de la distribution, du métabolisme et de l'excrétion (ADME) ainsi que les aspects toxicologiques. Les candidats médicaments peuvent être marqués à l'aide d'isotopes stables (H-2, C-13 or N-15), d'isotopes à période longue (H-3 or C-14) pour les études *in vitro* et *ex vivo* et des émetteurs de positrons à période brève (C-11 or F-18) pour les études *in vivo*.

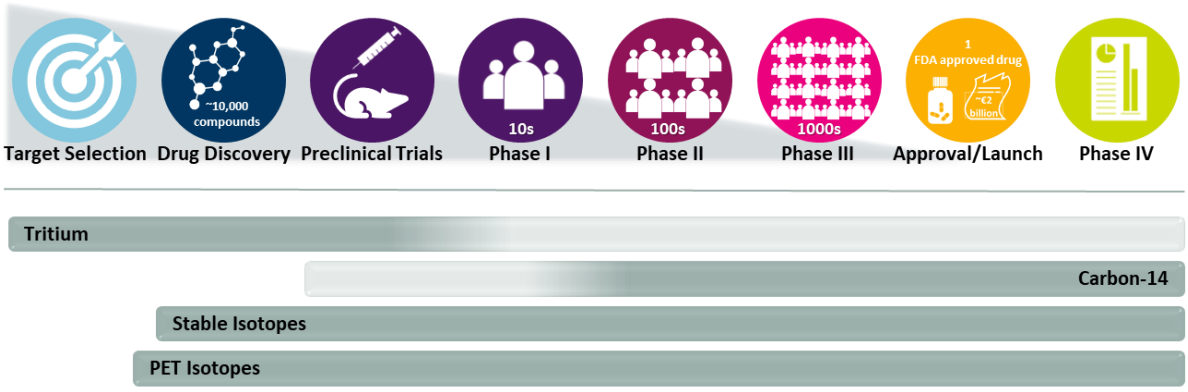

Figure 21 – Les 8 étapes du développement d'un nouveau médicament : à partir d'environ 10.000 composés, on peut espérer aboutir à 1 médicament mis sur le marché. Les différents isotopes utilisés au cours du processus sont indiqués en dessous.

Les produits marqués par des isotopes stables peuvent être suivis en spectrométrie de masse grâce à la signature isotopique particulière du compose marqué qui peut être utilisée pour la quantification absolue du composé d'origine et la quantification relative de ses métabolites dans des échantillons biologiques (Figure 22).[10]

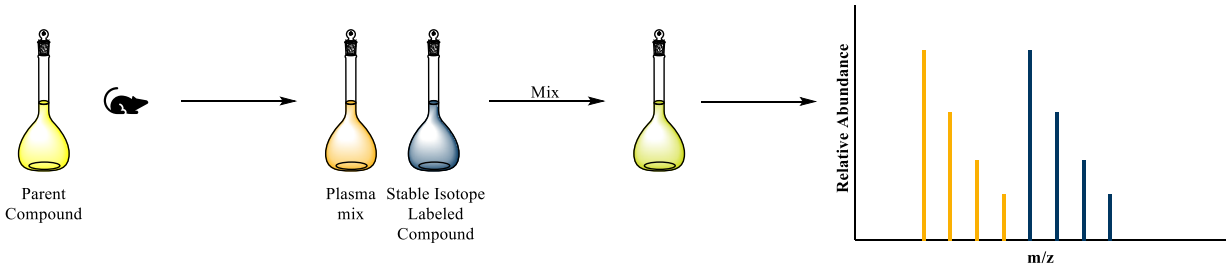

Figure 22 – Quantification des composés parents à l'aide d'isotopes stables mélangés au produit injecté en milieu biologique et analysé par chromatographie liquide couplée à de la spectrométrie de masse. Adapté d'Iglesias et al.[10]

Les composés marqués avec des isotopes radioactifs facilitent la détection, la traçabilité et la quantification du médicament et de ses métabolites par comptage ou imagerie béta pour les radio-isotopes à périodes longues (H-3, C-14) ou par imagerie par émission de positrons (TEP) pour les radio-isotopes à périodes brèves (C-11, F-18). Ainsi, le marquage avec des isotopes radioactifs de l'hydrogène, du carbone et du fluor ont trouvé de nombreuses applications pour l'identification de candidats médicaments ainsi que les études précliniques et les phases d'essais cliniques.

La synthèse de composés marqués (notamment par des isotopes radioactifs) est généralement semblable à celle des composés d'origine. Cependant, la position du marquage imposée par la métabolisation potentielle du candidat médicament influence considérablement les voies de synthèse à partir de précurseurs disponibles. L'introduction précoce du radiomarquage est générateur de déchets dont le traitement et coûteux. Inversement, l'introduction tardive du marquage radioactif, plus économique et plus écologique, pose des problèmes techniques liés à la complexité et la fragilité de molécules à haute valeur ajoutée. Ainsi, le radiochimiste dispose pour le moment d'un nombre limité de méthodes compatibles avec cette dernière approche, notamment dans le cas d'un marquage avec des radio-isotopes du carbone (C-11, C-14), méthodes à laquelle nous nous sommes intéressés au cours de cette thèse de doctorat.

La réaction de carbonylation avec le monoxyde de carbone (CO) radiomarqué est une technique intéressante pour l'incorporation tardive de radio-isotopes via des réactions de couplage polyvalentes et généralisables.[72,83] Les méthodes classiques de carbonylation utilisent la catalyse par des métaux de transition (par exemple le palladium) qui permettent l'incorporation de CO par formation de groupement cétones, acides carboxyliques, esters et amides dans des composés bio-actifs complexes.[65] Cependant, la plupart de ces méthodes ne

sont applicables qu'avec des substrats de type halogénures ou triflates d'aryle ou de vinyle.[96,97] Les procédures utilisant les halogénures utilisent généralement des excès de CO, ce qui est incompatible avec les conditions de marquage radioactif en raison des coûts de la matière première radiomarquée mais aussi du traitement des déchets radioactifs.[88]

Cette thèse présente un travail exploratoire sur le radiomarquage de médicaments et d'analogues, catalysé par le palladium sous lumière visible afin de permettre leur marquage par incorporation de CO en conditions quasi-stochiométriques (Scheme 45).[85] Nous avons choisi de marquer la fonction amide, groupe fonctionnel très fréquent dans de nombreux médicaments et qui est métaboliquement stable. Cette méthode, développée en C-12 peut être aisément appliquée au C-13 et C-14 en utilisant le *COgen comme source de marquage par le CO. Des rendements moyens ont été obtenus avec cette stratégie de marquage tardif pour une grande vérité de substrats de type alkyle tandis que les iodures d'aryles peuvent également être utilisés pour cette réaction. Il serait intéressant d'étendre la diversité chimique des substrats et de mieux comprendre le mécanisme de la réaction afin d'améliorer son efficacité.

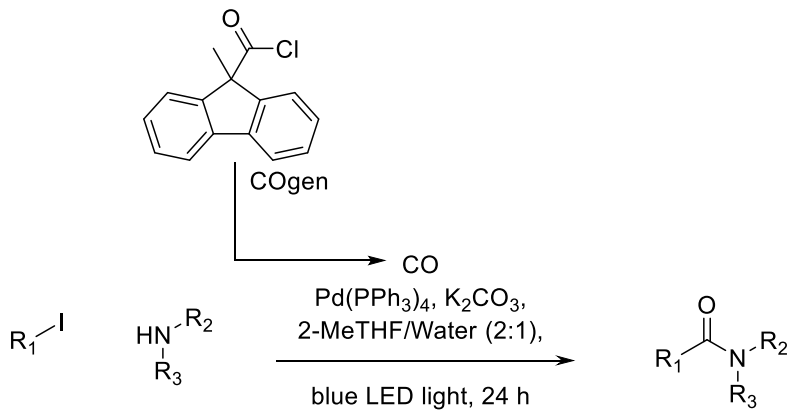

Scheme 45 – Formation d'alkyle carboxamides à partir de CO pour le radiomarquage tardif de médicaments.

Dans le travail précédent consacré au marquage à l'aide de CO, le précurseur solide COgen est synthétisé en deux étapes auxquelles s'ajoutent une étape de libération du CO. Afin de simplifier cette procédure de génération du CO marqué, nous avons tenté de mettre à profit les récentes avancées en matière de réduction directe du CO_2, éliminant ainsi les étapes intermédiaires de purification et d'isolement (Scheme 46). Les résultats préliminaires

présentés dans cette thèse ont montré que la réduction de CO_2 avec le disilane est très prometteuse pour le marquage d'une grande variété de molécules d'intérêt pharmaceutiques par le C-13 et le C-14 et pourrait être adaptée au marquage par le C-11.

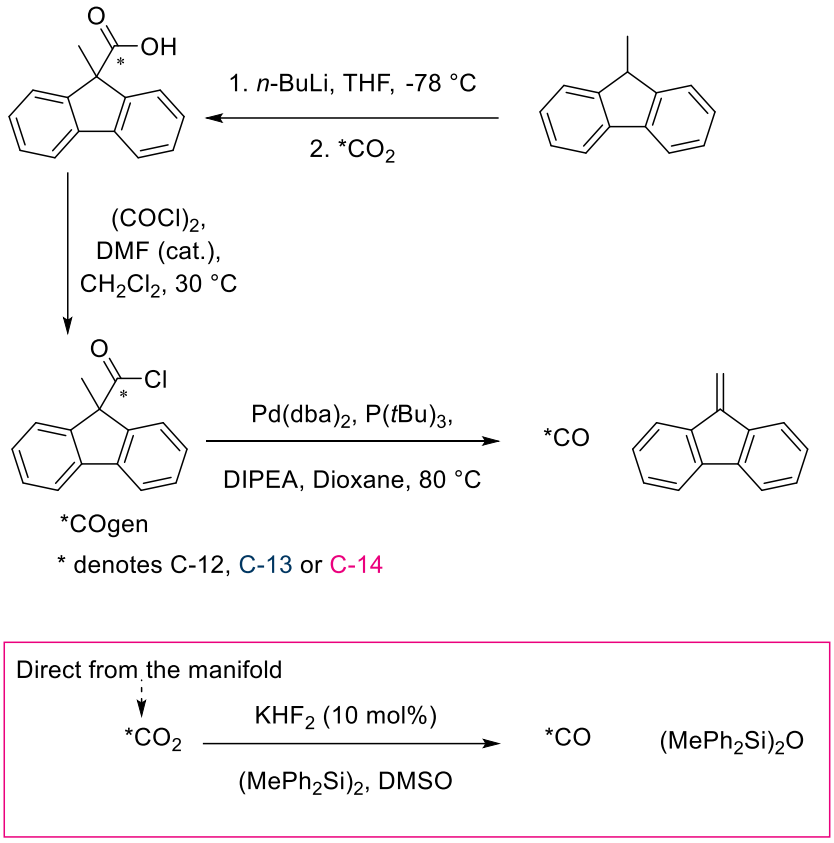

*Scheme 46 – Synthèse du *COgen en trois étapes (incluant la libération du *CO), comparée à la réduction en une étape du *CO_2 en *CO.*

Finalement, dans le cadre d'un détachement au Service Hospitalier Frédéric Joliot Curie (SHFJ) du CEA faisant partie du projet européen ISOTOPICS, j'ai eu l'opportunité de passer 3 mois dans les laboratoires de marquage pour l'imagerie TEP. La TEP est une méthode d'imagerie non-invasive et permet de cartographier la distribution *in vivo* de radionucléides émetteurs de positrons (radio-isotopes à très courte période) qui sont injectés à des mammifères. Les radio-isotopes les plus utilisés pour ces études sont C-11, F-18, N-13 et O-15 avec des périodes de respectivement 20.8 mn, 110 mn, 9.96 mn and 2.04 mn. Dans le cas de C-11, N-13 and O-15, il est indispensable qu'un cyclotron soit présent sur site compte-tenu des très courtes périodes de ces éléments tandis que le fluor-18 peut-être fourni par un producteur extérieur.[113] Ainsi les étapes de réaction, de traitement, de purification et de formulation peuvent être réalisées dans un délai correspondant à deux ou trois fois la période du radionucléide qui doit-être incorporé préférentiellement en dernière étape de synthèse.

Pour ce project de marquage, nous avons entrepris de développer un nouveau traceur pour l'imagerie TEP de la P-glycoprotein (P-gp) qui est un transporteur de la barrière hématoencéphalique jouant un rôle crucial dans l'efflux extra-cérébral de diverses substances exogènes et qui intervient également dans l'élimination des molécules anti-tumorales hors des cellules cancéreuses.[105,106]

Le crizotinib est un inhibiteur de tyrosine kinase inhibitor servant pour le traitement du cancer du poumon "non à petites cellules" dont l'accumulation intracérébrale est limitée par la P-gp, empêchant ainsi un traitement efficace des métastases dans le cerveau. Notre but était de développer un traceur TEP dérivé du crizotininb présentant une distribution intra-cérébrale non-altérée. Nous avons finalement choisi de marquer le crizotinib au F-18 sans en altérer la structure ni les propriétés biologiques selon une voie de synthèse décrite dans le Scheme 47 et aboutissant au of *(R,S)*-[^{18}F]crizotinib. A présent, les études sont en cours pour radiomarquer le *(R)*-[^{18}F]crizotinib énantiomériquement pur afin de réaliser l'imagerie TEP sur des rongeurs.

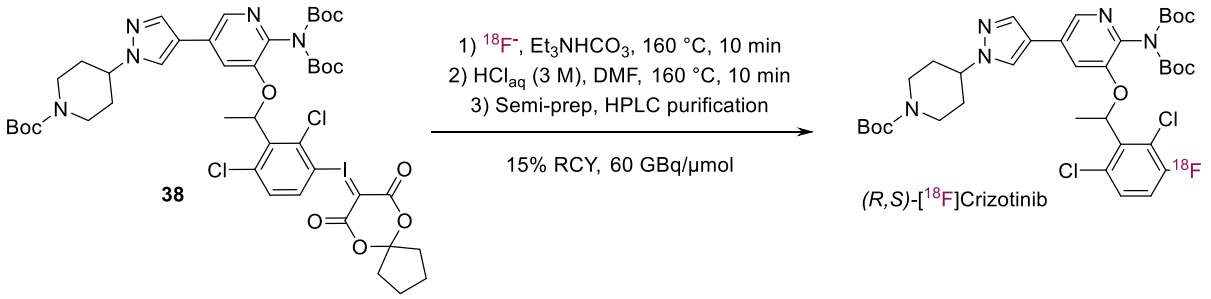

Scheme 47 – Radiofluoration du crizotinib pour l'imagerie TEP de la P-gp au niveau de la barrière hématoencéphalique.

Experimental

7. Experimental: Visible-Light Enabled Aminocarbonylation of Unactivated Alkyl Iodides with Stoichiometric Carbon Monoxide for Application on Late-Stage Carbon Isotope Labeling

7.1. General Information

General Reactions

All reagents were purchased from commercial suppliers and used without further purification, unless mentioned otherwise. Anhydrous solvents were purchased from Sigma Aldrich and stored under nitrogen atmosphere. 9-Methyl-9H-fluorene-9-carbonyl chloride and 9-Methylfluoren-9-[^{14}C]-carbonyl chloride (respectively, COgen and ^{14}COgen) was prepared according to the procedure of Skrydstrup et al[83] and commercially available two chamber glassware apparatus (COware) was purchased from Sytracks and used for the carbonylation reactions. Yields are based on the COgen and refer to purified, isolated, homogenous product and spectroscopically pure material, unless stated otherwise.

Reaction Setup

All reactions were carried out under a nitrogen atmosphere and were magnetically stirred. Electric heating plates and DrySyn were used for elevated temperatures and stated temperatures corresponds to the external DrySyn temperature. Blue S6 LED strips (15 V, 15W/meter, 4.67m, λ = 465.2 nm) were used, provided by LED Teknik Boras Sweden, no filters were used (see below for full LED report). The distance between the COware (borosilicate glass) and the blue LED strips is between 2 and 4 cm, reactions were repeated on all positions, and comparable results were obtained. Concentration was performed on a rotary evaporator at 40 °C at appropriate pressure.

Reaction mixture

Crude reaction mixture was assayed by GC-MS or LC-MS and quantified by NMR with anisole as internal standard. LC-MS analysis was performed on a Waters Acquity UP-LC using either

- Method A: BEH C18 column (50 mm x 2.1 mm, 1.7 µm particles) with a 10-90% gradient over 2 or 4 min with MeCN-NH_4/NH_4CO_3;
- Method B: BEH C18 column (50 mm x 2.1 mm, 1.8 µm particles) with a 10-90% gradient over 2 or 4 min with MeCN-formic acid and electrospray ionization.

GC-MS (EI) analysis was performed on a 7890A GC system and 5975C inert MSD system equipped with an Agilent 19091S-433L (30 m x 250 µ x 0.25 µm) capillary column using a gradient: 40-150 °C with a rate of 15 °C/min, followed by 150-300 °C with a rate of 60 °C/min, and electron impact ionization at 70 eV.

Thin layer chromatography was carried out using E. Merck silica glass plates (60F-254) with UV light (254 nm) and/or iodine vapor/potassium permanganate as the visualization agent.

Purification

Crude reaction mixtures were purified by either flash chromatography prepacked Isolute® SI columns or Biotage SNAP columns using a Biotage automated flash systems with UV detection or preparative reversed phase HPLC purifications using a Gilson 322 Pump equipped with a Gilson UV/Vis-152 lamp with an Xbridge™ Prep C-18 10 µm OBD™ 19 x 250 mm column.

Analysis

^{1}H NMR and ^{13}C NMR spectra were recorded on a Bruker AVANCE III system running at proton frequency of 500.1 MHz with a cryogenic probe or on a Bruker Avance Nanobay system at 400.13 MHz and processed with the NMR software MestreNova (Mestrelab Research SL). NMR experiments were run in $CDCl_3$ at 25°C, unless stated otherwise. ^{1}H chemical shifts are referenced relative to the residual solvent peak at 7.26 ppm, and ^{13}C chemical shifts are referenced to 77.67 for $CDCl_3$. Signals are listed in ppm, and multiplicity identified as s = singlet, br = broad, d = doublet, dt = doublet of a triplet, t = triplet, tt = triplet of a triplet, q = quartet, quin = quintet, h = hextet, m = multiplet; coupling constants in Hz; integration. ^{13}C NMR data is reported as with chemical shifts. For purity, quantitative NMR spectroscopy (qNMR) was performed with 2,3,5,6-tetrachloronitrobenzene (Tokyo Chemical Industry Co. Ltd. Japan, lot 242) (unless mentioned otherwise) as an internal calibrant in 0.6 mL $CDCl_3$ (glass ampules, Sigma Aldrich).[127] Purity was calculated with the NMR processing software, MestreNova. Accurate mass values were determined for compounds that have not been reported in the literature on a Waters Xevo Q-TOF mass spectrometer with an electro spray ion source in positive mode. Purity assays were also performed on the aforementioned LC-MS and GC-MS systems, if there was a substantial amount of UV signal. Radiochemical purity was determined by HPLC using either

- Setup 1: Waters 2695 Separations module equipped with Waters x Select CSH C18 2.5 µm, 3 x 100 mm column and with a radioactivity flow monitor using a Perkin-Elmer Radiomatic 500 TR with Ultima Gold cocktail. Gradient method was used for radiochemical purity determination with mobile phase A (water with 0.2% formic acid adjusted to pH 3) and B (95% MeCN/water 0.2% Formic acid pH 3) with gradient

elution (50% B for 0-3 minutes, then ramp to 100% B over 17 min and hold at 100% B for 5 min).

- Setup 2: Waters Acquity UPLC with Waters Xbridge C18 3.5 µm, 4.6 x 100mm column was used along with Perkin-Elmer TRI-CARB 2500 liquid scintillation analyser with Ultima Gold cocktail. Gradient method was used for radiochemical purity determination with mobile phase A (10mM NH_4HCO_3 buffered with NH_4OH) and B (MeCN) with gradient elution (5% for 0-3 minutes, then ramp to 95% over 22 min and hold at 95% for 5 minutes).

LED report of the blue LEDs

LED Integrated Testing System test report

test item:	LED spectrum analyse			
equipment:	Led test system			
Test Identifier	Product	Blue S6	Manufacturer:	Ledteknik
	Temperature	23 ° C	Humidity:	30 %
	Conner:	MOL	Date:	20120823
	Organ:	LEDteknik AB		

curve of spectrum power distributing

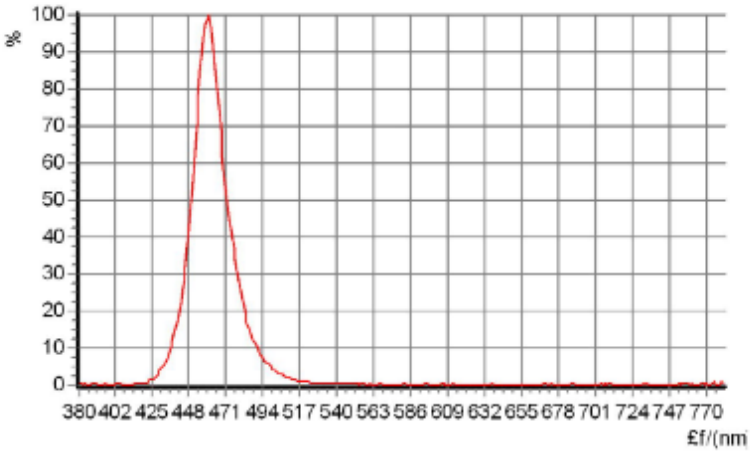

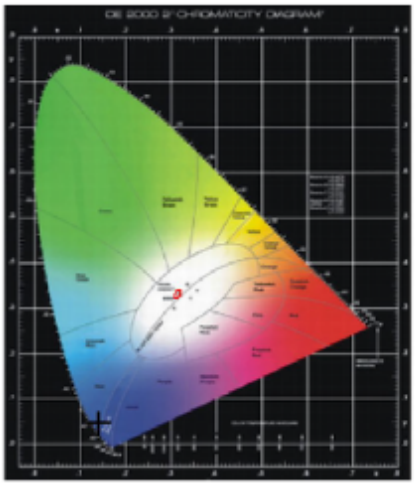

Spectrum		Electrical	
λ (Peak):	460.4 nm	I(test):	120.4 mA
λ (Main):	465.2 nm	V(Positive):	12.000 V
λ (Centroid):	450.7 nm	Φv:	33497.9 mlm
λ (Center):	451.0 nm	Light Effi:	23.185 lm/w
BandWidth:	23.0 nm	Light Power:	554.4217 mw
ColorTemp:	K		
(x, y):	0.1418, 0.0503		
(u, v):	0.1708, 0.0909		
Ra:	0.0		
Color Purity:	0.966		

7.2. General Procedures

General Procedure for Chamber B, CO Producing Chamber

Chamber B was loaded in the following order $Pd(dba)_2$ (5%, 0.03 mmol), toluene (3 mL), tri-tert-butyl phosphane (5%, 0.03 mmol) and N,N-diisopropylethylamine (1.5 equiv, 0.9 mmol). The chamber was sealed with Teflon-lined PTFE septa and stabilizing disc. The chamber is purged with N_2, after which COgen (1 equiv, 0.6 mmol in toluene, 2 mL) is added and the chamber is stirred and heated to 70 °C.

General Procedure for Aminocarbonylation Chamber A, CO Consuming Chamber

To chamber A was added $Pd(PPh_3)_4$ (5%, 0.03 mmol), K_2CO_3, (1 equiv, 0.6 mmol), 2-MeTHF (3.5 mL), alkyl iodide (1 equiv, 0.6 mmol), amine (3 equiv, 1.8 mmol) and water (1.5 mL). The chamber was sealed with a Teflon lined PTFE septa and stabilizing disk. The chamber was purged for 5 min. The chamber was irradiated with visible blue light and stirred for 24 h. The reaction mixture was extracted with CH_2Cl_2 (3 x 10 mL) over a phase separator and concentrated in vacuo, unless mentioned otherwise. Purification was performed using either manual system, Biotage automated normal purification system or reversed phase HPLC purification.

Characterization data

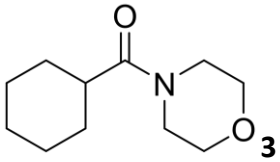

3

Preparation of c*yclohexyl(morpholino)methanone* ***3*** *(CAS 29338-96-3).*[94] Chamber A was loaded according to the general procedure with iodocyclohexane (78 µL, 0.6 mmol) and morpholine (155 µL, 1.80 mmol) in 2-MeTHF (3.5 mL) and water (1.5 mL) as solvent system. Chamber B was loaded according to the general procedure for CO releasing chamber. Purification was performed on a 25g SNAP column with 25% EtOAc in Heptane over 20 min. Fractions containing product were pooled and concentrated to give the desired product (72.2 mg, 61%).

Data for **3**: ^{1}H NMR (400 MHz, $CDCl_3$) δ 1.17 – 1.32 (m, 3H), 1.52 (m, 2H), 1.70 (d, J = 12.94 Hz, 5H), 2.42 (tt, J = 3.41, 3.41, 11.58, 11.58 Hz, 1H), 3.44 – 3.71 (m, 8H).

^{13}C{^{1}H} NMR (100.6 MHz, $CDCl_3$) δ 174.6, 67.0, 66.8, 45.8, 41.9, 40.2, 29.3, 25.75, 25.74.

NMR purity assay: 95%.

[^{13}C-*carbonyl*]3 – 1.2 mmol

Preparation of c*yclohexyl(morpholino)methanone* ***[^{13}C]3***. Chamber A was loaded according to the general procedure with iodocyclohexane (155 µL, 1.2 mmol), morpholine (311 µL, 3.6 mmol), K_2CO_3 (166 mg, 1.2 mmol), $Pd(PPh_3)_4$ (69.3 mg, 0.06 mmol) in 2-MeTHF (3.5 mL) and water (1.5 mL) as solvent system. Chamber B was loaded according to the general procedure CO releasing chamber with $Pd(dba)_2$ (34.5 mg, 0.06 mmol), P(*t*-Bu)$_3$ (60 µL, 0.06 mmol), N,N-diisopropylamine (315 µL, 1.81 mmol) in toluene (5 mL), and at last [^{13}C]COgen (292 mg, 1.2 mmol). Purification was performed on 25g SNAP column with 0-60% EtOAc in Heptane. Fractions containing product were pooled and concentrated to give the desired product (86.3 mg, 38%).

Data for **[^{13}C-*carbonyl*]3**: ^{1}H NMR (400 MHz, $CDCl_3$) δ 1.2 – 1.33 (m, 3H), 1.53 (q, 2H), 1.64 – 1.75 (m, 3H), 1.75 – 1.87 (m, 2H), 2.42 (dtd, 1H), 3.42 – 3.73 (m, 8H).

^{13}C NMR (101 MHz, $CDCl_3$) δ 174.9, 67.1, 40.7, 40.1, 29.5, 29.5, 25.99, 25.95.

NMR purity assay: 96.1%.

3 – 1.2 mmol

Preparation of c*yclohexyl(morpholino)methanone **3**.* Chamber A was loaded according to the general procedure with iodocyclohexane (155 µL, 1.2 mmol), morpholine (311 µL, 3.6 mmol), K_2CO_3 (166 mg, 1.2 mmol), $Pd(PPh_3)_4$ (69.3 mg, 0.06 mmol) in 2-MeTHF (3.5 mL) and water (1.5 mL) as solvent system. Chamber B was loaded according to the general procedure CO releasing chamber with $Pd(dba)_2$ (34.5 mg, 0.06 mmol), P(*t*-Bu)$_3$ (60 µL, 0.06 mmol), N,N-diisopropylamine (315 µL, 1.81 mmol) in toluene (1 mL), and at last COgen (291 mg, 1.2 mmol, 0.3M, 4 mL). Purification was performed on 25g SNAP column with 0-60% EtOAc in Heptane. Fractions containing product were pooled and concentrated to give the desired product (85 mg, 36%).

NMR purity assay: 96.6%.

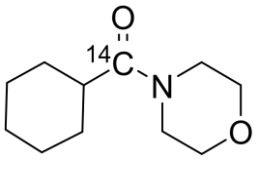

[^{14}C-*carbonyl*]3

Preparation of [^{14}C]c*yclohexyl(morpholino)methanone **3**.* Chamber A was loaded according to the general procedure and reaction procedure for **3**. Chamber B was loaded according to the general procedure for CO releasing chamber COgen (129 mg, 0.57 mmol) and [^{14}C]COgen (65.7 MBq, 0.03 mmol) was used. Purification was performed on a 20g Flash Si column with 25% EtOAc in Heptane. Fractions containing product were pooled and concentrated in vacuo to give the desired product (32.96 MBq, 0.117 TBq/mol, 50%).

Radio-HPLC (setup 1) 98.87%.

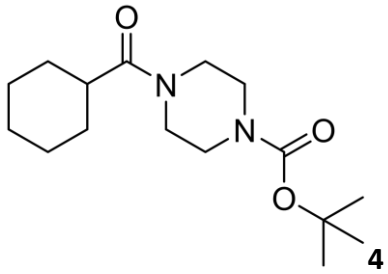

4

Preparation of tert-butyl 4-(cyclohexanecarbonyl)piperazine-1-carboxylate ***4*** (CAS 1328099-31-5). Chamber A was loaded according to general procedure iodocyclohexane (78 µL, 0.6 mmol) and tert-butyl piperazine-1-carboxylate (343.2 mg, 1.84 mmol). Chamber B was loaded according to the CO releasing chamber. Purification was performed on a 10g Flash Si column with 25% EtOAc in n-Heptane. Fractions containing product were pooled and concentrated in vacuo to give the desired product (88.7 mg, 50%).

Data for **4**: ^{1}H NMR (400 MHz, $CDCl_3$) δ 1.23 – 1.28 (m, 2H), 1.44 – 1.59 (m, 11H), 1.65 – 1.84 (m, 5H), 2.44 (tt, J = 11.6, 3.3 Hz, 1H), 3.31 – 3.65 (m, 8H).

^{13}C{^{1}H} NMR (101 MHz, $CDCl_3$) δ 174.9, 154.7, 80.4, 77.5, 77.4, 77.2, 76.8, 45.3, 43.9, 41.5(broad peaks due to conformation change), 40.6, 29.5, 28.5, 25.96, 25.94.

NMR purity assay 90%.

HRMS (ESI-TOF) m/z: $[M+H]^+$ Calcd for $C_{16}H_{28}N_2O_3$ 297.2178; Found 297.2195.

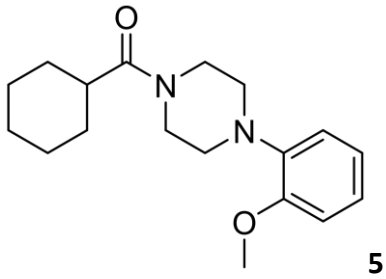

5

Preparation of cyclohexyl(4-(2-methoxyphenyl)piperazin-1-yl)methanone **5** (CAS 260553-25-1 - new). Chamber A was loaded according to the general procedure with iodocyclohexane (78 µL, 0.6 mmol) and 1-(2-methoxyphenyl)piperazine hydrochloride (2.52 equiv, 346 mg, 1.51 mmol). Chamber B was loaded according to the general procedure for the CO releasing chamber. Purification was performed *via* HPLC (5-70% MeCN – 0.1% TFA in water over 20 min, wavelength 220nm, 15mL/min). Fractions containing product were pooled and lyophilized to give product as TFA salt. The product was partitioned in 5 mL CH_2Cl_2 and 5 mL Na_2CO_3. The layers are separated over a phase separator. The aqueous layer was washed with CH_2Cl_2 (5 x 5mL). The organic layers were combined and concentrated to give the free product (67.1 mg, 37%).

Data for **5**: ^{1}H NMR (400 MHz, $CDCl_3$) δ 1.23 – 1.37 (m, 3H), 1.5 – 1.63 (m, 2H), 1.66 – 1.86 (m, 6H), 2.52 (tt, J = 3.31, 3.31, 11.55, 11.55 Hz, 1H), 3.05 (dt, J = 4.78, 4.78, 17.63 Hz, 4H), 3.67 – 3.73 (m, 2H), 3.79 – 3.84 (m, 2H), 3.89 (s, 3H), 6.87 – 6.97 (m, 3H), 7 – 7.1 (m, 1H).

^{13}C{^{1}H} NMR (101 MHz, $CDCl_3$) δ 174.6, 152.2, 123.6, 121.0, 118.5, 111.3, 77.3, 77.2, 77.0, 76.7, 55.4, 51.3, 50.7, 45.6, 41.7, 40.4, 29.4, 25.89, 25.86. A peak at 140 ppm missing, however strong correlation on HMBC suggests it is a quaternary aromatic carbon.

NMR purity assay: 96.7%.

LC-MS (Method B, 4min): 303.0 $[M+H]^+$, rt 2.07 min (100%).

HRMS (ESI-TOF) m/z: $[M+H]^+$ Calcd for $C_{18}H_{26}N_2O_2$ 303.2072; Found 303.2070.

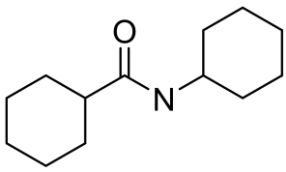

6

Preparation of N-cyclohexylcyclohexanecarboxamide ***6*** (CAS 7474-36-4).[89] Chamber A was loaded according to general procedure iodocyclohexane (78 µL, 0.60 mmol) and cyclohexanamine (206 µL, 1.80 mmol), 5 mL 2-methyl THF. Chamber B was loaded according to the CO releasing chamber. The reaction mixture concentrated *in vacuo*. Purification was performed on a 10g Flash Si column with 25% EtOAc in n-Heptane. Fractions containing product were pooled and concentrated in vacuo to give the desired product (72.1 mg, 57%).

Data for **6**: ^{1}H NMR (400 MHz, $CDCl_3$) δ 1.02 – 1.48 (m, 11H), 1.57 – 1.94 (m, 10H), 2.01 (tt, J = 3.40, 3.40, 11.83, 11.83 Hz, 1H), 3.68 – 3.82 (m, 1H), 5.24 (s, 1H).

^{13}C{^{1}H} NMR (151 MHz, $CDCl_3$) δ 175.1, 77.2, 77.0, 76.8, 47.7, 45.8, 33.3, 29.8, 25.8, 25.6, 24.9.

NMR purity assay 96.1%.

GC-MS: 209.2 [M], rt 9.83 min (100%).

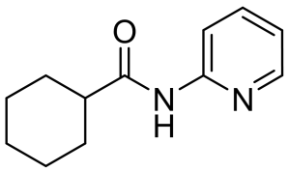

7

Preparation of N-(pyridin-2-yl)cyclohexanecarboxamide ***7*** (CAS 68134-77-0).[128] Chamber A was loaded according to general procedure iodocyclohexane (78 µL, 0.6 mmol) and pyridine-2-amine (165.2 mg, 1.76 mmol). Chamber B was loaded according to the CO releasing chamber. Purification was performed on a 10g SNAP column with 8-66% EtOAc in n-Heptane. Fractions containing product were pooled and concentrated in vacuo. The obtained product was further purified on a 10g Isolute SI column. Fractions containing product were pooled and concentrated in vacuo to give the product (22.4 mg, 18%).

Data for **7**: ^{1}H NMR (400 MHz, $CDCl_3$) δ 1.25 – 1.38 (m, 3H), 1.49 – 1.62 (m, 2H), 1.71 (d, J = 10.9 Hz, 1H), 1.79 – 1.88 (m, 2H), 2.01 (d, J = 13.0 Hz, 2H), 2.38 (t, J = 12.1 Hz, 1H), 7.14 (t, J = 6.6 Hz, 1H), 7.87 (t, J = 7.6 Hz, 1H), 8.21 (d, J = 5.1 Hz, 1H), 8.43 (d, J = 8.5 Hz, 1H), 9.35 (s, 1H).

^{13}C{^{1}H} NMR (100.59 MHz, $CDCl_3$) δ 176.08, 150.8, 142.6, 142.1, 119.4, 115.8, 46.5, 29.4, 25.7, 25.3.

NMR purity assay 88%.

LC-MS (Method B, 4 min): 205.07 $[M+H]^+$, rt 1.35 min (100%).

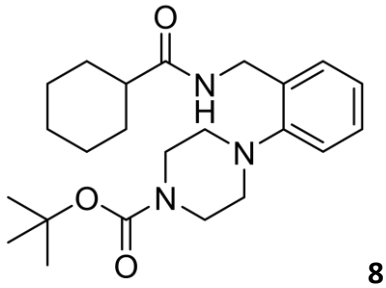

8

*Preparation of tert-butyl 4-(2-(cyclohexanecarboxamidomethyl)phenyl)piperazine-1-carboxylate **8** (CAS 2393928-95-5 - new)*. Chamber A was loaded according to the general procedure with iodocyclohexane (78 µL, 0.6 mmol) and tert-butyl 4-(2-(aminomethyl)phenyl)piperazine-1-carboxylate (522.5 mg, 1.79 mmol). Chamber B was loaded according to the general procedure for CO releasing chamber. Purification was performed on a 10g SNAP column with EtOAc in Heptane (0-70%) over 20 min. Fractions containing product were pooled and concentrated to give the desired product (70.2 mg, 29%).

Data for **8**: ^{1}H NMR (400 MHz, $CDCl_3$) δ 1.28 (m, 3H), 1.39 – 1.52 (m, 11H), 1.64 – 1.72 (m, 1H), 1.76 – 1.85 (m, 2H), 1.86 – 1.95 (m, 2H), 2.12 (tt, J = 3.48, 3.48, 11.73, 11.73 Hz, 1H), 2.82 – 2.92 (m, 4H), 3.58 (t, J = 4.90, 4.90 Hz, 4H), 4.55 (d, J = 5.57 Hz, 2H), 6.19 (t, J = 4.34, 4.34 Hz, 1H), 7.07 – 7.15 (m, 2H), 7.24 – 7.3 (m, 2H).

^{13}C{^{1}H} NMR (101 MHz, CDCl3, 26°C) δ 175.73, 154.74, 151.03, 133.1, 129.2, 128.4, 124.6, 120.2, 79.9, 77.3, 77.0, 76.7, 52.5, 45.7, 39.6, 29.8, 28.4, 25.8.

NMR purity assay: 98.9%.

HRMS (ESI-TOF) m/z: $[M+H]^+$ Calcd for $C_{23}H_{35}N_3O_3$ 402.2757; Found 402.2761.

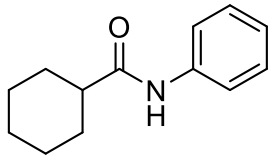

9

Preparation of N-phenylcyclohexanecarboxamide ***9*** (2719-26-8). Chamber A was loaded according to the general procedure with iodocyclohexane (78 µL, 0.60 mmol) and aniline (164 µL, 1.80 mmol), 5 mL 2-MeTHF. Chamber B was loaded according to the general procedure.

This reaction was also attempted with aqueous conditions using 2-MeTHF/water 2:1 (5mL) in chamber A. However, in both cases only a trace of product was observed on GC-MS.

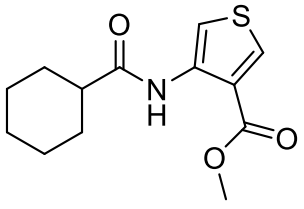

10

Preparation of N-phenylcyclohexanecarboxamide ***10***. Chamber A was loaded according to the general procedure with iodocyclohexane (78 µL, 0.60 mmol) and methyl 3-aminothiophene-2-carboxylate (270.8, 1.72 mmol), 5 mL 2-MeTHF/water (2:1). Chamber B was loaded according to the general procedure. Purification was performed on a 10 g SNAP column with 2 to 50% EtOAc in Heptane over 20 min. Fractions containing product were pooled and concentrated to give the desired product (7.3 mg, 4.5%) as light green crystals.

Many impurities were seen on the NMR. Due to the low recovery of the product, this product was discarded.

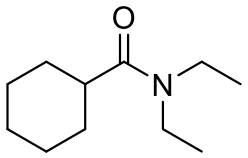

11

*Preparation of N,N-diethylcyclohexanecarboxamide **11** (5461-52-9).* Chamber A was loaded according to the general procedure with iodocyclohexane (78 µL, 0.60 mmol) and diethylamine (186 µL, 1.80 mmol) in 2-MeTHF (3.5 mL) and water (1.5 mL) as solvent system. Chamber B was loaded according to the general procedure for CO releasing chamber.

The reaction was also attempted without water, only using 2-MeTHF (5 mL). Only a trace on NMR and GC-MS was seen, and therefore purification was not pursued.

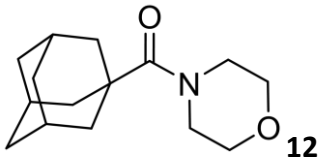

12

Preparation of adamantan-1-yl(morpholino)methanone **12** (CAS 22508-50-5).[89] Chamber A was loaded according to general procedure 1-iodoadamantane (158.4 mg, 0.60 mmol) and morpholine (155 µL, 1.8 mmol). Chamber B was loaded according to the CO releasing chamber. Purification was performed on a 10g Flash Si column with 25% EtOAc in n-Heptane. Fractions containing product were pooled and concentrated in vacuo to give the desired product (57.9 mg, 39%).

Data for **12**: ^{1}H NMR (400 MHz, $CDCl_3$) δ 1.66 – 1.78 (m, 6H), 1.97 – 2.01 (m, 6H), 2.02 – 2.07 (m, 3H), 3.63 – 3.73 (m, 8H).

$^{13}C\{^{1}H\}$ NMR (151 MHz, $CDCl_3$) δ 175.9, 77.2, 77.0, 76.8, 67.1, 46.0, 41.7, 39.0, 36.6, 28.5, 28.3.

NMR purity assay 92%.

LC-MS (Method B, 4 min): 250.1 $[M+H]^+$, rt 1.77 min (100%).

Preparation of adamantan-1-yl(morpholino)methanone **12** (CAS 22508-50-5) *from 1-bromoadamantane*. Chamber A was loaded according to general procedure 1-bromoadamantane (137.5 mg, 0.64 mmol) and morpholine (155 µL, 1.8 mmol). Chamber B was loaded according to the CO releasing chamber. Purification was performed on a 20 g Flash Si column with 0-25% EtOAc in n-Heptane. Fractions containing product were pooled and concentrated in vacuo to give the desired product (19.3 mg, 13%).

NMR purity assay 88%.

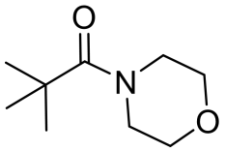

13

Preparation of 2,2-dimethyl-1-morpholinopropan-1-one **13** (CAS 70414-49-2).[129] Chamber A was loaded according to general procedure 2-iodo-2-methylpropane (72 µL, 0.60 mmol) and morpholine (155 µL, 1.80 mmol). Chamber B was loaded according to the CO releasing chamber. Purification was performed on a 20g Flash Si column with 0-25% EtOAc in n-Heptane. Fractions containing product were pooled and concentrated in vacuo to give the translucent crystals (15.8 mg, 15%).

Data for **13**: ^{1}H NMR (400 MHz, $CDCl_3$) δ 1.26 (s, 9H), 3.65 (d, J = 7.3 Hz, 8H).

$^{13}C\{^{1}H\}$ NMR (101 MHz, $CDCl_3$) δ 176.6, 77.5, 77.2, 76.9, 67.0, 45.9, 38.7, 28.4.

NMR purity assay 99%.

HRMS (ESI-TOF) m/z: $[M+H]^+$ Calcd for $C_9H_{17}NO_2$ 172.1337; Found 172.1326.

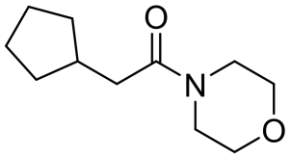

14

Preparation of 2-cyclopentyl-1-morpholinoethan-1-one **14** (CAS 1090938-36-5 - new). Chamber A was loaded according to the general procedure (iodomethyl)cyclopentane (127.9 mg, 0.61 mmol) and morpholine (155 µL, 1.80 mmol). Chamber B was loaded according to the general procedure. Purification was performed on a 10g SI column with 25% EtOAc in Heptane. Fractions containing product were pooled and concentrated to give product (42.3 mg, 36%).

Data for **14**: ^{1}H NMR (400 MHz, $CDCl_3$) δ 1.04 – 1.19 (m, 2H), 1.45 – 1.66 (m, 4H), 1.74 – 1.89 (m, 2H), 2.11 – 2.28 (m, 1H), 2.31 (d, J = 7.4 Hz, 2H), 3.38 – 3.51 (m, 2H), 3.53 – 3.68 (m, 6H).

^{13}C{^{1}H} NMR (101 MHz, $CDCl_3$) δ 171.7, 77.5, 77.2, 76.8, 67.2, 66.9, 46.3, 42.0, 39.2, 36.8, 32.9, 25.1.

NMR purity assay 85%.

LCMS (Method A, 4 min): 198 $[M+H]^+$, rt 1.16 min (100%).

HRMS (ESI-TOF) m/z: $[M+H]^+$ Calcd for $C_{11}H_{19}NO_2$ 198.1494; Found 198.1493.

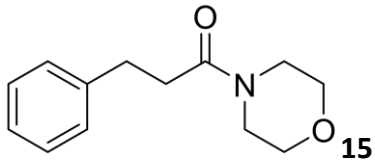

*Preparation of 1-morpholino-3-phenylpropan-1-one **15** (CAS 17077-46-2).*[130] Chamber A was loaded according to general procedure (2-iodoethyl)benzene (87 µL, 0.60 mmol) and morpholine (155 µL, 1.80 mmol). Chamber B was loaded according to the CO releasing chamber. Purification was performed on a 25g SNAP column with EtOAc in Heptane (2-100% EtOAc). Fractions were pooled, concentrated, and subjected to HPLC purification (5-75% MeCN - 0.2% NH3 in H_2O/MeCN (95:5) over 15 min, wavelength 220 nm, 15 mL/min). Fractions containing product were pooled and lyophilized to give the desired product (10.9 mg, 8%).

Data for **15**: ^{1}H NMR (400 MHz, $CDCl_3$) δ 2.58 – 2.66 (m, 2H), 2.94 – 3.03 (m, 2H), 3.31 – 3.41 (m, 2H), 3.47 – 3.56 (m, 2H), 3.62 (s, 4H), 7.18 – 7.24 (m, 3H), 7.27 – 7.32 (m, 2H).

^{13}C{^{1}H} NMR (101 MHz, $CDCl_3$) δ 171.0, 141.2, 128.7, 128.6, 126.4, 77.5, 77.2, 76.8, 67.0, 66.6, 46.1, 42.1, 35.0, 31.6.

LCMS (Method A, 4min): 220 $[M+H]^+$, rt 1.13 min (100%).

HRMS (ESI-TOF) m/z: $[M+H]^+$ Calcd for $C_{13}H_{17}NO_2$ 220.1137; found 220.1135.

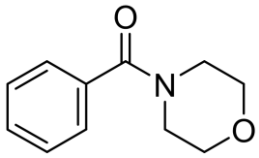

16

Preparation of morpholino(phenyl)methanone **16** (CAS 1468-28-6).[131] Chamber A was loaded according to general procedure with iodobenzene (67 µL, 0.6 mmol) and morpholine (155 µL, 1.8 mmol). Chamber B was loaded according to the CO releasing chamber. Purification was performed *via* HPLC (5-70% MeCN – 0.1% TFA in water over 20 min, wavelength 220nm, 15mL/min). Fractions containing product were pooled and lyophilized to give the desired product (69.7 mg, 61%).

Data for **16**: ^{1}H NMR (400 MHz, $CDCl_3$) δ 3.25 – 3.87 (m, 8H), 7.3 – 7.41 (m, 5H).

$^{13}C\{^{1}H\}$ NMR (101 MHz, $CDCl_3$) δ 170.3, 135.3, 129.8, 128.5, 127.0, 77.5, 77.2, 76.8, 66.8, 48.1, 42.5.

NMR purity assay: 98.1%.

LCMS (Method B, 4 min): 192.01 $[M+H]^+$, rt 0.87 min (100%).

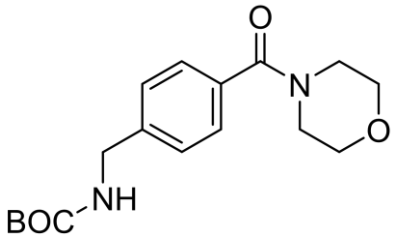

17

Preparation of tert-butyl (4-(morpholine-4-carbonyl)benzyl)carbamate **17** (CAS 1110964-59-4 - new). Chamber A was loaded according to general procedure tert-butyl (4-iodobenzyl)carbamate (204.5 mg, 0.61 mmol) and morpholine (155 µL, 1.80 mmol). Chamber B was loaded according to the CO releasing chamber. Purification was performed on a 20g Isolute SPE Si column with 25%-100% EtOAc in n-Heptane. Fractions containing product were pooled and concentrated in vacuo to give the desired product (133.9 mg, 70%).

Data for **17**: ^{1}H NMR (400 MHz, $CDCl_3$) δ 1.46 (s, 9H), 3.2 – 3.99 (m, 8H), 4.33 (d, J = 5.7 Hz, 2H), 4.92 (s, 1H), 7.28 – 7.41 (m, 4H).

^{13}C{^{1}H} NMR (101 MHz, $CDCl_3$) δ 170.3, 156.0, 141.2, 134.4, 127.6, 127.5, 79.9, 77.5, 77.4, 77.2, 76.8, 67.0, 44.4, 28.5. NMR purity assay: 88%.

HRMS (ESI-TOF) m/z: $[M+H]^+$ Calcd for $C_{17}H_{24}N_2O_4$ 321.1814; Found 321.1818.

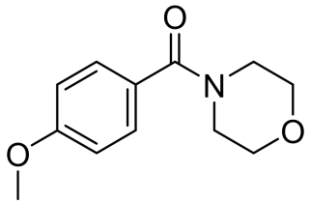

18

Preparation of (4-methoxyphenyl)(morpholino)methanone **18** (CAS 7504-58-7).[132] Chamber A was loaded according to general procedure 1-iodo-4-methoxybenzene (139 mg, 0.59 mmol) and morpholine (155 µL, 1.80 mmol). Chamber B was loaded according to the CO releasing chamber. Purification was performed on a 20 g Flash Si column with 40%-100% EtOAc in n-Heptane. Fractions containing product were pooled and concentrated in vacuo to give the desired product (92.8 mg, 70%).

Data for **18**: ^{1}H NMR (400 MHz, $CDCl_3$) δ 3.66 (d, J = 17.5 Hz, 8H), 3.82 (s, 3H), 6.82 – 6.98 (m, 2H), 7.29 – 7.44 (m, 2H).

$^{13}C\{^{1}H\}$ NMR (101 MHz, $CDCl_3$) δ 170.5, 161.0, 129.3, 127.5, 113.9, 77.5, 77.2, 76.8, 67.0, 55.5.

NMR purity assay: 83.6%.

HRMS (ESI-TOF) m/z: $[M+H]^+$ Calcd for $C_{12}H_{15}NO_3$ 222.1130; Found 222.1112.

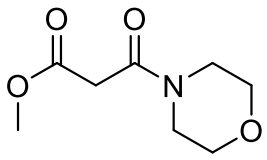

19

*Preparation of 3-morpholino-3-oxopropanoic acid **19**.* Chamber A was loaded according to the general procedure with ethyl 2-iodoacetate (71 µL, 0.60 mmol) and morpholine (155 µL, 1.80 mmol) in 2-MeTHF (3.5 mL) and water (1.5 mL) as solvent system. Chamber B was loaded according to the general procedure for CO releasing chamber.

The product was hydrolyzed during the reaction and it became very difficult to isolate this.

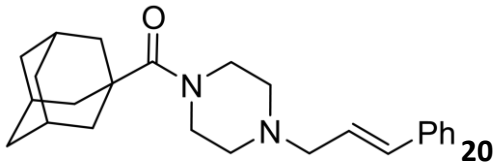

Preparation of 1-adamantyl-[4-[(E)-cinnamyl]piperazin-1-yl]methanone **20** (CAS 60277-86-3).[133] Chamber A was loaded according to the general procedure with 1-iodoadamantane (157 mg, 0.60 mmol) and trans 1-cinnamylpiperazine (364 mg, 1.80 mmol), 5 mL 2-MeTHF. Chamber B was loaded according to the general procedure. Purification was performed *via* HPLC (35-95% MeCN – 0.2% NH_3 in H_2O/MeCN (95:5) over 25 min, wavelength 250 nm, 20 mL/min). Fractions were pooled and lyophilized to give product as brown sticky oil (40.8 mg, 19%).

Data for **20**: ^{1}H NMR (400 MHz, $CDCl_3$) δ 1.66 – 1.77 (m, 6H), 1.95 – 2.06 (m, 9H), 2.42 – 2.53 (m, 4H), 3.12 – 3.19 (m, 2H), 3.64 – 3.81 (m, 4H), 6.25 (dt, J = 15.8, 6.8 Hz, 1H), 6.52 (d, J = 15.9 Hz, 1H), 7.2 – 7.26 (m, 1H), 7.28 – 7.34 (m, 2H), 7.35 – 7.39 (m, 2H).

^{13}C{^{1}H} NMR (101 MHz, $CDCl_3$) δ 175.8, 136.9, 133.6, 128.7, 127.8, 126.5, 126.1, 77.5, 77.2, 76.8, 61.1, 53.6, 45.4, 41.8, 39.2, 36.8, 28.6.

NMR purity assay: 87.7%.

LC-MS (Method A, 4 min) 365 $[M+H]^+$, rt 263 min (87%)

HRMS (ESI-TOF) m/z: [M+H]+ Calcd for $C_{24}H_{32}N_2O$ 365.2593; Found 365.2589.

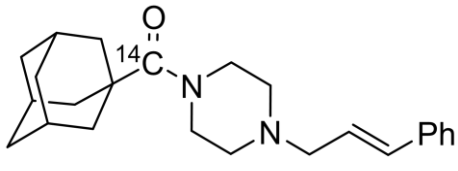

[^{14}C-*carbonyl*]20

Preparation of 1-adamantyl-[4-[(E)-cinnamyl]piperazin-1-yl]methanone **[^{14}C-*carbonyl*]20**. Chamber A was loaded according to the general procedure with 1-iodoadamantane (157 mg, 0.60 mmol) and trans 1-cinnamylpiperazine (384 mg, 1.90 mmol), 5 mL 2-MeTHF. Chamber B was loaded according to the general procedure for CO releasing chamber COgen (128.5 mg, 0.57 mmol) and [^{14}C]COgen (69.06 MBq, 0.03 mmol) was used. Purification was performed *via* HPLC (60-80% MeCN – 0.2% NH_3 in H_2O/MeCN (95:5) over 15 min, wavelength 250 nm, 20 mL/min). Fractions were pooled and lyophilized to give product as light-yellow sticky oil (14.31 MBq, 0.106 TBq/mol, 23%).

Radio-HPLC (setup 2) 97.48%.

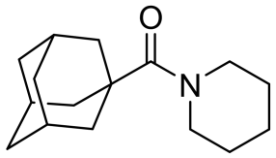

21

Preparation of Adamantan-1-yl(piperidin-1-yl)methanone **21** (CAS 22508-49-2).[89] Chamber A was loaded according to general procedure 1-iodoadamantane (157 mg, 0.60 mmol) and piperidine (178 µL, 1.80 mmol). Chamber B was loaded according to the CO releasing chamber. Purification was performed on a 25g SNAP column with 0-25% EtOAc in n-Heptane. Fractions containing product were pooled and concentrated in vacuo to give the translucent crystals (42 mg, 28.3).

Data for **21**: ^{1}H NMR (400 MHz, $CDCl_3$) δ 1.49 – 1.59 (m, 4H), 1.61 – 1.67 (m, 2H), 1.69 – 1.77 (m, 6H), 1.97 – 2.07 (m, 9H), 3.52 – 3.67 (m, 4H).

^{13}C{^{1}H} NMR (101 MHz, $CDCl_3$) δ 175.7, 77.5, 77.2, 76.8, 46.6, 41.9, 39.2, 36.9, 28.7, 26.5, 25.0.

NMR purity assay: 96%.

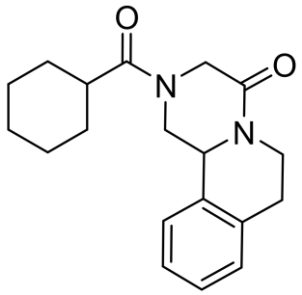

22

Preparation of 2-(cyclohexanecarbonyl)-1,2,3,6,7,11b-hexahydro-4H-pyrazino[2,1-a]isoquinolin-4-one **22** (Praziquantel, CAS 55268-74-1).[134] Chamber A was loaded according to the general procedure with 1-iodocyclohexane (78 µL, 0.60 mmol) and 1,2,3,6,7,11b-hexahydro-4H-pyrazino[2,1-a]isoquinolin-4-one (350.9 mg, 1.73 mmol). Chamber B was loaded according to the general procedure. Purification was performed on a 25g SNAP column with 12-100% EtOAc in n-Heptane. Fractions containing product were pooled and concentrated in vacuo to give product (53.5 mg, 28.5%). This was subjected to recrystallization by dissolution in warm EtOH, and then stored in the freezer. Filtration gave fluffy crystals (24.8 mg, 13%).

Data for **22**: ^{1}H NMR (500 MHz, $CDCl_3$) δ 1.23 – 1.42 (m, 3.3H, major + minor), 1.48 – 1.65 (m, 2H, major + minor), 1.7 – 1.9 (m, 5.4H, major + minor), 2.43 – 2.62 (m, 1H, major + minor), 2.76 – 3.05 (m, 4H), 3.27 (t, J = 11.7 Hz, 0.21H, minor), 3.88 (d, J = 18.5 Hz, 0.21H, minor), 4.10 (d, J = 17.4 Hz, 0.76H, major), 4.39 (d, J = 12.8 Hz, 0.21H, minor), 4.49 (d, J = 17.4 Hz, 0.77H, major), 4.75 – 4.96 (m, 2.3H, major + minor), 5.18 (d, J = 13.1 Hz, 0.76H, major), 7.15 – 7.25 (m, 1.3H), 7.27 – 7.36 (m, 2.7H).

^{13}C{^{1}H} NMR (126 MHz, $CDCl_3$) δ 174.8 (major), 174.3 (minor), 165.6 (minor), 164.4 (major), 135.5 (minor), 134.7 (major), 132.8 (major), 132.1 (minor), 129.7 (minor), 129.3 (major), 127.7 (minor), 127.5 (major), 127.0, 125.5 (major), 125.2 (minor), 55.8 (minor), 55.0 (major), 49.6

(minor), 49.0 (major), 46.3 (minor), 45.2 (major), 40.8, 39.1 (major), 38.7 (minor), 29.5 (minor), 29.3 (major), 29.2 (minor), 29.0 (major), 28.9 (minor), 28.7 (major), 25.7.

NMR purity assay: 96.6%.

HRMS (ESI-TOF) m/z: $[M+H]^+$ Calcd for $C_{19}H_{24}N_2O_2$ 313.1916; Found 313.1908.

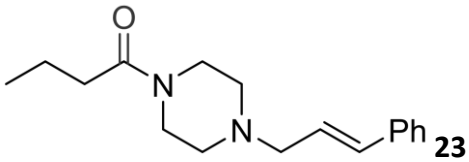

Preparation of 1-(4-cinnamylpiperazin-1-yl)butan-1-one **23** (Bucinnazine, CAS 17719-89-0).[92] Chamber A was loaded according to the general procedure with 1-iodopropane (59 µL, 0.60 mmol) and trans 1-cinnamylpiperazine (364 mg, 1.80 mmol), 5 mL 2-MeTHF. Chamber B was loaded according to the general procedure. Purification was performed *via* HPLC (30-90% MeCN – 0.2% NH_3 in H_2O/MeCN (95:5) over 25 min, wavelength 250 n, 20 ml/min. Fractions were pooled and lyophilized to give product (5.37 mg, 3%).

Data for **23**: ^{1}H NMR (400 MHz, $CDCl_3$) δ 0.97 (t, J = 7.4 Hz, 3H), 1.67 (h, J = 7.4 Hz, 2H), 2.30 (t, J = 7.5 Hz, 2H), 2.97 (broad s, 4H), 3.39 – 4.15 (m, 6H), 6.27 (dt, J = 15.4, 7.3 Hz, 1H), 6.69 (d, J = 15.8 Hz, 1H), 7.28 – 7.43 (m, 5H).

^{13}C{^{1}H} NMR (126 MHz, $CDCl_3$) δ 171.4, 128.8, 126.9, 77.3, 77.0, 76.8, 59.8, 51.5, 43.2, 39.1, 34.9, 18.6, 13.9.

8. Experimental: Reduction of $^{14}CO_2$ to ^{14}CO, comparison of two methods

8.1. General Information

Organic solvents (Aldrich) were used without further purification. Purifications of reactions products were carried out using Merck silica gel (40-63 µm). 1H NMR (400 MHz) was measured on a Brucker Avance 400 MHz spectrometer. Chemical shifts are reported in parts per million (ppm, δ) downfield from residual solvents peaks and coupling constants are reported as Hertz (Hz). Splitting patterns are designated as singlet (s), doublet (d), triplet (t). Splitting patterns that could not be interpreted or easily visualized are designated as multiplet (m). Electrospray mass spectra were obtained using an ESI-Quadripole autopurify, Waters (pump 2545, mass: ZQ2000) mass Spectrometer. Unless otherwise noted, all other commercially available reagents and solvents were used without further purification. Carbonylations for ^{13}C experiments were performed using carbon-13 CO_2 (99.2% enrichment) provided by Isotec.inc.

The double chamber system and the apparatus for electroreduction were provided by Professor Troels Skrydstrup.

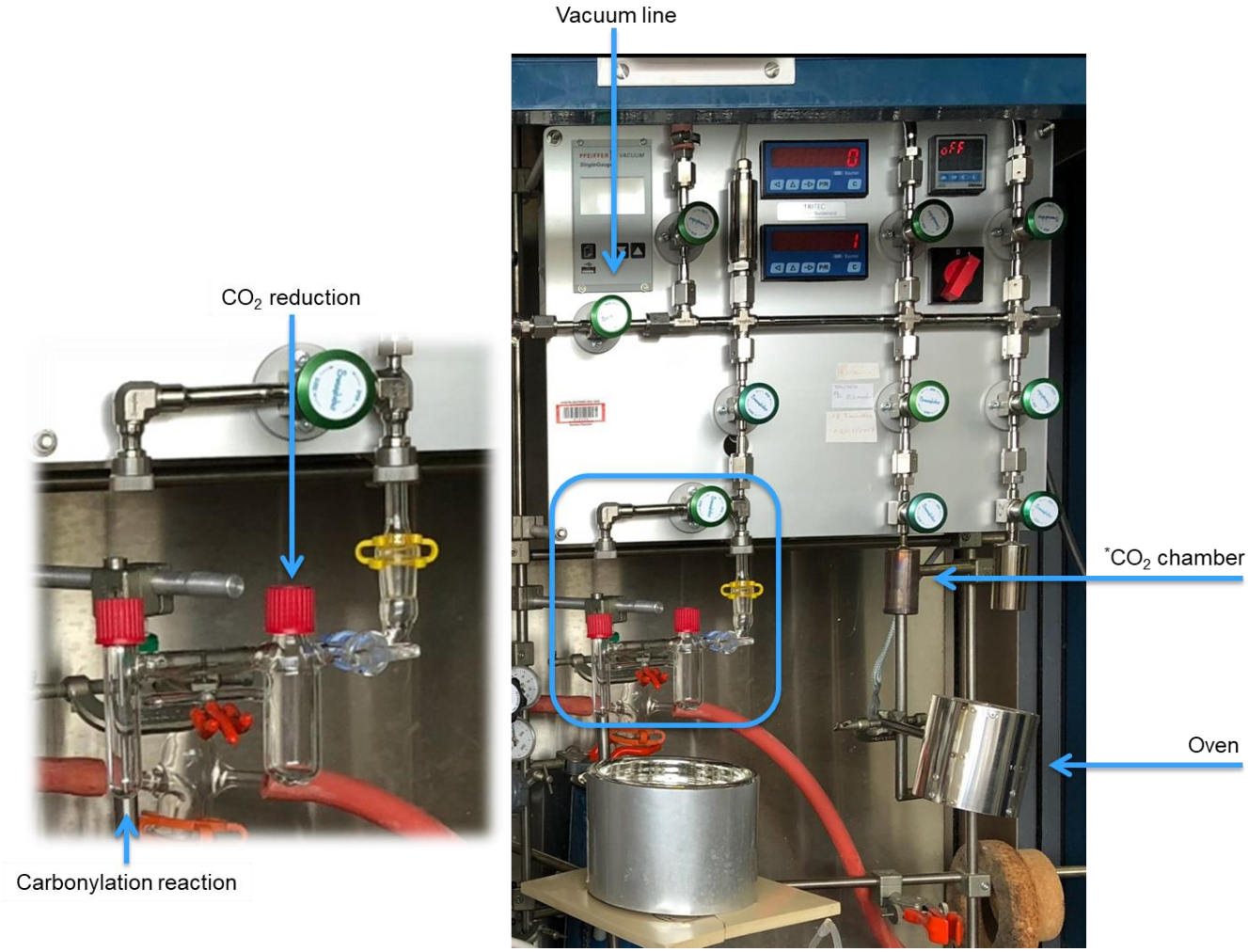

Figure 23 – Setup of the reaction at CEA-SCBM with the double chamber system.

8.2. Procedures and characterization

Electrochemical reduction

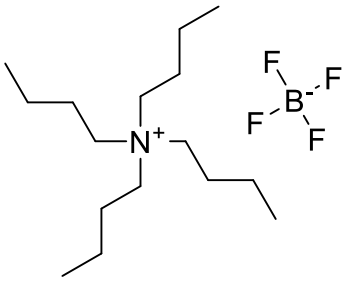

Preparation of tetrabutylammonium tetrafluoroborate (TBABF$_4$). Sodium tetrafluoroborate (2.74 g, 25 mmol) is dissolved in water (25 mL). To this, Tetrabutylammonium bromide (8.06 g, 25mmol) in DCM (25 mL) is added. The resulting two phases are stirred at ambient temperature for 24 h. The two phases were separated, and the organic phase was washed with 3x10mL water. The organic phase was dried over Mg_2SO_4, filtered, and concentrated *in vacuo* to give white solids. These solids were dried in a vacuum stove at 80 °C overnight to give the TBABF$_4$ salt in 7.21 g and 88% yield.

Data for TBABF$_4$: ^{1}H NMR (400 MHz, CD_3CN) δ 0.96 (t, J = 7.34, 7.34 Hz, 12H), 1.27 – 1.42 (m, 8H), 1.52 - 1.66 (m, 8H), 3.01 – 3.11 (m, 8H).

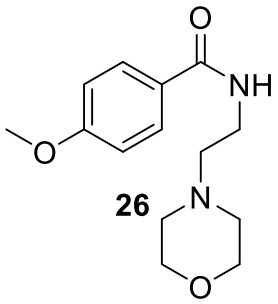

26

Preparation of 4-methoxy-N-(2-morpholinoethyl)benzamide (moclobemide) ***26***. Chamber A was loaded with $Pd(dba)_2$ (0.015 g, 0.03 mmol), PPh_3 (0.013 g, 0.05 mmol), 4-iodoanisole (0.119 g, 0.51 mmol), 1,4-dioxane (3 mL), 2-morpholinoethan-1-amine (0.131 mL, 1 mmol) and Et_3N (0.142 mL, 1.02 mmol). The chamber is sealed with a PTFE/silicone seal. Chamber B is charged with FeTTP (6 mg, 8.52 µmol), $TBABF_4$ (1.10 g, 3.34 mmol), 2,2,2-trifluoroethan-1-ol (2 mL, 27.45 mmol) and DMF (35 mL). Electrodes are mounted and the glassware was sealed with screw caps fitted with PTFE/silicone seal. Chamber B was bubbled through for 10 min with CO_2 with an outlet in chamber A. Both chambers were stirred for 18 h, while Chamber A is at 80 °C and chamber B is kept at room temperature. After which, the contents of chamber A is transferred to a round bottom flask and concentrated *in vacuo*. The residue is subjected to normal phase purification using 2% MeOH in DCM, to give the desired product (65 mg, 48%).

Data for **26**: ^{1}H NMR (400 MHz, $CDCl_3$) δ 2.46 – 2.53 (m, 4H), 2.59 (t, J = 6.0 Hz, 2H), 3.53 (d, J = 5.3 Hz, 2H), 3.68 – 3.75 (m, 4H), 3.83 (s, 3H), 6.76 (s, 1H), 6.91 (d, J = 8.9 Hz, 2H), 7.74 (d, J = 8.9 Hz, 2H).

LCMS (12 min): 265 $[M+H]^+$, rt 4.50 min (93%).

Preparation of [^{13}C-carbonyl]4-methoxy-N-(2-morpholinoethyl)benzamide ***[^{13}C]26***. Chamber A was loaded as described above. Chamber B is charged with FeTTP (2.06 mg, 2.92 µmol), $TBABF_4$ (0.395 g, 1.2 mmol), 2,2,2-trifluoroethan-1-ol (0.942 mL, 9.41 mmol) and DMF (12 mL). The glassware was charged with 0.5 mmol of $^{13}CO_2$ with the Tritec manifold. Both chambers were stirred for 18 h, while Chamber A is at 80 °C and chamber B is kept at room temperature.

No product formation was seen on TLC/LCMS.

Reduction of $^{13}CO_2$ by disilanes catalyzed by F^-

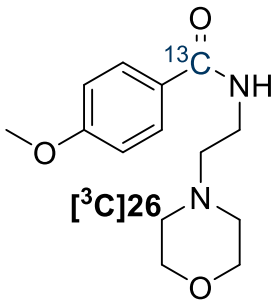

Preparation of [^{13}C-carbonyl]4-methoxy-N-(2-morpholinoethyl)benzamide (moclobemide) ***[^{13}C]26***.[98] Chamber A was loaded with $Pd(dba)_2$ (0.015 g, 0.03 mmol), PPh_3 (0.013 g, 0.05 mmol), 4-iodoanisole (0.119 g, 0.51 mmol), 1,4-dioxane (3 mL), 2-morpholinoethan-1-amine (0.131 mL, 1 mmol) and Et_3N (0.142 mL, 1.02 mmol). Chamber B was loaded with KHF_2 (3.91 mg, 0.05 mmol), $(MePh_2Si)_2$ (197 mg, 0.50 mmol) and DMSO (12 mL). Both chambers are sealed with a screw cap lined with PTFE/silicone seal. The glassware is charged with 0.50 mmol $^{13}CO_2$ using the Tritec manifold. Chamber A is heated at 80 °C, while Chamber B is heated at 30 °C for 18 h. After which, the contents of chamber A are transferred to a round bottom flask and concentrated *in vacuo*. The crude product is subjected to silica purification using 2% MeOH in DCM to give the product **[^{13}C]26** as white crystals (22.9 mg, 29%).

Data for **[^{13}C]26**: ^{1}H NMR (400 MHz, $CDCl_3$) δ 2.46 – 2.53 (m, 4H), 2.59 (t, J = 6.0 Hz, 2H), 3.53 (d, J = 5.3 Hz, 2H), 3.68 – 3.75 (m, 4H), 3.83 (s, 3H), 6.76 (s, 1H), 6.91 (d, J = 8.9 Hz, 2H), 7.74 (d, J = 8.9 Hz, 2H).

^{13}C NMR (101 MHz, $CDCl_3$) δ 166.65, 166.32, 166.00, 137.57, 133.25, 128.79, 128.74, 128.38, 128.36, 66.91, 56.87, 53.46, 53.31, 36.09.

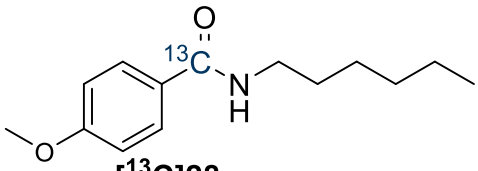

[^{13}C]28

Preparation of [^{13}C-carbonyl]N-hexyl-4-methoxybenzamide ***[^{13}C]28***.[103] Chamber A is loaded with 4-iodoanisole **24** (117 mg, 0.50 mmol), n-hexyl amine **27** (0.132 mL, 1.00 mmol), $Pd(dba)_2$ (14.38 mg, 0.03 mmol), PPh_3 (13.11 mg, 0.05 mmol), Et_3N (0.139 mL, 1.00 mmol) and 1,4-dioxane (3 mL). Chamber B was loaded with KHF_2 (3.91 mg, 0.05 mmol), $(MePh_2Si)_2$ (197 mg, 0.50 mmol) and DMSO (12 mL). Both chambers are sealed with a screw cap lined with PTFE/silicone seal. The glassware is charged with 0.50 mmol $^{13}CO_2$ using the Tritec manifold. Chamber A is heated at 80 °C, while Chamber B is heated at 30 °C for 18 h. After which, the contents of chamber A are transferred to a round bottom flask and concentrated *in vacuo*. The crude is the purified over silica using 10-20% EtOAc in n-Heptane. Fractions containing product were pooled and concentrated to give the desired product **[^{13}C]28** (63.6 mg, 54%).

Data for **[^{13}C]28**: ^{1}H NMR (400 MHz, $CDCl_3$) δ 0.86 – 0.91 (m, 3H), 1.24 – 1.43 (m, 6H), 1.54 – 1.65 (m, 2H), 3.38 – 3.47 (m, 2H), 3.84 (s, 3H), 6.04 (s, 1H), 6.83 – 7 (m, 2H), 7.62 – 7.81 (m, 2H).

9. Experimental: Radiosynthesis of ^{18}F-Crizotinib, a potential radiotracer for PET imaging of the P-glycoprotein transport function at the blood-brain barrier

9.1. General Information

General Reactions

All reagents were purchased from commercial suppliers and used without further purification, unless mentioned otherwise. Anhydrous solvents were purchased from Sigma Aldrich and stored under nitrogen atmosphere. Yields and refer to purified, isolated, homogenous product and spectroscopically pure material, unless stated otherwise.

Reaction Setup

All reactions were carried out under a nitrogen atmosphere and were magnetically stirred. Electric heating plates and DrySyn were used for elevated temperatures and stated temperatures corresponds to the external DrySyn temperature. Concentration was performed on a rotary evaporator at 40 °C at appropriate pressure.

Reaction mixture

Crude reaction mixture was assayed by GC-MS or LC-MS and quantified by NMR with anisole as internal standard. LC-MS analysis was performed on a Waters Acquity UPLC using either

- Method A: BEH C18 column (50 mm x 2.1 mm, 1.7 µm particles) with a 10-90% gradient over 2 or 4 min with MeCN-NH_4/NH_4CO_3;
- Method B: BEH C18 column (50 mm x 2.1 mm, 1.8 µm particles) with a 10-90% gradient over 2 or 4 min with MeCN-formic acid and electrospray ionization;

- Method C: Kinetex 2.6u XB-C18 column (50 mm x 3.0 mm, 2.6 µm particles) with a 5-100% gradient over 2, 5 or 6 min with MeCN-TFA).

GCMS (EI) analysis was performed on a 7890A GC system and 5975C inert MSD system equipped with an Agilent 19091S-433L (30 m x 250 µ x 0.25 µm) capillary column using a gradient: 40-150 °C with a rate of 15 °C/min, followed by 150-300 °C with a rate of 60 °C/min, and electron impact ionization at **70** eV.

Thin layer chromatography was carried out using E. Merck silica glass plates (60F-254) with UV light (254 nm) and/or iodine vapor/potassium permanganate as the visualization agent.

Purification

Crude reaction mixtures were purified by either flash chromatography prepacked Biotage SNAP columns using a Biotage automated flash systems with UV detection or preparative reversed phase HPLC purifications using a Gilson 322 Pump equipped with a Gilson UV/Vis-152 lamp with a Xbridge™ Prep C-18 10 µm OBD™ 19x250 mm column or preparative SFC-MS with Waters Kromasil DIOL (30 mm x 250 mm, 10 µm) column.

Analysis

^{1}H NMR and ^{13}C NMR spectra were recorded on a Bruker AVANCE III system running at proton frequency of 500.1 MHz with a cryogenic probe or on a Bruker Avance Nanobay system at 400.13 MHz and processed with the NMR software MestreNova (Mestrelab Research SL). NMR experiments were run in $CDCl_3$ or DMSO-d_6 at 25°C, unless stated otherwise. ^{1}H chemical shifts are referenced relative to the residual solvent peak at 7.26 ppm, and ^{13}C chemical shifts are referenced to 77.67 for $CDCl_3$. Signals are listed in ppm, and multiplicity identified as s =

singlet, br = broad, d = doublet, dt = doublet of a triplet, t = triplet, tt = triplet of a triplet, q = quartet, quin = quintet, h = hextet, m = multiplet; coupling constants in Hz; integration. ^{13}C NMR data is reported as with chemical shifts. For purity, quantitative NMR spectroscopy (qNMR) was performed with 2,3,5,6-tetrachlorobenzene (purity 99%) (unless mentioned otherwise) as an internal calibrant in $CDCl_3$ or DMSO-d_6.[127] Purity assays were also performed on the aforementioned LC-MS.

Radio synthesis

Automated radiosynthesis of [^{18}F]crizotinib from precursor **9** was performed using a TRACERlab FX_{FN} synthesizer (GE Healthcare, USA) equipped with a 501 HPLC Pump (Waters, USA) and a UV detector K-2501 (Knauer, Germany). No carrier-added [^{18}F]fluoride ion is produced via the $^{18}O(p, n)^{18}F$ nuclear reaction by irradiation of a 2 mL [^{18}O]water (> 97% enriched, CortecNet, France) target with an IBA Cyclone-18/9 (IBA, Belgium) cyclotron. $^{18}F^-$ (20-30 GBq) is trapped on an ion exchange resin QMA light (Waters) and eluted with a solution of base (2 mg) in a mixture of MeCN (1.2 mL) and water (300 µL). The resulting complex is azeotropically dried upon heating at 60 °C for 5 min under vacuum and a stream of helium followed by heating. Another 500 µL of MeCN was added and dried again. A solution of the precursor **22** (2.7 mg) in DMF 700 µL is added and the mixture is heated at 160 °C for 10 min. After which 3M HCl (300 µL) is added for the deprotection, and heated for another 160 °C for 10 min. The reaction mixture is cooled to 50 °C and diluted with water HPLC eluant (10 4 mL) is added and passed before passing through a Sep-pak® Alumina-N cartridge (Waters, USA). Semi-preparative HPLC purification was realized on a reverse phase Symmetry® C18 column (300 x 7.8 mm, 7 µm) using a mixture of H2O/CH3OH/THF/TFA (70/20/10/0.1 v/v/v/v) as

eluent at 5 mL/min with gamma and UV (λ = 254 nm) detection. The collected peak (retention time = 11-13 min) of [18F]crizotinib is diluted with water (20 mL) and loaded on a Sep-Pak® C18 cartridge (Waters). The cartridge is rinsed with water (10 mL) and the product is eluted with ethanol (2 mL) and further diluted with aq. 0.9 % NaCl (8 mL). Ready-to-inject [^{18}F]crizotinib was obtained within 70 min from end of beam (EOB) in 15 ± 5% (n = 7) decay-corrected radiochemical yield (d.c. RCY).

Quality control

Quality control was performed on a 717plus Autosampler HPLC system equipped with a 1525 binary pump and a 2996 photodiode array detector (Waters) and a Flowstar LB 513 (Berthold, France) gamma detector. The system was monitored with the Empower 3 (Waters) software. HPLC were realized on a reverse phase analytical Symmetry C18 (150 mm x 4.6 mm, 3.5 µm, Waters) column using a mixture of H_2O/MeOH/THF/TFA (70/20/10/0.1 v/v/v/v, 1.5 mL/min) as eluent. UV detection was performed at 333 nm. Identification of the peak was assessed by comparing the retention time of [^{18}F]crizotinib with the retention time of the non-radioactive reference crizotinib (rt ref). For acceptance, the retention time must be within the retention time of the reference ± 10% range. Radiochemical and chemical purities were calculated as the ratio of the area under the curve (AUC) of the crizotinib peak over the sum of the AUCs of all other peaks on gamma and UV chromatograms respectively. Radiochemical and chemical purities are the mean values of three consecutive runs. Molar activity was calculated as the ratio of the activity of the collected peak of [^{18}F]crizotinib (Capintec®, Berthold) over the molar quantity of crizotinib determined using calibration curves. Molar activity is calculated as the mean value of three consecutive runs.

9.2. Procedures and characterization data

*Precursor synthesis: hypervalent iodine(III) precursor **38***

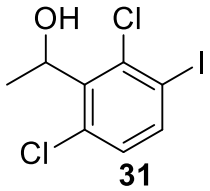

31

*Preparation of 1-(2,6-dichloro-3-iodophenyl)ethan-1-ol **31** (new).* Into a 250-mL 3-necked round-bottom flask purged and maintained with an inert atmosphere of nitrogen, was placed diisopropyl amine (8.2 g, 81.04 mmol, 1.10 equiv), tetrahydrofuran (100 mL). This was followed by the addition of *n*-butyllithium (31 mL, 8.23 mmol, 1.05 equiv, 2.5 mol/L) dropwise with stirring at -30 °C in 20 min. The resulting solution was stirred for 1 h at -30 °C. Into another 500-mL 3-necked round-bottom flask purged and maintained with an inert atmosphere of nitrogen, was placed a solution of 2,4-dichloro-1-iodobenzene (20 g, 73.29 mmol, 1.00 equiv) in THF (200 mL). To this was added the resulting solution in the first flask dropwise with stirring at -78 °C in 20 min. The resulting solution was stirred for 2 h at -78 °C. To the mixture was added acetaldehyde (6.8 g, 154.36 mmol, 2.10 equiv) dropwise with stirring at -78 °C in 15 min. The resulting solution was stirred for 1 h at -78 °C. The reaction was then quenched by the addition of 100 mL of $NH_4Cl_{(aq)}$. The resulting solution was extracted with 2x200 mL of ethyl acetate and the organic layers combined. The resulting mixture was washed with 1x100 mL of brine. The mixture was dried over anhydrous sodium sulfate and concentrated under vacuum. The residue was applied onto a silica gel column with ethyl acetate/petroleum ether (0:1-1:5). The fractions containing product were pooled and

concentrated to give the product, 1-(2,6-dichloro-3-iodophenyl)ethan-1-ol **31**, was isolated at a light-yellow oil (16 g, 69%).

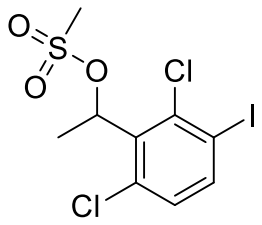

32

*Preparation of 1-(2,6-dichloro-3-iodophenyl)ethyl methanesulfonate **32** (new).* Into a 500-mL 3-necked round-bottom flask purged and maintained with an inert atmosphere of nitrogen, was placed 1-(2,6-dichloro-3-iodophenyl)ethan-1-ol **31** (15 g, 47.33 mmol, 1.00 equiv), DCM (200 mL), DIEA (12.2 g, 94.40 mmol, 2.00 equiv). This was followed by the addition of methanesulfonyl chloride (7.0 g, 61.11 mmol, 1.30 equiv) dropwise with stirring at 0 °C in 5 min. The resulting solution was stirred for 1.5 h at 0 °C. The resulting solution was diluted with 100 mL of DCM. The resulting mixture was washed with 2x100 mL of brine. The mixture was dried over anhydrous sodium sulfate and concentrated under vacuum. The residue was purified on a silica gel column with ethyl acetate/petroleum ether (0:1-1:5). The fractions containing product were pooled and concentrated to give, 1-(2,6-dichloro-3-iodophenyl)ethyl methanesulfonate **32**, as off-white solid (12.6 g, 67%).

Data for **32**: ^{1}H NMR (300 MHz, $CDCl_3$) δ 1.796 – 1.854 (m, 3H), 2.884 – 2.924 (s, 3H), 6.502 – 6.570 (m, 1H), 7.085 – 7.113 (d, J = 8.4, 1H), 7.814 – 7.842 (d, J = 8.4).

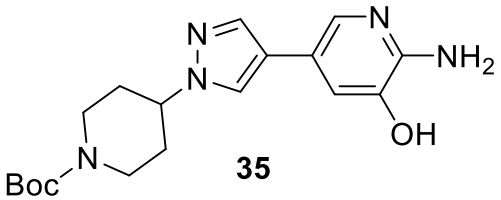

Preparation of tert-butyl 4-[4-(6-amino-5- hydroxypyridin-3-yl)-1H-pyrazol-1-yl]piperidine-1-carboxylate **35** (CAS 2322541-37-5 - new). Into a 500-mL 3-necked round-bottom flask purged and maintained with an inert atmosphere of nitrogen, was placed tert-butyl 4-[4-(tetramethyl-1,3,2-dioxaborolan-2-yl)-1H-pyrazol-1-yl]piperidine-1-carboxylate **33** (9.8 g, 25.97 mmol, 1.00 equiv), 2-amino-5-bromopyridin-3-ol **34** (5.9 g, 30.16 mmol, 1.20 equiv), Pd(dppf)Cl_2 (2.0 g, 2.73 mmol, 0.10 equiv), 1,4-dioxane (200 mL), Na_2CO_3 (5.5 g, 51.40 mmol, 2.00 equiv), water (20 mL). The resulting solution was stirred for 16 h at 100 °C. The reaction mixture was cooled to 25 °C with a water/ice bath. The residue was applied onto a silica gel column with dichloromethane/methanol (1:0-10:1). Fractions containing product were pooled and concentrated to give the desired product, *tert*-butyl 4-[4-(6-amino-5-hydroxypyridin-3-yl)-1H-pyrazol-1-yl]piperidine-1-carboxylate **35**, as a light brown solid (4.5, 48%).

Data for **35**: LCMS (Method C, 2 min): 360 $[M+H]^+$, rt 0.786 min (82%).

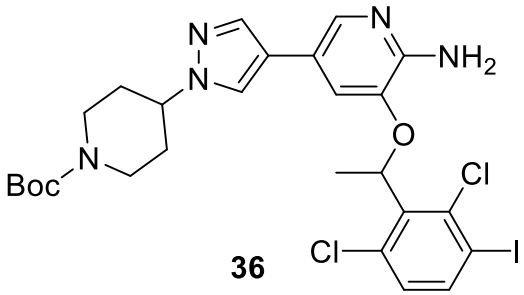

36

*Preparation of tert-butyl 4-(4-[6-amino-5-[1-(2,6-dichloro-3-iodophenyl)ethoxy]pyridin-3-yl]-1H-pyrazol-1-yl)piperidine-1- carboxylate **36** (new)*. Into a 250-mL round-bottom flask purged and maintained with an inert atmosphere of nitrogen, was placed *tert*-butyl 4-[4-(6-amino-5-hydroxypyridin-3-yl)-1H-pyrazol-1-yl]piperidine-1-carboxylate **35** (4.4 g, 12.24 mmol, 1.00 equiv), 1-(2,6-dichloro-3-iodophenyl)ethyl methanesulfonate **32** (4.8 g, 12.15 mmol, 1.00 equiv), acetonitrile (120 mL), Cs_2CO_3 (12 g, 36.83 mmol, 3.00 equiv). The resulting solution was stirred for 4 h at 60 °C. The reaction mixture was cooled to 25 °C with a water bath. The residue was applied onto a silica gel column with ethyl acetate/petroleum ether (0:1-1:0). Fractions containing product were pooled and concentrated in vacuo to give the product, *tert*-butyl 4-(4-[6-amino-5-[1-(2,6-dichloro-3-iodophenyl)ethoxy]pyridin-3-yl]-1H-pyrazol-1-yl) piperidine-1-carboxylate **36**, as a light brown solid (3.9 g, 48%).

Data for **36**: ^{1}H NMR (300 MHz, DMSO-d_6) δ 1.157 – 1.205 (t, J = 7.2, 1H), 1.427 (s, 9H), 1.750 – 1.795 (m, 5H), 1.996 – 2.027 (m, 3H), 2.918 (m, 2H), 4.000 – 4.098 (m, 3H), 4.287 – 4.338 (m, 1H), 6.100-6.122 (m, 2H), 6.833 – 6.837 (m, 1H), 7.243 – 7.271 (d, J = 8.4, 1H), 7.517 (s, 1H), 7.747 – 7.752 (m, 1H), 7.907 – 7.950 (m, 2H).

LC-MS (Method C, 2 min): 658 [M], 699 $[M+MeCN+H]^+$, rt 1.135 (69%).

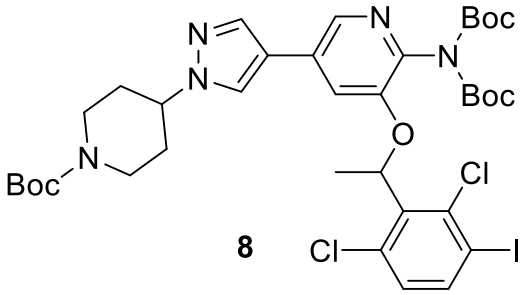

8

Preparation of tert-butyl 4-[4-(6-[bis[(tert-butoxy)carbonyl]amino]-5-[1-(2,6-dichloro-3-iodophenyl)ethoxy]pyridin-3-yl)-1H-pyrazol-1-yl]piperidine-1-carboxylate ***37*** *(new).* Into a 250-mL round-bottom flask purged and maintained with an inert atmosphere of nitrogen, was placed tert-butyl 4-(4-[6-amino-5-[1-(2,6-dichloro-3-iodophenyl)ethoxy]pyridin-3-yl]-1H-pyrazol-1-yl)piperidine-1-carboxylate **36** (3.9 g, 5.92 mmol, 1.00 equiv), tetrahydrofuran (100 mL), DIEA (2.3 g, 17.80 mmol, 3.00 equiv), $(Boc)_2O$ (3.9 g, 17.87 mmol, 3.00 equiv), 4-dimethylaminopyridine (700 mg, 5.73 mmol, 1.00 equiv). The resulting solution was stirred for 16 h at 25 °C. The residue was applied onto a silica gel column with EtOAc/petroleum ether (0:1-1:1). Fractions containing product were pooled and concentrated to give the desired product, *tert*-butyl 4-[4-(6-[bis[(*tert*-butoxy)carbonyl]amino]-5-[1-(2,6-dichloro-3-iodophenyl) ethoxy]pyridin-3-yl)-1H-pyrazol-1-yl]piperidine-1-carboxylate **37**, as a white solid (3.6 g, 71%)

Data for **37**: ^{1}H NMR (300 MHz, DMSO-d_6): δ 1.231 - 1.431 (m, 27H), 1.742 - 1.856 (m, 5H), 2.041 - 2.074 (m, 2H), 2.942 (m, 2H), 4.046 - 4.087 (m, 2H), 4.364 - 4.416 (m, 1H), 6.285 - 6.307 (m, 1H), 7.252 - 7.280 (m, 1H), 7.566 (s, 1H), 7.910 - 7.954 (m, 2H), 8.282 - 8.287 (m, 1H), 8.382 (s, 1H).

NMR purity assay 97.65%.

LC-MS (Method C, 6 min): 858 $[M+H]^+$, rt 3.687 min (97%).

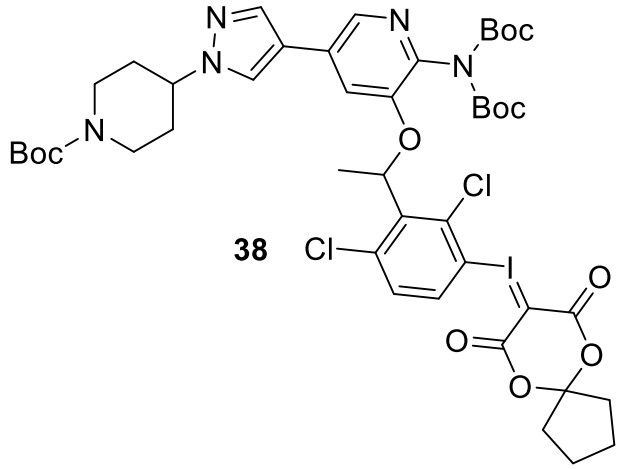

38

*Preparation of tert-butyl 4-(4-(6-(bis(tert-butoxycarbonyl)amino)-5-(1-(2,6-dichloro-3-((7,9-dioxo-6,10-dioxaspiro[4.5]decan-8-ylidene)-l3-iodaneyl)phenyl)ethoxy)pyridin-3-yl)-1H-pyrazol-1-yl)piperidine-1-carboxylate **38** (new).* Into a 250-mL round-bottom flask, was placed tert-butyl 4-[4-(6-[bis[(tert-butoxy)carbonyl]amino]-5-[1-(2,6-dichloro-3-iodophenyl)ethoxy] pyridin-3-yl)-1H-pyrazol-1-yl]piperidine-1-carboxylate **37** (1.5 g, 1.75 mmol, 1.00 equiv), acetone (16 mL), AcOH (4 mL). This was followed by the addition of dimethyldioxirane (50 mL) dropwise with stirring at 0 °C in 5 min. The resulting solution was stirred for 2 h at 0 °C. The mixture was concentrated under vacuum. To this was added ethanol (20 mL), 6,10-dioxaspiro[4.5]decane-7,9-dione (600 mg, 3.53 mmol, 2.00 equiv). The pH value of the solution was adjusted to 10 with 10% $Na_2CO_{3(aq)}$. The resulting solution was stirred for 2 h at 25 °C. The resulting solution was diluted with 100 mL of water. The resulting solution was extracted with 3x100 mL of ethyl acetate and the organic layers combined. The resulting mixture was washed with 2x100 mL of brine. The mixture was dried over anhydrous sodium sulfate and concentrated under vacuum. The residue was applied onto a silica gel column with ethyl acetate/petroleum ether (0:1-1:0). The resulting mixture was purified by Prep-HPLC. Fractions containing the product were pooled and concentrated to give the product, tert-butyl 4-(4-(6-(bis(*tert*-butoxycarbonyl)amino)-5-(1-(2,6-dichloro-3-((7,9-dioxo-6,10-

dioxaspiro[4.5]decan-8-ylidene)-l3-iodaneyl)phenyl)ethoxy)pyridin-3-yl)-1H-pyrazol-1-yl)piperidine-1-carboxylate **38**, as an off-white solid (275 mg, 15%).

Data for **38**: ^{1}H NMR (300 MHz, DMSO-d_6): δ 1.231 - 1.434 (m, 27H), 1.586 - 1.635 (m, 4H), 1.717 - 1.738 (m, 3H), 1.7954 - 1.921 (m, 6H), 2.041 - 2.082 (m, 2H), 2.735 - 2.973 (m, 2H), 4.048 - 4.090 (m, 2H), 4.392 -4.443 (m, 1H), 6.297 - 6.321 (m, 1H), 7.565 - 7.635 (m, 2H), 7.775 - 7.803 (m, 1H), 7.953 (s, 1H), 8.300 - 8.350 (m, 2H).

NMR purity assay: 98.16%.

LC-MS (Method C, 5 min): 1026 $[M+H]^+$, rt 3.031 min (98%).

The racemic product was dissolved in EtOH (50 mg/mL) and purified over a chiral column, Chiralcel OD column (250x20mm, particle size 5 µm), with n-Heptane/EtOH/TEA (80/20/0.1, v/v/v) to obtain ***(R)*-38**.

*Precursor synthesis: Deoxyfluorination precursor **50***

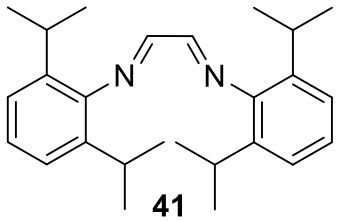

*Preparation of (1E,2E)-N1,N2-bis(2,6-diisopropylphenyl)ethane-1,2-diimine **41**.*[135] 2,6-diisopropylaniline **39** (17.73 g, 100 mmol) and acetic acid (0.105 g, 1.75 mmol) in methanol (25 mL) was heated to 50 °C. To this was added oxalaldehyde **40** (7.25 g, 49.97 mmol) in methanol (25 mL) and the mixture stirred at 50 °C for 15 min. The reaction was stirred at RT overnight. A yellow precipitate had formed in the red/brownish solution. The solid was filtered and the filter cake washed with methanol (3 x 15 mL). The product (1E,2E)-N1,N2-bis(2,6-diisopropylphenyl)ethane-1,2-diimine **41** (14.12 g, 75 %) was afforded as a yellow solid.

Data for **41**: ^{1}H NMR (400 MHz, $CDCl_3$) δ: 1.21 (d, J = 6.9 Hz, 24H), 2.90-2.98 (m, 4H), 7.13-7.21 (m, 6H), 8.10 (s, 2H).

^{13}C NMR (100 MHz, $CDCl_3$) δ: 163.2, 148.1, 136.9, 125.3, 123.3, 28.2, 23.5.

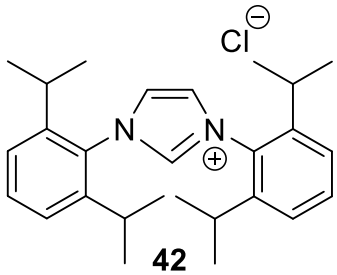

42

*Preparation of 1,3-bis(2,6-diisopropylphenyl)-1H-imidazol-3-ium **42**.*[135] In air, (1E,2E)-N1,N2-*bis*(2,6-diisopropylphenyl)ethane-1,2-diimine **41** (12,9 g, 34,25 mmol) and paraformaldehyde (1.060 g, 35.28 mmol) were combined in ethyl acetate (320 mL) and heated to 70 °C. Under vigorous stirring, chlorotrimethylsilane (4.48 ml, 35.28 mmol) in ethyl acetate (5 mL) was added very gradually. The mixture was stirred at 70 °C for 2.5 hours. The mixture was then cooled to 10 °C while stirring. The mixture was filtered under reduced pressure and the filter cake washed with ethyl acetate (4 x 25 mL). The product 1,3-bis(2,6-diisopropylphenyl)-1H-imidazol-3-ium **42** was afforded as a slightly rose-colored solid.

Data for **42**: ^{1}H NMR (400 MHz, CD_3CN) δ: 1.19 (d, J = 6.9 Hz, 12H), 1.23 (d, J = 6.8 Hz, 12H), 2.40 (hept, J = 6.8 Hz, 4H), 7.42 (d, J = 7.8 Hz, 4H), 7.60 (t, J = 7.8 Hz, 2H), 7.88 (d, J = 1.5 Hz, 2H), 10.69 (t, J = 1.4 Hz, 1H).

^{13}C NMR (100 MHz, CD_3CN) δ: 146.3, 141.0, 132.8, 126.6, 125.5, 29.9, 24.7, 23.7.

LCMS (Method A, 4 min): 389 $[M]^+$, rt 1.69 min (100%).

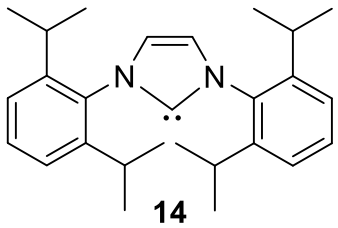

14

Preparation of 1,3-bis(2,6-diisopropylphenyl)-1H-imidazol-3-ium-2-ide ***43***.[135] 1,3-*bis*(2,6-diisopropylphenyl)-1H-imidazol-3-ium chloride **42** (4.25 g, 10 mmol) is placed in an oven-dried round bottom flask. The flask was evacuated and backfilled with N_2 gas, then potassium 2-methylpropan-2-olate in THF (10.00 ml, 10.00 mmol) and THF (10.00 ml) was added. The mixture was stirred at room temperature for 3.5 hours, the solvent was evaporated in vacuo. The residue was dissolved in toluene (21 mL) with gentle heating (50-60 °C) and the hot solution was filtered through a pad of celite eluting with toluene. The filtrate was concentrated and dried in vacuo.

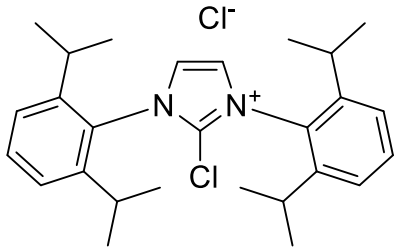

29

*Preparation of 2-chloro-1,3-bis(2,6-diisopropylphenyl)-1H-imidazol-3-ium **29**.*[135] To a mixture of 1,3-bis(2,6-diisopropylphenyl)-1H-imidazol-3-ium-2-ide **43** (3.89 g, 10 mmol) and THF (23.87 ml) was added hexachloroethane (2.60 g, 11.00 mmol) at -78 °C. The mixture was warmed to 23 °C and stirred for 20 h. The reaction mixture was filtered, the filter cake was washed with THF (3x10mL) and toluene (3x10 mL) and dried in vacuo to give the product as an off-white solid (3.302 g, 72%).

Data for **29**: ^{1}H NMR (400 MHz, $CDCl_3$) δ 1.23 (d, J = 6.89 Hz, 12H), 1.32 (d, J = 6.79 Hz, 12H), 2.25 – 2.47 (m, 4H), 7.45 (d, J = 7.86 Hz, 4H), 7.68 (t, J = 7.86, 7.86 Hz, 2H), 8.80 (s, 2H).

LCMS (Method B, 4 min): 423 $[M]^+$, rt 1.95 min (98%).

*Preparation of 2-chloro-1,3-bis(2,6-diisopropylphenyl)-1H-imidazol-3-ium silver(I) carbonate chloride **44**.* 2-chloro-1,3-bis(2,6-diisopropylphenyl)-1H-imidazol-3-ium **29** (500 mg, 1.09 mmol, 1 equiv) and Ag_2CO_3 (150 mg, 0.54 mmol, 0.5 equiv) are mixed and stored in an amber colored vial.

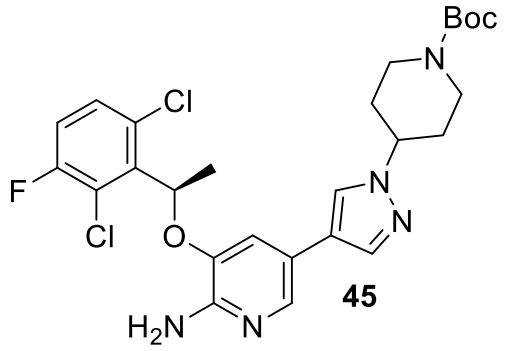

Preparation of tert-butyl (R)-4-(4-(6-amino-5-(1-(2,6-dichloro-3-fluorophenyl)ethoxy)pyridin-3-yl)-1H-pyrazol-1-yl)piperidine-1-carboxylate ***45*** *(CAS 877399-51-4).*[136] Boc_2O (0.634 mL, 2.76 mmol, 1.1 eq) in one portion to a solution of crizotinib (1.13 g, 2.51 mmol, 1 eq) and N,N-dimethylpyridin-4-amine (31 mg, 0.25 mmol, 0.1 eq) in THF (33.3 mL) under a N_2 atmosphere. The resulting solution was stirred for 18 hours at room temperature. The reaction mixture was diluted with water (20 mL) and washed with EtOAc (100 mL). The organic layer was dried over anhydrous magnesium sulfate , filtered, and evaporated to afford *tert*-butyl (R)-4-(4-(6-amino-5-(1-(2,6-dichloro-3-fluorophenyl)ethoxy)pyridin-3-yl)-1H-pyrazol-1-yl)piperidine-1-carboxylate **45** (1.260 g, 2.30 mmol, 91%) as a beige solid.

Data for **45**: ^{1}H NMR (400 MHz, $CDCl_3$) δ 1.48 (s, 9H), 1.85 (d, J = 6.7 Hz, 3H), 1.93 (td, J = 12.3, 4.3 Hz, 2H), 2.13 (d, J = 11.0 Hz, 2H), 2.89 (t, J = 11.7 Hz, 2H), 4.24 (ddq, J = 11.4, 8.0, 3.9 Hz, 3H), 4.87 (s, 2H), 6.07 (q, J = 6.7 Hz, 1H), 6.87 (d, J = 1.7 Hz, 1H), 7.05 (dd, J = 8.8, 8.0 Hz, 1H), 7.30 (dd, J = 8.9, 4.8 Hz, 1H), 7.48 (s, 1H), 7.56 (s, 1H), 7.74 (d, J = 1.8 Hz, 1H).

^{13}C NMR (101 MHz, $CDCl_3$) δ 154.74, 149.01, 140.03, 137.04, 136.01, 135.27, 129.10, 122.78, 120.09, 119.22, 117.00, 116.77, 115.17, 80.07, 77.48, 77.16, 76.84, 72.63, 59.54, 48.41, 32.51, 28.56, 19.04.

LCMS (Method B, 4 min): 552 $[M+H]^+$, rt 2.08 min (100%).

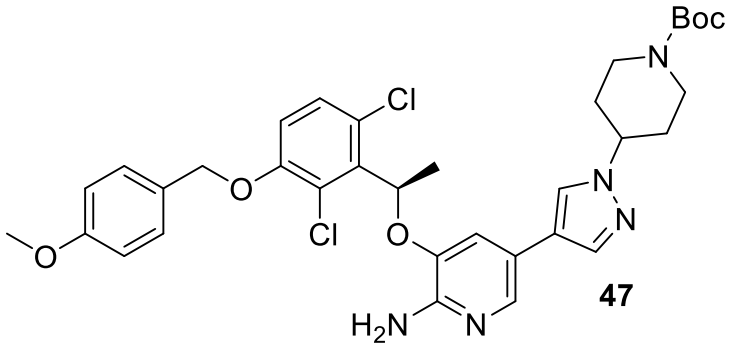

Preparation of tert-butyl (R)-4-(4-(6-amino-5-(1-(2,6-dichloro-3-((4-methoxybenzyl) oxy)phenyl)ethoxy)-pyridin-3-yl)-1H-pyrazol-1-yl)piperidine-1-carboxylate ***47*** *(new). Tert-*butyl (R)-4-(4-(6-amino-5-(1-(2,6-dichloro-3-fluorophenyl)ethoxy)pyridin-3-yl)-1H-pyrazol-1-yl) piperidine-1-carboxylate (275.3 mg, 0.50 mmol, 1 eq), (4-methoxyphenyl)methanol **46** (68 µl, 0.55 mmol, 1.1 eq) and sodium hydride (28.8 mg, 0.60 mmol, 1.2 eq) were suspended in DMF (3.2 mL) and sealed into a microwave tube (2-5 mL) under nitrogen atmosphere. The reaction was heated to 120 °C for 30 min in the microwave reactor and cooled to RT, to give a light brown solution. The reaction mixture was cooled and quenched with MeOH (5 mL) and concentrated in vacuo. The crude was dissolved in 50 mg/mL DCM/EtOH (1:1) and purified over SFC-MS with 10% MeOH/DEA (100:0.5) in CO_2 150 bar. The desired product, *tert*-butyl (R)-4-(4-(6-amino-5-(1-(2,6-dichloro-3-((4-methoxybenzyl)oxy)-phenyl)ethoxy)pyridin-3-yl)-1H-pyrazol-1-yl)piperidine-1-carboxylate, was obtained as a beige solid (182.9 mg, 55%).

Data for **47**: ^{1}H NMR (400 MHz, $CDCl_3$) δ 1.47 (s, 9H), 1.84 (d, J = 6.7 Hz, 3H), 1.92 (tt, J = 12.2, 6.2 Hz, 2H), 2.11 (d, J = 11.9 Hz, 2H), 2.88 (t, J = 11.8 Hz, 2H), 3.80 (s, 3H), 4.23 (ddq, J = 11.4, 7.9, 3.8 Hz, 3H), 4.76 (s, 2H), 5.02 (s, 2H), 6.11 (q, J = 6.5 Hz, 1H), 6.82 (d, J = 8.9 Hz, 1H), 6.86 – 6.93 (m, 3H), 7.20 (d, J = 8.9 Hz, 1H), 7.32 (d, J = 8.6 Hz, 2H), 7.49 (s, 1H), 7.58 (s, 1H), 7.74 (s, 1H).

^{13}C NMR (101 MHz, $CDCl_3$) δ 159.73, 154.72, 149.16, 136.15, 136.05, 135.37, 128.99, 127.91, 125.54, 122.79, 120.32, 115.16, 114.21, 114.07, 80.03, 77.48, 77.16, 76.84, 72.76, 71.18, 59.47, 55.41, 28.56, 19.04.

LCMS (Method B, 4 min): 668 $[M+H]^+$, rt 2.42 min (97%).

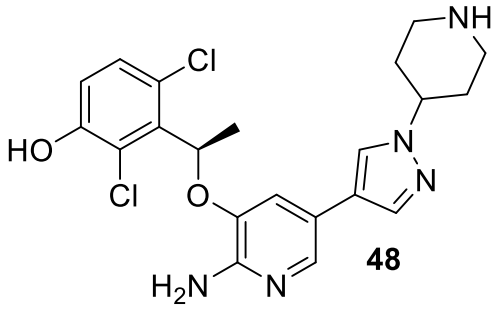

48

· 2 TFA

Preparation of (R)-3-(1-((2-amino-5-(1-(piperidin-4-yl)-1H-pyrazol-4-yl)pyridin-3-yl)oxy)ethyl)-2,4-dichlorophenol TFA salt **48**. *Tert*-butyl (R)-4-(4-(6-amino-5-(1-(2,6-dichloro-3-((4-methoxybenzyl)oxy)phenyl)ethoxy)pyridin-3-yl)-1H-pyrazol-1-yl)piperidine-1-carboxylate **47** (250 mg, 0.37 mmol, 1 eq) is dissolved in DCM (1 mL). To the yellow solution, 2,2,2-trifluoroacetic acid (0.9 mL, 11.68 mmol, 31.2 eq) is added dropwise via a syringe. After 1 h, the reaction mixture is concentrated in vacuo and the crude is used as it is.

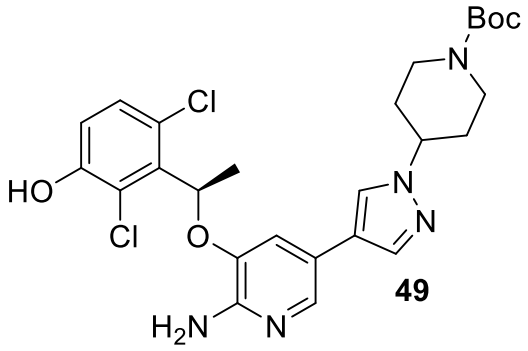

49

Preparation of tert-butyl (R)-4-(4-(6-amino-5-(1-(2,6-dichloro-3-hydroxyphenyl)ethoxy)pyridin-3-yl)-1H-pyrazol-1-yl)piperidine-1-carboxylate ***49****.* To (R)-3-(1-((2-amino-5-(1-(piperidin-4-yl)-1H-pyrazol-4-yl)pyridin-3-yl)oxy)ethyl)-2,4-dichlorophenol *bis* (2,2,2-trifluoroacetate) **48** (0.074 g, 0.11 mmol, 1 eq) was added sodium hydrogen carbonate (0.9 mL, 0.99 mmol). pH was checked and adjusted to pH 8~9 by adding solid NaHCO3. Dioxane (1 mL) was added and $(Boc)_2O$ (0.025 mL, 0.11 mmol, 1 eq) was added dropwise. The reaction mixture was stirred overnight at room temperature. The reaction mixture was concentrated and re-dissolved in DCM. The solids were filtered off and the filtrate was concentrated to give the product in quantitative yield.

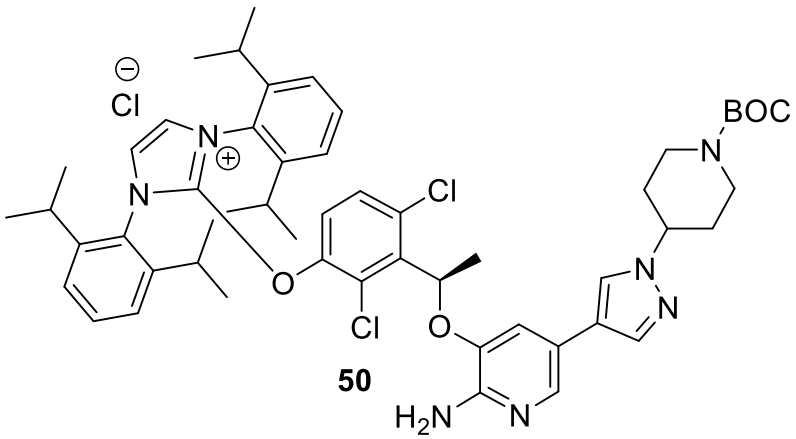

50

Preparation of (R)-2-(3-(1-((2-amino-5-(1-(1-(tert-butoxycarbonyl)piperidin-4-yl)-1H-pyrazol-4-yl)pyridin-3-yl)oxy)ethyl)-2,4-dichlorophenoxy)-1,3-bis(2,6-diisopropylphenyl)-1H-imidazol-3-ium chloride ***50.*** 2-chloro-1,3-bis(2,6-diisopropylphenyl)-1H-imidazol-3-ium disilver(I) carbonate chloride **44** (0.081 g, 0.11 mmol, 1 eq) and 2-chloro-1,3-bis(2,6-diisopropylphenyl)-1H-imidazol-3-ium disilver(I) carbonate chloride (0.081 g, 0.11 mmol, 1 eq) are dissolved in chloroform (0.15 mL) in a small vial and stirred at 60 °C until completion. The reaction mixture cooled, filtered and the filtrate is concentrated to give the product in quantitative yield.

Failed strategies for protection and deprotection

Strategy 1: Boc protection aniline, followed by DDQ deprotection of phenol

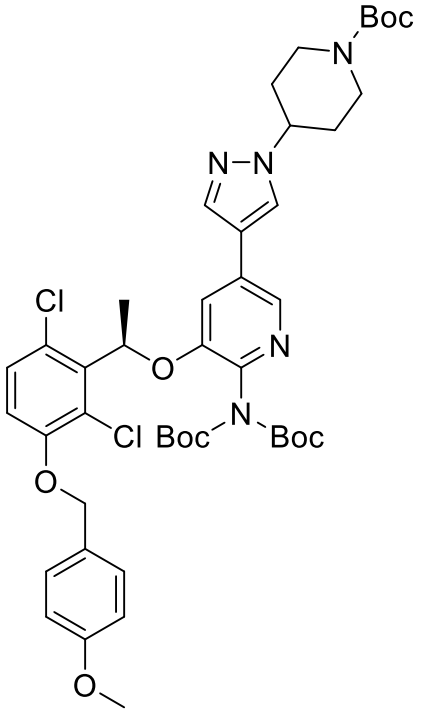

Preparation of tert-butyl (R)-4-(4-(6-(bis(tert-butoxycarbonyl)amino)-5-(1-(2,6-dichloro-3-((4-methoxybenzyl)oxy)phenyl)ethoxy)pyridin-3-yl)-1H-pyrazol-1-yl)piperidine-1-carboxylate.

$(Boc)_2O$ (508.7 mg, 2.32 mmol) was dissolved in THF (10 mL) and added in one portion to *tert*-butyl (R)-4-(4-(6-amino-5-(1-(2,6-dichloro-3-((4-methoxybenzyl)oxy)phenyl)ethoxy)pyridin-3-yl)-1H-pyrazol-1-yl)piperidine-1-carboxylate **47** (250 mg, 0.37 mmol), TEA (0.45 mL, 3.24 mmol) and N,N-dimethylpyridin-4-amine (5.3 mg, 0.04 mmol) and stirred at room temperature over the weekend in a nitrogen atmosphere. The conversion confirmed on TLC. The reaction mixture was concentrated *in vacuo*. The crude residue was re-dissolved in 15 mL DCM and washed with water (3 x 20 mL). The DCM layer was dried over Na_2SO_4 and concentrated *in vacuo*.

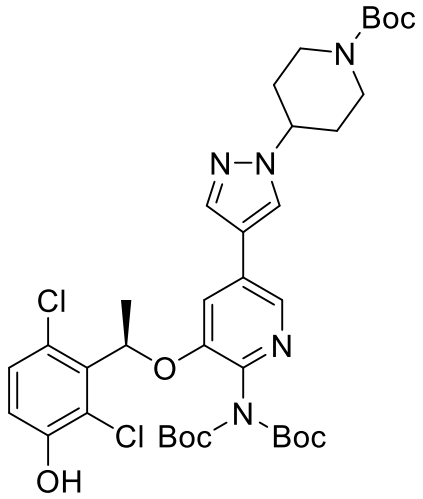

Preparation of tert-butyl (R)-4-(4-(6-(bis(tert-butoxycarbonyl)amino)-5-(1-(2,6-dichloro-3-hydroxyphenyl)ethoxy)pyridin-3-yl)-1H-pyrazol-1-yl)piperidine-1-carboxylate.

(R)-4-(4-(6-(bis(tert-butoxycarbonyl)amino)-5-(1-(2,6-dichloro-3-((4-methoxybenzyl)oxy) phenyl)ethoxy)pyridin-3-yl)-1H-pyrazol-1-yl)piperidine-1-carboxylate (50 mg, 0.06 mmol) was dissolved in DCM (7 mL) and water (0.7 mL). To this DDQ (52.3 mg, 0.23 mmol) was added and stirred for 1 h.[137] The TLC showed many spots, and the product could not be identified on LC-MS. Yet, a work up was attempted. $NaHCO_{3(sat\ aq)}$ was added to the reaction mixture and separated. The aqueous phase is extracted with EtOAc (3 x 10 mL). The organic layers are combined and washed with 10 mL water and 10 mL brine, dried over Na_2SO_4 and concentrated *in vacuo*. LC-MS is still unclear; therefore, this method was abandoned.

Second strategy: Acid deprotection of phenol and piperidone, followed by Boc-protection of piperidine and aniline.

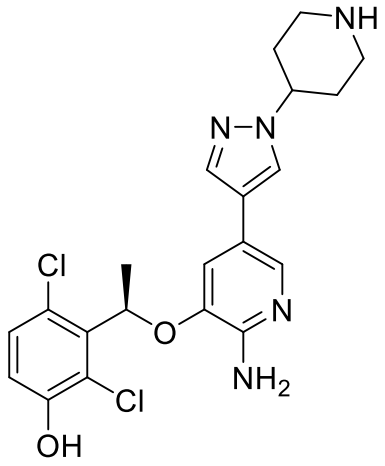

Preparation of (R)-3-(1-((2-amino-5-(1-(piperidin-4-yl)-1H-pyrazol-4-yl)pyridin-3-yl)oxy)ethyl)-2,4-dichlorophenol. *tert*-butyl (R)-4-(4-(6-amino-5-(1-(2,6-dichloro-3-((4-methoxybenzyl)oxy) phenyl)ethoxy)pyridin-3-yl)-1H-pyrazol-1-yl)piperidine-1-carboxylate **47** (250 mg, 0.37 mmol) is dissolved in DCM (1 mL). The yellow solution is cooled with an ice-bath and TFA (0.9 mL, 11.68 mmol) is added dropwise. The ice-bath is removed, and the dark red solution is left stirring for 1 h. The reaction mixture is concentrated ad use as it is in the next step.

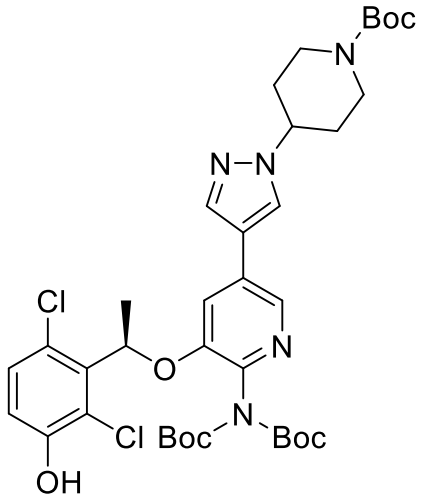

Preparation of tert-butyl (R)-4-(4-(6-(bis(tert-butoxycarbonyl)amino)-5-(1-(2,6-dichloro-3-hydroxyphenyl)ethoxy)pyridin-3-yl)-1H-pyrazol-1-yl)piperidine-1-carboxylate. $(Boc)_2O$ (0.263 mL, 1.15 mmol) was dissolved in THF (5.5 mL) and added in one portion to (R)-3-(1-((2-amino-5-(1-(piperidin-4-yl)-1H-pyrazol-4-yl)pyridin-3-yl)oxy)ethyl)-2,4-dichlorophenol and N,N-dimethylpyridin-4-amine (5.5 mg, 0.05 mmol) in a nitrogen atmosphere. The reaction mixture was stirred at room temperature for 18 h. The reaction mixture was evaporated to dryness ad redissolved in DCM (12 mL) and washed with water (3 x 12 mL). The organic layer is dried over Na_2SO_4, filtered and concentrated *in vacuo*. A normal phase purification was performed using EtOAc:n-Heptane (8:2). Fractions containing product were pooled and concentrated to give 45 mg of product (16%). The NMR showed addition of two Boc-groups, on the piperidine and one possibly on the phenol. The protons of the aniline are visible at 4.77 ppm.

^{1}H NMR (400 MHz, $CDCl_3$) δ 1.48 (s, 9H), 1.55 (s, 9H), 1.85 (d, J = 6.7 Hz, 3H), 1.95 (dq, J = 12.1, 6.1, 5.1 Hz, 2H), 2.12 (d, J = 12.1 Hz, 2H), 2.89 (s, 2H), 4.24 (ddq, J = 11.5, 8.0, 4.0 Hz, 3H), 4.77 (s, 2H), 6.08 (q, J = 6.7 Hz, 1H), 6.84 (d, J = 1.4 Hz, 1H), 7.12 (d, J = 8.7 Hz, 1H), 7.33 (d, J = 8.7 Hz, 1H), 7.48 (s, 1H), 7.55 – 7.62 (m, 1H), 7.75 (d, J = 1.7 Hz, 1H).

Strategy 3, removal of boc-group in presence of PMB:

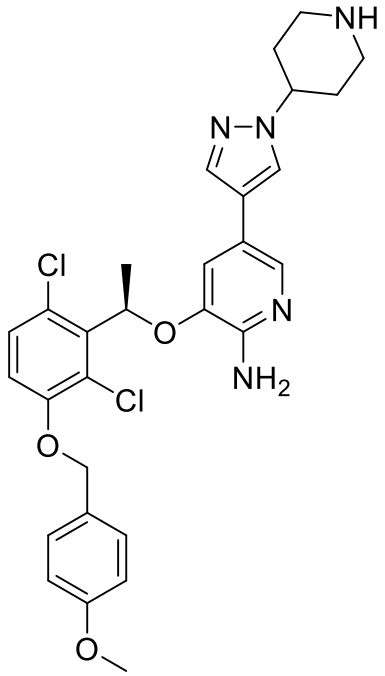

Preparation of (R)-3-(1-(2,6-dichloro-3-((4-methoxybenzyl)oxy)phenyl)ethoxy)-5-(1-(piperidin-4-yl)-1H-pyrazol-4-yl)pyridin-2-amine. *tert*-butyl (R)-4-(4-(6-amino-5-(1-(2,6-dichloro-3-((4-methoxybenzyl)oxy)phenyl)ethoxy)pyridin-3-yl)-1H-pyrazol-1-yl)piperidine-1-carboxylate **47** (50 mg, 0.07 mmol) is suspended/dissolved in MeCN (1 mL). To this, cesium carbonate (36.5 mg, 0.11 mmol) and 1H-imidazole (7.64 mg, 0.11 mmol) were added and stirred at 70 °C.[138] TLC was made after 2 h, overnight and two nights, but no product formation was observed. Therefore, this reaction was discarded.

Preparation of (R)-3-(1-(2,6-dichloro-3-((4-methoxybenzyl)oxy)phenyl)ethoxy)-5-(1-(piperidin-4-yl)-1H-pyrazol-4-yl)pyridin-2-amine. *tert*-butyl (R)-4-(4-(6-amino-5-(1-(2,6-dichloro-3-((4-methoxybenzyl)oxy)phenyl)ethoxy)pyridin-3-yl)-1H-pyrazol-1-yl)piperidine-1-carboxylate **47** (50 mg, 0.07 mmol) was suspended in water (1 mL) and stirred at 100 °C in a sealed vial.[139] TLC was made after 2 h, overnight and two nights, but no product formation was observed. Therefore, this reaction was discarded.

Strategy 4: start from the beginning

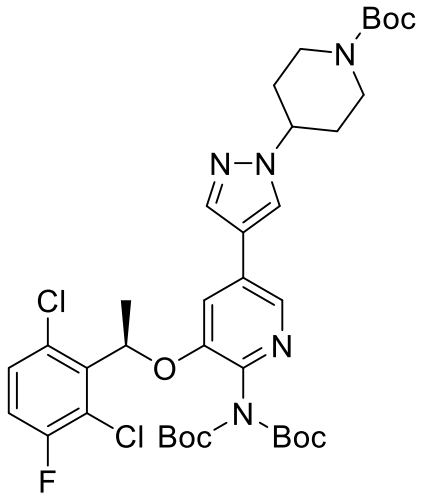

Preparation of tert-butyl (R)-4-(4-(6-(bis(tert-butoxycarbonyl)amino)-5-(1-(2,6-dichloro-3-fluorophenyl)ethoxy)pyridin-3-yl)-1H-pyrazol-1-yl)piperidine-1-carboxylate. Crizotinib (250 mg, 0.56 mmol) is dissolved in DMF (1 mL). To this, a solution of N,N-dimethylpyridin-4-amine (13.56 mg, 0.11 mmol) and $(Boc)_2O$ (0.638 mL, 2.78 mmol) was added dropwise. The solution was left overnight for stirring. The reaction mixture was diluted with $NaHCO_{3(sat.\ aq.)}$ and washed with DCM (3 x 100 mL). DCM layers were combined, washed with water, brine and dried over Na_2SO_4, filtered and concentrated to give product as white foam.

^{1}H NMR (400 MHz, $CDCl_3$) δ 1.46 (s, 19H), 1.62 (s, 9H), 1.82 (d, J = 6.7 Hz, 3H), 1.89 – 2.02 (m, 2H), 2.15 (d, J = 13.5 Hz, 2H), 2.78 – 2.99 (m, 2H), 4.18 – 4.39 (m, 3H), 6.04 (q, J = 6.7 Hz, 1H), 7.06 (dd, J = 8.9, 7.9 Hz, 1H), 7.16 (d, J = 1.8 Hz, 1H), 7.31 (dd, J = 8.9, 4.8 Hz, 1H), 7.61 – 7.73 (m, 2H), 8.17 (d, J = 1.9 Hz, 1H).

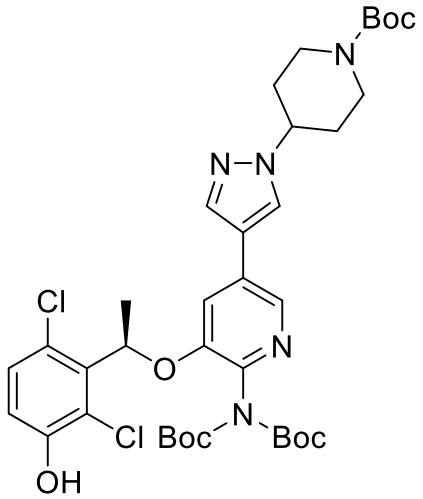

Preparation of tert-butyl (R)-4-(4-(6-(bis(tert-butoxycarbonyl)amino)-5-(1-(2,6-dichloro-3-hydroxyphenyl)ethoxy)pyridin-3-yl)-1H-pyrazol-1-yl)piperidine-1-carboxylate. tert-butyl (R)-4-(4-(6-(bis(tert-butoxycarbonyl)amino)-5-(1-(2,6-dichloro-3-fluorophenyl)ethoxy)pyridin-3-yl)-1H-pyrazol-1-yl)piperidine-1-carboxylate (50 mg, 0.07 mmol) is dissolved in 1,3-dimethylimidazolidin-2-one (1 mL, 0.07 mmol) with NaOH (18 mg, 0.45 mmol) and stirred at 140 °C. After 2 h a new spot is observed on TLC.

Unfortunately, it was difficult to remove the solvent, due to its high boiling point. A workup was attempted; however, an acidic deprotection gave partial deprotection. Thus, this method was abandoned.

10. References

(1) Dugave, C. ISOTOPICS, a European project for de-risking drug innovation https://www.openaccessgovernment.org/isotopics-a-european-project-for-de-risking-drug-innovation/44411/ (accessed Sep 11, 2019).

(2) Horien, C.; Yuan, P. Drug Development. *Yale Journal of Biology and Medicine*. Yale Journal of Biology and Medicine 2017, pp 1–3.

(3) Microdose Radiopharmaceutical Diagnostic Drugs: Nonclinical Study Recommendations https://www.fda.gov/regulatory-information/search-fda-guidance-documents/microdose-radiopharmaceutical-diagnostic-drugs-nonclinical-study-recommendations (accessed Oct 14, 2019).

(4) Dugave, C. ISOTOPICS http://www.isotopics-project.eu/.

(5) Kummar, S.; Doroshow, J. H.; Tomaszewski, J. E.; Calvert, A. H.; Lobbezoo, M.; Giaccone, G. Phase 0 Clinical Trials: Recommendations from the Task Force on Methodology for the Development of Innovative Cancer Therapies. *Eur. J. Cancer* **2009**, *45* (5), 741–746. https://doi.org/10.1016/J.EJCA.2008.10.024.

(6) Fuloria, N. K.; Fuloria, S.; Vakiloddin, S. Phase Zero Trials: A Novel Approach in Drug Development Process. *Ren. Fail.* **2013**, *35* (7), 1044–1053. https://doi.org/10.3109/0886022X.2013.810543.

(7) Borden, E. C.; Dowlati, A. Phase I Trials of Targeted Anticancer Drugs: A Need to Refocus. *Nat. Rev. Drug Discov.* **2012**, *11* (12), 889–890. https://doi.org/10.1038/nrd3909.

(8) Schellekens, R. C. A.; Stellaard, F.; Woerdenbag, H. J.; Frijlink, H. W.; Kosterink, J. G. W. Applications of Stable Isotopes in Clinical Pharmacology. *Br. J. Clin. Pharmacol.* **2011**, *72* (6), 879–897. https://doi.org/10.1111/j.1365-2125.2011.04071.x.

(9) Atzrodt, J.; Derdau, V.; Kerr, W. J.; Reid, M. Deuterium- and Tritium-Labelled Compounds: Applications in the Life Sciences. *Angewandte Chemie - International Edition*. John Wiley & Sons, Ltd February 12, 2018, pp 1758–1784. https://doi.org/10.1002/anie.201704146.

(10) Iglesias, J.; Sleno, L.; Volmer, D. A. Isotopic Labeling of Metabolites in Drug Discovery Applications. *Curr. Drug Metab.* **2012**, *13*, 1213–1225. https://doi.org/10.2174/138920012803341357.

(11) Elmore, C. S. The Use of Isotopically Labeled Compounds in Drug Discovery. *Annual Reports in Medicinal Chemistry*. Elsevier 2009, pp 515–534. https://doi.org/10.1016/S0065-7743(09)04425-X.

(12) Harbeson, S. L.; Tung, R. D. Deuterium in Drug Discovery and Development. *Annu. Rep. Med. Chem.* **2011**, *46*, 403–417. https://doi.org/10.1016/B978-0-12-386009-5.00003-5.

(13) Notman, N. 2Heavy drugs gaining momentum https://www.chemistryworld.com/features/2heavy-drugs-gaining-momentum/1010186.article (accessed Oct 14, 2019).

(14) Tokunaga, E.; Yamamoto, T.; Ito, E.; Shibata, N. Understanding the Thalidomide Chirality in Biological Processes by the Self-Disproportionation of Enantiomers. *Sci. Rep.* **2018**, *8* (1), 17131. https://doi.org/10.1038/s41598-018-35457-6.

(15) Yamamoto, T.; Tokunaga, E.; Nakamura, S.; Shibata, N.; Toru, T. Synthesis and Configurational Stability of (S)- and (R)-Deuteriothalidomides. *Chem. Pharm. Bull. (Tokyo).* **2010**, *58* (1), 110–112. https://doi.org/10.1248/cpb.58.110.

(16) Jacques, V.; Czarnik, A. W.; Judge, T. M.; Van der Ploeg, L. H. T.; DeWitt, S. H. Differentiation of Antiinflammatory and Antitumorigenic Properties of Stabilized Enantiomers of Thalidomide

Analogs. *Proc. Natl. Acad. Sci.* **2015**, 201417832. https://doi.org/10.1073/pnas.1417832112.

(17) Narayanaswami, V.; Dahl, K.; Bernard-Gauthier, V.; Josephson, L.; Cumming, P.; Vasdev, N. Emerging PET Radiotracers and Targets for Imaging of Neuroinflammation in Neurodegenerative Diseases: Outlook Beyond TSPO. *Mol. Imaging* **2018**, *17*, 153601211879231. https://doi.org/10.1177/1536012118792317.

(18) Schou, M.; Halldin, C.; Pike, V. W.; Mozley, P. D.; Dobson, D.; Innis, R. B.; Farde, L.; Hall, H. Post-Mortem Human Brain Autoradiography of the Norepinephrine Transporter Using (S,S)-[18F]FMeNER-D2. *Eur. Neuropsychopharmacol.* **2005**, *15* (5), 517–520. https://doi.org/10.1016/j.euroneuro.2005.01.007.

(19) Rami-Mark, C.; Zhang, M.-R.; Mitterhauser, M.; Lanzenberger, R.; Hacker, M.; Wadsak, W. [18F]FMeNER-D2: Reliable Fully-Automated Synthesis for Visualization of the Norepinephrine Transporter. *Nucl. Med. Biol.* **2013**, *40* (8), 1049–1054. https://doi.org/10.1016/j.nucmedbio.2013.08.007.

(20) Schou, M.; Halldin, C.; Sóvágó, J.; Pike, V. W.; Hall, H.; Gulyás, B.; Mozley, P. D.; Dobson, D.; Shchukin, E.; Innis, R. B.; Farde, L. PET Evaluation of Novel Radiofluorinated Reboxetine Analogs as Norepinephrine Transporter Probes in the Monkey Brain. *Synapse* **2004**, *53* (2), 57–67. https://doi.org/10.1002/syn.20031.

(21) Krauser, J. A. A Perspective on Tritium versus Carbon-14: Ensuring Optimal Label Selection in Pharmaceutical Research and Development. *J. Label. Compd. Radiopharm.* **2013**, *56* (9–10), 441–446. https://doi.org/10.1002/jlcr.3085.

(22) Isin, E. M.; Elmore, C. S.; Nilsson, G. N.; Thompson, R. A.; Weidolf, L. Use of Radiolabeled Compounds in Drug Metabolism and Pharmacokinetic Studies. *Chem. Res. Toxicol.* **2012**, *25* (3), 532–542. https://doi.org/10.1021/tx2005212.

(23) Weissleder, R.; Ross, B. D.; Rehemtulla, A.; Gambjir, S. S. Radiochemistry of Positron Emission Tomography. In *Molecular Imaging*; People's Medical Publishin House- USA: Shelton, Connecticut, 2010; pp 304–326.

(24) Hein, P.; Michel, M. Radioligand Binding Studies in Cardiovascular Research (Saturation and Competition Binding Studies). In *Receptor and Binding Studies*; Springer Berlin Heidelberg, 2005; pp 723–783. https://doi.org/https://doi.org/10.1007/3-540-26574-0_37.

(25) Smith, E.; Collins, I. Photoaffinity Labeling in Target-and Binding-Site Identification. *Future Medicinal Chemistry*. Future Science February 1, 2015, pp 159–183. https://doi.org/10.4155/fmc.14.152.

(26) Surapaneni, S. Regulatory Drug Disposition and NDA Package Including Mist. In *ADME-Enabling Tehcnologies in Drug Design and Development*; Zhang, D., Surapaneni, S., Eds.; John Wiley & Sons, Ltd: Hoboken, New Jersey, 2012; pp 3–14.

(27) McEwen, A.; Henson, C. Quantitative Whole-Body Autoradiography: Past, Present and Future. *Bioanalysis*. Future Science Ltd March 1, 2015, pp 557–568. https://doi.org/10.4155/bio.15.9.

(28) Wang, L.; Hong, H.; Zhang, D. Applications of Quantitative Whole-Body Autoradiography (QWBA) in Drug Discovery and Development. In *ADME-Enabling Tehcnologies in Drug Design and Development*; Zhang, D., Surapaneni, S., Eds.; John Wiley & Sons, Ltd: Hoboken, New Jersey, 2012; pp 419–434.

(29) Wang, L.; He, K.; Maxwell, B.; Grossman, S. J.; Tremaine, L. M.; Humphreys, W. G.; Zhang, D. Tissue Distribution and Elimination of [14 C]Apixaban in Rats. *Drug Metab. Dispos.* **2011**, *39* (2), 256–264. https://doi.org/10.1124/dmd.110.036442.

(30) Solon, E. G. Chapter 6. Autoradiography in Pharmaceutical Discovery and Development. In *Biomedical Imaging: The Chemistry of Labels, Probes and Contrast Agents*; 2011; pp 309–342. https://doi.org/10.1039/9781849732918-00309.

(31) Wotherspoon, A. T.; Safavi-Naeini, M.; Banati, R. B. Microdosing, Isotopic Labeling, Radiotracers and Metabolomics: Relevance in Drug Discovery, Development and Safety. *Bioanalysis*. Future Science Ltd London, UK December 24, 2017, pp 1913–1933. https://doi.org/10.4155/bio-2017-0137.

(32) Atzrodt, J.; Allen, J. Synthesis of Radiolabeled Compounds for Clinical Studies. In *Drug Discovery and Evaluation: Methods in Clinical Pharmacology*; Springer Berlin Heidelberg, 2011; pp 105–118. https://doi.org/10.1007/978-3-540-89891-7_12.

(33) Mignot, A. Why, When, and How to Conduct 14C Human Studies. *SGS' Life Science News*. 2009.

(34) Hinsinger, K.; Pieters, G. The Emergence of Carbon Isotope Exchange. *Angewandte Chemie - International Edition*. July 15, 2019, pp 9678–9680. https://doi.org/10.1002/anie.201905368.

(35) Ruben, S.; Kamen, M. D. Long-Lived Radioactive Carbon: C14. *Phys. Rev.* **1941**, *59* (4), 349–354. https://doi.org/10.1103/PhysRev.59.349.

(36) Raaen, V. F.; Ropp, G. A.; Raaen, H. P. *Carbon-14 - McGraw-Hill Series in Advanced Chemistry*; McGraw-Hill: New York, 1968.

(37) Voges, R.; Heys, J. R.; Moenius, T. Barium [14C]Carbonate and the Preparation of Carbon-14-Labeled Compounds via One-Carbon Building Blocks of the [14C]Carbon Dioxide Tree. In *Preparation of Compounds with Tritium and Carbon-14*; John Wiley & Sons, Ltd: West Sussex, 2009; pp 211–286.

(38) Voges, R.; Heys, J.; Moenius, T. Preparation of Carbon-14-Labeled Compounds via the [14C]Cyanide Tree. In *Preparation of Compounds with Tritium and Carbon-14*; John Wiley & Sons, Ltd: West Sussex, 2009; pp 393–439.

(39) Derdau, V. New Trends and Applications in Cyanation Isotope Chemistry. *Journal of Labelled Compounds and Radiopharmaceuticals*. Wiley-Blackwell December 25, 2018, pp 1012–1023. https://doi.org/10.1002/jlcr.3630.

(40) Matloubi, H.; Ghandi, M.; Zarrindast, M.-R.; Saemian, N. Modified Synthesis of 11-[14C]-Clozapine. *Appl. Radiat. Isot.* **2001**, *55* (6), 789–791. https://doi.org/10.1016/S0969-8043(01)00134-8.

(41) Sunay, U. B.; Talbot, K. C.; Galullo, V. Synthesis of Carbon-14 and Tritium Labelled Analogs of the Noval Antischizophrenic Agent Clozapine. *J. Label. Compd. Radiopharm.* **1992**, *31* (12), 1041–1047. https://doi.org/10.1002/jlcr.2580311212.

(42) Loreau, O.; Georgin, D.; Taran, F.; Audisio, D. Palladium-Catalyzed Decarboxylative Cyanation of Aromatic Carboxylic Acids Using [^{13}C] and [^{14}C]-KCN. *J. Label. Compd. Radiopharm.* **2015**, *58* (11–12), 425–428. https://doi.org/10.1002/jlcr.3330.

(43) Voges, R.; Heys, J.; Moenius, T. Preparation of Carbon-14-Labeled Compounds via the [14C2]Acetylene Tree. In *Preparation of Compounds with Tritium and Carbon-14*; John Wiley & Sons, Ltd: West Sussex, 2009; pp 441–463.

(44) Elmore, C. S.; Dorff, P. N. Synthesis of Triphenylsilyl[14C2]Acetylene for Use in a Sonogashira Reaction. *J. Label. Compd. Radiopharm.* **2011**, *54* (1), 51–53. https://doi.org/10.1002/jlcr.1808.

(45) Voges, R.; Heys, J.; Moenius, T. Preparation of Carbon-14-Labeled Compounds via the [14C]Cyanamide Tree. In *Preparation of Compounds with Tritium and Carbon-14*; John Wiley & Sons, Ltd: West Sussex, 2009; pp 465–478.

(46) Murthy, A.; Ullas, G. Synthesis of [^{14}C] Labeled 2-Methoxypyrimidine-5-Carboxylic Acid. *J. Label. Compd. Radiopharm.* **2009**, *52* (4), 114–116. https://doi.org/10.1002/jlcr.1577.

(47) Dauben, W.; Reid, J.; Yankwich, P. Techniques in Using Carbon 14. *Anal. Chem.* **1947**, *19* (11), 828–832. https://doi.org/10.1021/ac60011a003.

(48) Zwiebel, N.; Turkevich, J.; Miller, W. W. Preparation of Radioactive CO2 from BaCO3. *J. Am. Chem. Soc.* **1949**, *71* (1), 376–377. https://doi.org/10.1021/ja01169a520.

(49) Voges, R.; Heys, J. R.; Moenius, T. *Preparation of Compounds Labeled with Tritium and Carbon-14*; John Wiley & Sons, Ltd: West Sussex, 2009.

(50) Hesk, D.; Borges, S.; Dumpit, R.; Hendershot, S.; Koharski, D.; McNamara, P.; Ren, S.; Saluja, S.; Truong, V.; Voronin, K. Synthesis of 3 H, 2 H 4 , and 14 C-MK 3814 (Preladenant). *J. Label. Compd. Radiopharm.* **2017**, *60* (4), 194–199. https://doi.org/10.1002/jlcr.3490.

(51) Latli, B.; Hrapchak, M.; Cheveliakov, M.; Reeves, J. T.; Marsini, M.; Busacca, C. A.; Senanayake, C. H. Potent and Selective CC Chemokine Receptor 1 Antagonists Labeled with Carbon-13, Carbon-14, and Tritium. *J. Label. Compd. Radiopharm.* **2018**, *61* (10), 764–772. https://doi.org/10.1002/jlcr.3635.

(52) McGhee, W.; Riley, D. Replacement of Phosgene with Carbon Dioxide: Synthesis of Alkyl Carbonates. *J. Org. Chem.* **1995**, *60* (19), 6205–6207. https://doi.org/10.1021/jo00124a044.

(53) Dean, D. C.; Wallace, M. A.; Marks, T. M.; Melillo, D. G. Efficient Utilization of [14C]Carbon Dioxide as a Phosgene Equivalent for Labeled Synthesis. *Tetrahedron Lett.* **1997**, *38* (6), 919–922. https://doi.org/10.1016/S0040-4039(96)02513-0.

(54) Del Vecchio, A.; Caillé, F.; Chevalier, A.; Loreau, O.; Horkka, K.; Halldin, C.; Schou, M.; Camus, N.; Kessler, P.; Kuhnast, B.; Taran, F.; Audisio, D. Late-Stage Isotopic Carbon Labeling of Pharmaceutically Relevant Cyclic Ureas Directly from CO_2. *Angew. Chemie Int. Ed.* **2018**, *57* (31), 9744–9748. https://doi.org/10.1002/anie.201804838.

(55) Destro, G.; Loreau, O.; Marcon, E.; Taran, F.; Cantat, T.; Audisio, D. Dynamic Carbon Isotope Exchange of Pharmaceuticals with Labeled CO_2. *J. Am. Chem. Soc.* **2019**, *141* (2), 780–784. https://doi.org/10.1021/jacs.8b12140.

(56) Cruickshank, W. Some Observations on Different Hydrocarbonates and Combinations of Carbone with Oxygen. *J. Nat. Philos., Chem. Art* **1801**, No. 5, 201–211.

(57) Brennführer, A.; Neumann, H.; Beller, M. Palladium-Catalyzed Carbonylation Reactions of Aryl Halides and Related Compounds. *Angew. Chemie Int. Ed.* **2009**, *48* (23), 4114–4133. https://doi.org/10.1002/anie.200900013.

(58) Schoenberg, A.; Bartoletti, I.; Heck, R. F. Palladium-Catalyzed Carboalkoxylation of Aryl, Benzyl, and Vinylic Halides. *J. Org. Chem.* **1974**, *39* (23), 3318–3326. https://doi.org/10.1021/jo00937a003.

(59) Heck, R. F. A Synthesis of Diaryl Ketones from Arylmercuric Salts. *J. Am. Chem. Soc.* **1968**, *90* (20), 5546–5548. https://doi.org/10.1021/ja01022a040.

(60) Schoenberg, A.; Heck, R. F. Palladium-Catalyzed Amidation of Aryl, Heterocyclic, and Vinylic Halides. *J. Org. Chem.* **1974**, *39* (23), 3327–3331. https://doi.org/10.1021/jo00937a004.

(61) Schoenberg, A.; Heck, R. F. Palladium-Catalyzed Formylation of Aryl, Heterocyclic, and Vinylic Halides. *J. Am. Chem. Soc.* **1974**, *96* (25), 7761–7764. https://doi.org/10.1021/ja00832a024.

(62) Ye, S.; Xiang, T.; Li, X.; Wu, J. Metal-Catalyzed Radical-Type Transformation of Unactivated Alkyl Halides with C–C Bond Formation under Photoinduced Conditions. *Org. Chem. Front.* **2019**, *6* (13), 2183–2199. https://doi.org/10.1039/C9QO00272C.

(63) Heck, R. F.; Breslow, D. S. *Catalyzed Carboxyalkylation Reactions Carboxyalkylation Reactions Catalyzed by Cobalt Carbonylate Ion*; Vol. 99.

(64) Clayden, J.; Greeves, N.; Warren, S.; Wothers, P. Organometallic Chemistry. In *Organic Chemistry*; Oxford University Press Inc.: New York, 2001; pp 1311–1344.

(65) Nielsen, D. U.; Neumann, K. T.; Lindhardt, A. T.; Skrydstrup, T. Recent Developments in Carbonylation Chemistry Using [13C]CO, [11C]CO, and [14C]CO. *Journal of Labelled*

Compounds and Radiopharmaceuticals. John Wiley & Sons, Ltd November 1, 2018, pp 949–987. https://doi.org/10.1002/jlcr.3645.

(66) Edwin Hargraves, H.; Lashford, A. G.; Rees, A. T.; Roughley, B. S. The Radiolysis of [14C]Carbon Monoxide. *J. Label. Compd. Radiopharm.* **2007**, *50* (5–6), 435–436. https://doi.org/10.1002/jlcr.1179.

(67) Weinhouse, S. PREPARATION OF CARBON MONOXIDE [1]. *J. Am. Chem. Soc.* **1948**, *70* (1), 442–443. https://doi.org/10.1021/ja01181a538.

(68) Huston, J. L.; Norris, T. H. Production of Radioactive Carbon Monoxide and Phosgene from Barium Carbonate. *J. Am. Chem. Soc.* **1948**, *70* (5), 1968–1969. https://doi.org/10.1021/JA01185A509.

(69) Dahl, K.; Ulin, J.; Schou, M.; Halldin, C. Reduction of [11 C]CO 2 to [11 C]CO Using Solid Supported Zinc. *J. Label. Compd. Radiopharm.* **2017**, *60* (13), 624–628. https://doi.org/10.1002/jlcr.3561.

(70) Melville, D. B.; Pierce, J. G.; Partridge, C. W. H. THE PREPARATION OF C14-LABELED BIOTIN AND A STUDY OF ITS STABILITY DURING CARBON DIOXIDE FIXATION. *J. Biol. Chem.* **1949**, No. 180, 299–306.

(71) Jagadish, B.; Iyengar, B. S.; Sólyom, A. M.; Remers, W. A.; Dorr, R. T.; Shin Yu, J.; Gupta, S.; Mash, E. A. Synthesis of [14 C]-Imexon. *J. Label. Compd. Radiopharm.* **2005**, *48* (3), 165–170. https://doi.org/10.1002/jlcr.911.

(72) Elmore, C. S.; Dean, D. C.; Melillo, D. G. A Convenient Method for [14C]Carbonylation Reactions. *J. Labelled Comp. Radiopharm.* **2000**, No. 43, 1135–1144.

(73) Elmore, C. S.; Dean, D. C.; DeVita, R. J.; Melillo, D. G. Synthesis of Two Non-Peptidyl GnRH Receptor Antagonists via [14C]Carbonylation. *J. Label. Compd. Radiopharm.* **2003**, *46* (10), 993–1000. https://doi.org/10.1002/jlcr.733.

(74) Simeone, J. P.; Braun, M. P.; Liu, L.; Natarajan, S. R. Palladium-Catalyzed Hydroxycarbonylation as the Key Step in the Synthesis of a Carbon-14 Labeled Maxi-K Channel Blocker. *J. Label. Compd. Radiopharm.* **2010**, *53* (7), n/a-n/a. https://doi.org/10.1002/jlcr.1755.

(75) Cacchi, S.; Fabrizi, G.; Goggiamani, A. Palladium-Catalyzed Synthesis of Aldehydes from Aryl Iodides and Acetic Formic Anhydride. *J. Comb. Chem.* **2004**, *6* (5), 692–694. https://doi.org/10.1021/cc049906h.

(76) Latli, B.; Hrapchak, M.; Li, G.; Lorenz, J.; Horan, J.; Busacca, C. A.; Senanayake, C. H. Synthesis of Highly Potent Lymphocyte Function-Associated Antigen-1 Antagonists Labeled with Carbon-14 and with Stable Isotopes, Part 3. *J. Label. Compd. Radiopharm.* **2019**, *62* (2), 77–85. https://doi.org/10.1002/jlcr.3698.

(77) Elmore, C. S.; Brush, K.; Schou, M.; Palmer, W.; Dorff, P. N.; Powell, M. E.; Hoesch, V.; Hall, J. E.; Hudzik, T.; Halldin, C.; Dantzman, C. L. Synthesis of a Delta Opioid Agonist in [2H 6], [2H 4], [11C], and [14C] Labeled Forms. *J. Label. Compd. Radiopharm.* **2011**, *54* (14), 847–854. https://doi.org/10.1002/jlcr.1939.

(78) ELMORE, C. S.; FRIETZE, W. E.; ANDISIK, D. W.; ERNST, G. E.; HEYS, J. R.; DANTZMAN, C. L. SYNTHESIS OF A C-14 LABELED DELTA-OPIOID RECEPTOR AGONIST BY CARBONYLATION. *J. Label. Compd. Radiopharm.* **2010**, *53*, 394–397. https://doi.org/10.1002/jlcr.1773.

(79) Whitehead, D. M.; Hartmann, S.; Ilyas, T.; Taylor, K. R.; Kohler, A. D.; Ellames, G. J. A Convenient Method to Produce [14 C]Carbon Monoxide and Its Application to the Radiosynthesis of [Carboxyl - 14 C]Celivarone, [Carboxyl - 14 C]SSR149744. *J. Label. Compd. Radiopharm.* **2013**, *56* (2), 36–41. https://doi.org/10.1002/jlcr.3009.

(80) Villeneuve, G. B.; Chan, T. H. A Rapid, Mild and Acid-Free Procedure for the Preparation of Acyl Chlorides Including Formyl Chloride. *Tetrahedron Lett.* **1997**, *38* (37), 6489–6492.

https://doi.org/10.1016/S0040-4039(97)01511-6.

(81) Roeda, D.; Crouzel, C.; Dollé, F. A Rapid, Almost Quantitative Conversion of [11C]Carbon Dioxide into [11C]Carbon Monoxide via [11C]Formate and [11C]Formyl Chloride. *Radiochim. Acta* **2004**, *92* (4–6). https://doi.org/10.1524/ract.92.4.329.35604.

(82) Elmore, C. S.; Dorff, P. N.; Richard Heys, J. Syntheses of the Tricyclic Cores of Clozapine, Dibenzo[b,f][1,4]Thiazepin-11(10H)-One, and Dibenzo[b,f][1,4]Oxazepin-11(10H)-One in C-14 Labeled Form by [14C]Carbonylation. *J. Label. Compd. Radiopharm.* **2010**, *53* (13), 787–792. https://doi.org/10.1002/jlcr.1802.

(83) Lindhardt, A. T.; Simonssen, R.; Taaning, R. H.; Gøgsig, T. M.; Nilsson, G. N.; Stenhagen, G.; Elmore, C. S.; Skrydstrup, T. 14Carbon Monoxide Made Simple - Novel Approach to the Generation, Utilization, and Scrubbing of 14carbon Monoxide. *J. Label. Compd. Radiopharm.* **2012**, *55* (11), 411–418. https://doi.org/10.1002/jlcr.2962.

(84) Hermange, P.; Lindhardt, A. T.; Taaning, R. H.; Bjerglund, K.; Lupp, D.; Skrydstrup, T. Ex Situ Generation of Stoichiometric and Substoichiometric 12CO and 13CO and Its Efficient Incorporation in Palladium Catalyzed Aminocarbonylations. *J. Am. Chem. Soc.* **2011**, *133* (15), 6061–6071. https://doi.org/10.1021/ja200818w.

(85) Sardana, M.; Bergman, J.; Ericsson, C.; Kingston, L. P.; Schou, M.; Dugave, C.; Audisio, D.; Elmore, C. S. Visible-Light-Enabled Aminocarbonylation of Unactivated Alkyl Iodides with Stoichiometric Carbon Monoxide for Application on Late-Stage Carbon Isotope Labeling. *J. Org. Chem.* **2019**, *84* (24), 16076–16085. https://doi.org/10.1021/acs.joc.9b02575.

(86) Kondo, T.; Sone, Y.; Tsuji, Y.; Watanabe, Y. Photo-, Electro-, and Thermal Carbonylation of Alkyl Iodides in the Presence of Group 7 and 8-10 Metal Carbonyl Catalysts. *J. Organomet. Chem.* **1994**, *473* (1–2), 163–173. https://doi.org/10.1016/0022-328X(94)80117-7.

(87) Kondo, T.; Tsuji, Y.; Watanabe, Y. Photochemical Carbonylation of Alkyl Iodides in the Presence of Various Metal Carbonyls. *Tetrahedron Lett.* **1988**, *29* (31), 3833–3836. https://doi.org/10.1016/S0040-4039(00)82127-9.

(88) Sumino, S.; Fusano, A.; Fukuyama, T.; Ryu, I. Carbonylation Reactions of Alkyl Iodides through the Interplay of Carbon Radicals and Pd Catalysts. *Acc. Chem. Res.* **2014**, *47* (5), 1563–1574. https://doi.org/10.1021/ar500035q.

(89) Chow, S. Y.; Odell, L. R.; Eriksson, J. Low-Pressure Radical 11 C-Aminocarbonylation of Alkyl Iodides through Thermal Initiation. *European J. Org. Chem.* **2016**, No. 36, 5980–5989. https://doi.org/10.1002/ejoc.201601106.

(90) Rahman, O.; Långström, B.; Halldin, C. Alkyl Iodides and [11 C]CO in Nickel-Mediated Cross-Coupling Reactions: Successful Use of Alkyl Electrophiles Containing a β Hydrogen Atom in Metal-Mediated [11 C]Carbonylation. *ChemistrySelect* **2016**, *1* (10), 2498–2501. https://doi.org/10.1002/slct.201600643.

(91) Tasker, S. Z.; Standley, E. A.; Jamison, T. F. Recent Advances in Homogeneous Nickel Catalysis. *Nature* **2014**, *509* (7500), 299–309. https://doi.org/10.1038/nature13274.

(92) Neumann, K. T.; Donslund, A. S.; Andersen, T. L.; Nielsen, D. U.; Skrydstrup, T. Synthesis of Aliphatic Carboxamides Mediated by Nickel NN2-Pincer Complexes and Adaptation to Carbon-Isotope Labeling. *Chem. - A Eur. J.* **2018**, *24* (56), 14946–14949. https://doi.org/10.1002/chem.201804077.

(93) Nguyen, J. D.; D'Amato, E. M.; Narayanam, J. M. R.; Stephenson, C. R. J. Engaging Unactivated Alkyl, Alkenyl and Aryl Iodides in Visible-Light-Mediated Free Radical Reactions. *Nat. Chem.* **2012**, *4* (10), 854–859. https://doi.org/10.1038/nchem.1452.

(94) Chow, S. Y.; Stevens, M. Y.; Åkerbladh, L.; Bergman, S.; Odell, L. R. Mild and Low-Pressure Fac -Ir(Ppy) 3 -Mediated Radical Aminocarbonylation of Unactivated Alkyl Iodides through Visible-Light Photoredox Catalysis. *Chem. - A Eur. J.* **2016**, *22* (27), 9155–9161.

https://doi.org/10.1002/chem.201601694.

(95) Roslin, S.; Odell, L. R. Palladium and Visible-Light Mediated Carbonylative Suzuki–Miyaura Coupling of Unactivated Alkyl Halides and Aryl Boronic Acids. *Chem. Commun.* **2017**, *53* (51), 6895–6898. https://doi.org/10.1039/C7CC02763J.

(96) Friis, S. D.; Lindhardt, A. T.; Skrydstrup, T. The Development and Application of Two-Chamber Reactors and Carbon Monoxide Precursors for Safe Carbonylation Reactions. *Acc. Chem. Res.* **2016**, *49* (4), 594–605. https://doi.org/10.1021/acs.accounts.5b00471.

(97) Zhang, J.; Hou, Y.; Ma, Y.; Szostak, M. Synthesis of Amides by Mild Palladium-Catalyzed Aminocarbonylation of Arylsilanes with Amines Enabled by Copper(II) Fluoride. *J. Org. Chem.* **2019**, *84* (1), 338–345. https://doi.org/10.1021/acs.joc.8b02874.

(98) Collin, H. P.; Reis, W. J.; Nielsen, D. U.; Lindhardt, A. T.; Valle, M. S.; Freitas, R. P.; Skrydstrup, T. COtab: Expedient and Safe Setup for Pd-Catalyzed Carbonylation Chemistry. *Org. Lett.* **2019**, *21* (15), 5775–5778. https://doi.org/10.1021/acs.orglett.9b01423.

(99) Purwanto; Deshpande, R. M.; Chaudhari, R. V.; Delmas, H. Solubility of Hydrogen, Carbon Monoxide, and 1-Octene in Various Solvents and Solvent Mixtures. *J. Chem. Eng. Data* **2002**, *41* (6), 1414–1417. https://doi.org/10.1021/je960024e.

(100) Elmore, C. S.; Schenk, D. J.; Arent, R.; Kingston, L. Evaluation of UV-HPLC and Mass Spectrometry Methods for Specific Activity Determination. *J. Label. Compd. Radiopharm.* **2014**, *57* (11), 645–651. https://doi.org/10.1002/jlcr.3234.

(101) Jensen, M. T.; Rønne, M. H.; Ravn, A. K.; Juhl, R. W.; Nielsen, D. U.; Hu, X. M.; Pedersen, S. U.; Daasbjerg, K.; Skrydstrup, T. Scalable Carbon Dioxide Electroreduction Coupled to Carbonylation Chemistry. *Nat. Commun.* **2017**, *8* (1), 489. https://doi.org/10.1038/s41467-017-00559-8.

(102) Taddei, C.; Bongarzone, S.; Gee, A. D. Instantaneous Conversion of [11C]CO2to [11C]CO via Fluoride-Activated Disilane Species. *Chem. - A Eur. J.* **2017**, *23* (32), 7682–7685. https://doi.org/10.1002/chem.201701661.

(103) Lescot, C.; Nielsen, D. U.; Makarov, I. S.; Lindhardt, A. T.; Daasbjerg, K.; Skrydstrup, T. Efficient Fluoride-Catalyzed Conversion of CO_2 to CO at Room Temperature. *J. Am. Chem. Soc.* **2014**, *136* (16), 6142–6147. https://doi.org/10.1021/ja502911e.

(104) Taddei, C.; Gee, A. D. Recent Progress in [^{11}C]Carbon Dioxide ([^{11}C]CO_2) and [^{11}C]Carbon Monoxide ([^{11}C]CO) Chemistry. *J. Label. Compd. Radiopharm.* **2018**. https://doi.org/10.1002/jlcr.3596.

(105) Verbeek, J.; Eriksson, J.; Syvänen, S.; Labots, M.; de Lange, E. C. M.; Voskuyl, R. A.; Mooijer, M. P. J.; Rongen, M.; Lammertsma, A. A.; Windhorst, A. D. [11C]Phenytoin Revisited: Synthesis by [11C]CO Carbonylation and First Evaluation as a P-Gp Tracer in Rats. *EJNMMI Res.* **2012**, *2* (1), 36. https://doi.org/10.1186/2191-219X-2-36.

(106) Syvänen, S.; Eriksson, J. Advances in PET Imaging of P-Glycoprotein Function at the Blood-Brain Barrier. *ACS Chem. Neurosci.* **2013**, *4* (2), 225–237. https://doi.org/10.1021/cn3001729.

(107) Mairinger, S.; Erker, T.; Muller, M.; Langer, O. PET and SPECT Radiotracers to Assess Function and Expression of ABC Transporters In Vivo. *Curr. Drug Metab.* **2011**, *12* (8), 774–792. https://doi.org/10.2174/138920011798356980.

(108) Barth, V. N.; Joshi, E. M.; Silva, M. D. Target Engagement for PK/PD Modeling and Translational Imaging Biomarkets. In *ADME-Enabling Tehcnologies in Drug Design and Development*; Zhang, D., Surapaneni, S., Eds.; John Wiley & Sons, Ltd: Hoboken, New Jersey, 2012; pp 493–512.

(109) Shukla, A.; Kumar, U. Positron Emission Tomography: An Overview. *Journal of Medical Physics*. Medknow Publications and Media Pvt. Ltd 2006, pp 13–21. https://doi.org/10.4103/0971-6203.25665.

(110) Berger, A. How Does It Work? Positron Emission Tomography. *BMJ* **2003**, *326* (7404), 1449. https://doi.org/10.1136/bmj.326.7404.1449.

(111) Van Der Born, D.; Pees, A.; Poot, A. J.; Orru, R. V. A.; Windhorst, A. D.; Vugts, D. J. Fluorine-18 Labelled Building Blocks for PET Tracer Synthesis. *Chemical Society Reviews*. The Royal Society of Chemistry July 31, 2017, pp 4709–4773. https://doi.org/10.1039/c6cs00492j.

(112) Nordberg, A.; Rinne, J. O.; Kadir, A.; Långström, B. The Use of PET in Alzheimer Disease. *Nat. Rev. Neurol.* **2010**, *6* (2), 78–87. https://doi.org/10.1038/nrneurol.2009.217.

(113) Itsenko, O. Photoinitiated Radical Carbonylation Using [11C]Carbon Monoxide, 2005.

(114) Chapy, H.; Saubaméa, B.; Tournier, N.; Bourasset, F.; Behar-Cohen, F.; Declèves, X.; Scherrmann, J.-M.; Cisternino, S. Blood-Brain and Retinal Barriers Show Dissimilar ABC Transporter Impacts and Concealed Effect of P-Glycoprotein on a Novel Verapamil Influx Carrier. *Br. J. Pharmacol.* **2016**, *173* (3), 497–510. https://doi.org/10.1111/bph.13376.

(115) Bankstahl, J. P.; Kuntner, C.; Abrahim, A.; Karch, R.; Stanek, J.; Wanek, T.; Wadsak, W.; Kletter, K.; Muller, M.; Loscher, W.; Langer, O. Tariquidar-Induced P-Glycoprotein Inhibition at the Rat Blood-Brain Barrier Studied with (R)-11C-Verapamil and PET. *J. Nucl. Med.* **2008**, *49* (8), 1328–1335. https://doi.org/10.2967/jnumed.108.051235.

(116) Chuan Tang, S.; Nguyen, L. N.; Sparidans, R. W.; Wagenaar, E.; Beijnen, J. H.; Schinkel, A. H. Increased Oral Availability and Brain Accumulation of the ALK Inhibitor Crizotinib by Coadministration of the P-Glycoprotein (ABCB1) and Breast Cancer Resistance Protein (ABCG2) Inhibitor Elacridar. *Int. J. Cancer* **2014**, *134* (6), 1484–1494. https://doi.org/10.1002/ijc.28475.

(117) Cui, J. J.; Tran-Dubé, M.; Shen, H.; Nambu, M.; Kung, P.-P.; Pairish, M.; Jia, L.; Meng, J.; Funk, L.; Botrous, I.; McTigue, M.; Grodsky, N.; Ryan, K.; Padrique, E.; Alton, G.; Timofeevski, S.; Yamazaki, S.; Li, Q.; Zou, H.; Christensen, J.; Mroczkowski, B.; Bender, S.; Kania, R. S.; Edwards, M. P. Structure Based Drug Design of Crizotinib (PF-02341066), a Potent and Selective Dual Inhibitor of Mesenchymal-Epithelial Transition Factor (c-MET) Kinase and Anaplastic Lymphoma Kinase (ALK). *J. Med. Chem.* **2011**, *54* (18), 6342–6363. https://doi.org/10.1021/jm2007613.

(118) Wislez, M.; Giroux-Leprieur, E.; Fallet, V.; Cadranel, J. Spotlight on Crizotinib in the First-Line Treatment of ALK-Positive Advanced Non-Small-Cell Lung Cancer: Patients Selection and Perspectives. *Lung Cancer Targets Ther.* **2016**, 83. https://doi.org/10.2147/LCTT.S99303.

(119) Radaram, B.; Pisaneschi, F.; Rao, Y.; Yang, P.; Piwnica-Worms, D.; Alauddin, M. M. Novel Derivatives of Anaplastic Lymphoma Kinase Inhibitors: Synthesis, Radiolabeling, and Preliminary Biological Studies of Fluoroethyl Analogues of Crizotinib, Alectinib, and Ceritinib. *Eur. J. Med. Chem.* **2019**, *182*, 111571. https://doi.org/10.1016/j.ejmech.2019.111571.

(120) Lin, Q.; Zhang, Y.; Fu, Z.; Hu, B.; Si, Z.; Zhao, Y.; Shi, H.; Cheng, D. Synthesis and Evaluation of 18F Labeled Crizotinib Derivative [18F]FPC as a Novel PET Probe for Imaging c-MET-Positive NSCLC Tumor. *Bioorganic Med. Chem.* **2020**, *28* (15), 115577. https://doi.org/10.1016/j.bmc.2020.115577.

(121) Cai, L.; Lu, S.; Pike, V. W. Chemistry with [18F]Fluoride Ion. *European J. Org. Chem.* **2008**, *2008* (17), 2853–2873. https://doi.org/10.1002/ejoc.200800114.

(122) Coenen, H. H. Fluorine-18 Labeling Methods: Features and Possibilities of Basic Reactions. In *PET Chemistry*; Springer Berlin Heidelberg; pp 15–50. https://doi.org/10.1007/978-3-540-49527-7_2.

(123) Rotstein, B. H.; Stephenson, N. A.; Vasdev, N.; Liang, S. H. Spirocyclic Hypervalent Iodine(III)-Mediated Radiofluorination of Non-Activated and Hindered Aromatics. *Nat. Commun.* **2014**, *5* (1), 4365. https://doi.org/10.1038/ncomms5365.

(124) Rotstein, B. H.; Wang, L.; Liu, R. Y.; Patteson, J.; Kwan, E. E.; Vasdev, N.; Liang, S. H. Mechanistic Studies and Radiofluorination of Structurally Diverse Pharmaceuticals with

Spirocyclic Iodonium(III) Ylides. *Chem. Sci.* **2016**, *7* (7), 4407–4417. https://doi.org/10.1039/c6sc00197a.

(125) Neumann, C. N.; Hooker, J. M.; Ritter, T. Concerted Nucleophilic Aromatic Substitution with 19F− and 18F−. *Nature* **2016**, *534* (7607), 369–373. https://doi.org/10.1038/nature17667.

(126) Liang, S. H.; Yokell, D. L.; Jackson, R. N.; Rice, P. A.; Callahan, R.; Johnson, K. A.; Alagille, D.; Tamagnan, G.; Lee Collier, T.; Vasdev, N. Microfluidic Continuous-Flow Radiosynthesis of [18F]FPEB Suitable for Human PET Imaging. *Medchemcomm* **2014**, *5* (4), 432–435. https://doi.org/10.1039/c3md00335c.

(127) Pauli, G. F.; Chen, S.-N.; Simmler, C.; Lankin, D. C.; Gödecke, T.; Jaki, B. U.; Friesen, J. B.; McAlpine, J. B.; Napolitano, J. G. Importance of Purity Evaluation and the Potential of Quantitative 1 H NMR as a Purity Assay. *J. Med. Chem.* **2014**, *57* (22), 9220–9231. https://doi.org/10.1021/jm500734a.

(128) Liu, Y.; Sun, H.; Huang, Z.; Ma, C.; Lin, A.; Yao, H.; Xu, J.; Xu, S. Metal-Free Synthesis of N -(Pyridine-2-Yl)Amides from Ketones via Selective Oxidative Cleavage of C(O)–C(Alkyl) Bond in Water. *J. Org. Chem.* **2018**, *83* (23), 14307–14313. https://doi.org/10.1021/acs.joc.8b01956.

(129) Nguyen, T. T.; Hull, K. L. Rhodium-Catalyzed Oxidative Amidation of Sterically Hindered Aldehydes and Alcohols. *ACS Catal.* **2016**, *6* (12). https://doi.org/10.1021/acscatal.6b02541.

(130) Jang, Y. K.; Krückel, T.; Rueping, M.; El-Sepelgy, O. Sustainable Alkylation of Unactivated Esters and Amides with Alcohols Enabled by Manganese Catalysis. *Org. Lett.* **2018**, *20* (24), 7779–7783. https://doi.org/10.1021/acs.orglett.8b03184.

(131) Ghosh, S. C.; Ngiam, J. S. Y.; Seayad, A. M.; Tuan, D. T.; Chai, C. L. L.; Chen, A. Copper-Catalyzed Oxidative Amidation of Aldehydes with Amine Salts: Synthesis of Primary, Secondary, and Tertiary Amides. *J. Org. Chem.* **2012**, *77* (18), 8007–8015. https://doi.org/10.1021/jo301252c.

(132) Fang, W.; Deng, Q.; Xu, M.; Tu, T. Highly Efficient Aminocarbonylation of Iodoarenes at Atmospheric Pressure Catalyzed by a Robust Acenaphthoimidazolyidene Allylic Palladium Complex. *Org. Lett.* **2013**, *15* (14), 3678–3681. https://doi.org/10.1021/ol401550h.

(133) Sugimoto, M.; Yamamoto, F.; Honna, K.; Kurisaki, K.; Sugahara, H.; Watanabe, K.; Fujimoto, Y.; Ryu, S. Adamantane-Piperazine Derivatives. US4001223, 1975.

(134) Dhanasekaran, S.; Suneja, A.; Bisai, V.; Singh, V. K. Approach to Isoindolinones, Isoquinolinones, and THIQs via Lewis Acid-Catalyzed Domino Strecker-Lactamization/Alkylations. *Org. Lett.* **2016**, *18* (4), 634–637. https://doi.org/10.1021/acs.orglett.5b03331.

(135) Tang, P.; Wang, W.; Ritter, T. Deoxyfluorination of Phenols. *J. Am. Chem. Soc.* **2011**, *133* (30), 11482–11484. https://doi.org/10.1021/ja2048072.

(136) Markovic, T.; Murray, P. R. D.; Rocke, B. N.; Shavnya, A.; Blakemore, D. C.; Willis, M. C. Heterocyclic Allylsulfones as Latent Heteroaryl Nucleophiles in Palladium-Catalyzed Cross-Coupling Reactions. *J. Am. Chem. Soc.* **2018**, *140* (46), 15916–15923. https://doi.org/10.1021/jacs.8b09595.

(137) Hanessian, S.; Marcotte, S.; Machaalani, R.; Huang, G. Total Synthesis and Structural Confirmation of Malayamycin A: A Novel Bicyclic C-Nucleoside from Streptomyces Malaysiensis. *Org. Lett.* **2003**, *5* (23), 4277–4280. https://doi.org/10.1021/ol030095k.

(138) Durugkar, D. K. M. K. A. Efficient and Selective Cleavage of the Tert-Butoxycarbonyl (Boc) Group under Basic Condition. *Arkivoc* **2005**, *2005* (14), 20–28. https://doi.org/10.3998/ark.5550190.0006.e03.

(139) Zinelaabidine, C.; Souad, O.; Zoubir, J.; Malika, B.; Nour-Eddine, A. A Simple and Efficient Green Method for the Deprotection of N-Boc in Various Structurally Diverse Amines under Water-

Mediated Catalyst-Free Conditions. *Int. J. Chem.* **2012**, *4* (3). https://doi.org/10.5539/ijc.v4n3p73.

ÉCOLE DOCTORALE
Sciences Chimiques : Molécules, Matériaux, Instrumentation et Biosystèmes (2MIB)

Titre : Développement de Nouvelles Méthodes de Marquage Tardif avec Carbone Marqué et Fluor-18

Mots clés : Radiochimie, Carbonylation, Radiofluorination, Marquage tardif

Résumé : Le marquage isotopique est un outil précieux pour la découverte de nouveaux médicaments. Nous présentons dans cette thèse la conception et l'application de méthodes de marquage tardif de molécules bioactives avec du carbone et du fluor.
Les réactions de carbonylation utilisant le monoxide de carbone sont connues pour être compatibles avec un marquage isotopique tardif des substances bioactives dans des conditions douces. La première partie de cette thèse décrit une réaction de photocarbonylation à partir d'iodures d'alkyles catalysée par le palladium sous lumière visible. Cette réaction polyvalente utilisant le 9-methylfluorene-9-carbonyl chloride (COgen) et réalisée dans des conditions douces est compatible avec un marquage en carbone-14.
La synthèse de COgen radioactif nécessitant plusieurs étapes, nos efforts ont porté sur la production de monoxyde de carbone marqué, par réduction du dioxyde de carbone correspondant avec un disilane.
La dernière partie de la thèse aborde la synthèse d'un nouveau traceur marqué au fluor-18 pour la tomographie par émission de positrons, spécifique de la P-glycoprotéine (P-gp), un transporteur de la barrière hématoencéphalique. Nous avons ainsi marqué au fluor-18 le Crizotinib, anticancéreux approuvé pour le traitement du cancer du poumon non à petites cellules et qui voit son accumulation fortement diminuée par le P-gp. Les études de biodistribution et d'imagerie cérébrale chez les rongeurs sont actuellement en cours.

Title: Development of New Late-Stage Labeling Methods with Labeled Carbon and Fluorine-18

Keywords: Radiochemistry, Carbonylation, Radiofluorination, Late-stage Labeling

Abstract: Isotope labeling is a crucial tool in drug discovery. Therefore, expanding the toolbox of a radiochemist with methods that allow late-stage labeling is highly important. The work presented in this thesis describes the development and utilization of late-stage labeling methods with carbon and fluorine.
Carbonylation reactions with carbon monoxide are particularly known as mild and compatible with the late-stage labeling. The first part of the thesis describes the development of visible-light mediated palladium-catalysis using alkyl iodides as the coupling partner for the carbonylation. The mild and versatile radical aminocarbonylation protocol has shown good substrate compatibility. The use of 9-Methylfluorene-9-carbonyl chloride (COgen) allowed easy translation between unlabeled and labeled reaction.
In order to bypass the synthesis of COgen which proceeds in two steps plus one step for the liberation of CO, we focused our efforts towards the one step reduction of labeled CO_2 to labeled CO using disilanes catalyzed by fluorides.
The last part of this thesis discusses the development of a new positron emission tomography (PET) radiotracer for P-glycoprotein (P-gp), an active transporter at the blood-brain barrier. Crizotinib is an approved treatment for non-small cell lung carcinoma and its brain accumulation is restricted by P-gp. Crizotinib was successfully labeled with ^{18}F, and rodent studies to map P-gp and improve the delivery of crizotinib to the brain are ongoing.

Université Paris-Saclay
Espace Technologique / Immeuble Discovery
Route de l'Orme aux Merisiers RD 128 / 91190 Saint-Aubin, France